Bedrock scallop distribution and morphology in upland river channels

ALEX GEORGE HALL

Bedrock scallop distribution and morphology in upland river channels

Alex G. Hall

Abstract

Scallops are contiguous concave features bound by steep ridges that occur on bedrock surfaces in cave and surface river channel environments. Scallops are useful indicators in hydraulics as their morphology is related to flow velocity and direction. However, previous research has focused on cave scallops, with limited quantitative analysis of scallop lengths and orientations in surface channel environments. A dataset of 13,641 scallop length and orientation measurements was collected from surface channel scallops. Analysis revealed that Trout Beck and Rough Sike had Sauter mean scallop lengths of 5.1 cm (S_{32} = 0.2, n = 1,185) and 3.1 cm (S_{32} = 0.2, n = 12,456) respectively. A negative relationship was present between the Sauter mean scallop length and the height at which they were located above the water surface. The statistical distributions of scallop length measurements are found to not follow the typical unimodal, log-normal distribution suggested for cave scallops, potentially due to other factors such as weathering and abrasion modifying the scallop morphology in surface channels. No significant relationships were observed between the Sauter mean scallop length or scallop abundance and the unit stream power at Trout Beck or Rough Sike. Scallops typically were oriented in the direction towards the primary flow in the channel, suggesting that the morphological context of the scalloped location must be considered when inferring paleo-flow directions. This study provides the first quantitative analysis of scallop morphology in surface channels, developing the understanding of how scallops form under varying environmental conditions. A first-order estimate of the scallop development timescales for a range of scallop sizes was generated under two different dissolution rates, providing the first such estimate for surface channel scallops on limestone surfaces.

Bedrock scallop distribution and morphology in upland river channels

Alex George Hall

A thesis submitted for the degree of

Masters by Research (By Thesis)

Geography

Durham University

2024

Table of Contents

List of Tables

List of Figures

Statement of Copyright

Introduction

Bedrock rivers are key drivers of morphological change in landscapes (Turowski *et al.*, 2008; Whipple *et al.*, 2013). Bedrock rivers are characterised as channels which flow over a bedrock surface, differing from alluvial rivers which flow over a sediment bed (Tinkler and Wohl, 1998; Turowski *et al.*, 2008; Whipple, 2004). A mix of these river types can also be observed, known as mixed bedrock-alluvial channels, where a bedrock channel has alluvial cover in some sections (Turowski *et al.*, 2008). In the upstream section of alluvial rivers, partial or complete bedrock segments are frequently observed, suggesting that a change has occurred in the balance between sediment conveyance and supply (Sharma, 2016).

Erosion refers to the removal and transport of a surficial surface, whereas weathering is the process of wearing down a natural surface in place due to exposure to the atmosphere (Whipple *et al.*, 2000). Erosion is the primary driver of morphological change in bedrock channels, with abrasion, plucking and chemical erosion being the dominant processes (Charlton, 2009). Abrasion refers to the wearing away of a surface from impacts by sediment transported in a fluid (Richardson and Carling, 2005; Wilson, 2009). Plucking is the hydraulic removal of blocks of rock, typically which have been weakened or 'prepared' by other processes, such as sub-aerial weathering (Charlton, 2009; Hancock *et al.*, 1998). Chemical erosion in bedrock rivers is driven by dissolution, which refers to the breaking down of the rock by water as soluble minerals dissolve (Wilson, 2009). The examination of forms sculpted by erosion in bedrock channels can provide useful insights into the dominant erosional and weathering mechanisms present within the channel (Richardson and Carling, 2005).

Dissolution by turbulent (continual mixing/irregularity) water in cave conduits and surface streams with soluble bedrock boundaries (e.g. limestone, gypsum) can develop contiguous concave microtopography bound by steep ridges known as scallops (Figure 1). Scallop-like forms can also develop on a range of other surfaces, such as ice (Bushuk *et al.*, 2019; Ristroph, 2018; Santanatoglia, 2023), snow (Goodchild and Ford, 1971; Jahn and Kłapa, 1968), meteorites (Henderson and Perry, 1958), carbon steel piping (Burrill and Cheluget, 1999; Villien *et al.*, 2001, 2005), and experimentally on plaster (Blumberg and Curl, 1974; Goodchild and Ford,

1971; Villien *et al.*, 2005). The fluids (e.g., water, air) and mechanisms of removal (e.g., dissolution, melting) which develop these scallop forms vary, however they all have a unifying similarity that they develop due to the turbulent flow of a fluid adjacent to an erodible surface (Bushuk *et al.*, 2019). Scallops developed by the flow of turbulent water over a carbonate rock surface have been studied in detail in cave systems (e.g., Bortel, 2021; Bretz, 1942; Faulkner, 2022; Gradziński, 2002; Hall, 2019; Lundberg *et al.*, 2017; Simms and Hunt, 2007; Skoglund and Lauritzen, 2005). Extensive assemblages of scallops can occur in surface streams but research on them is limited, therefore the processes which develop and modify their morphology and distribution are not well constrained (Coleman, 1945; Richardson and Carling, 2005). It is also unclear whether the morphology of scallops vary between cave and surface stream environments.

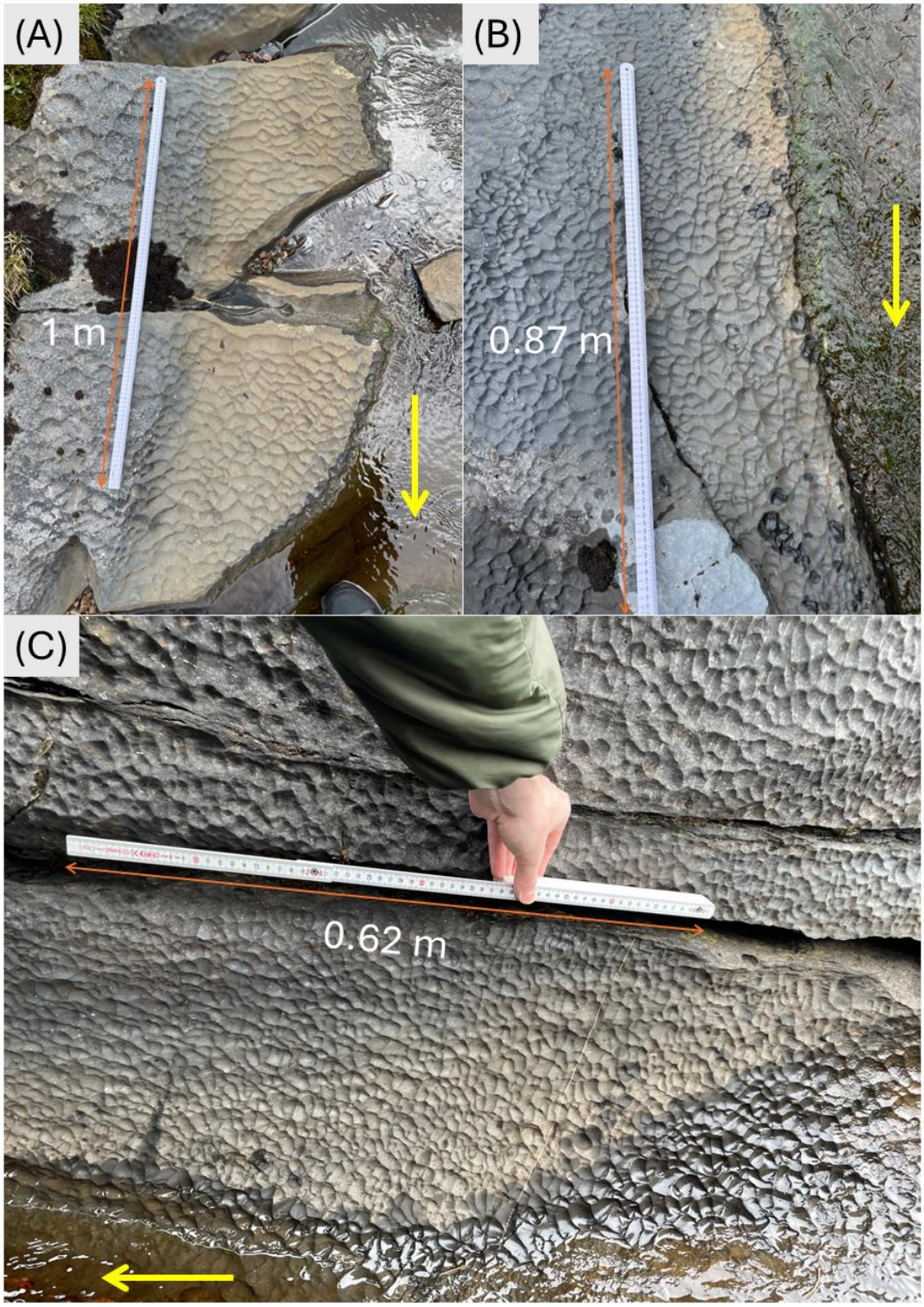

Figure 1: Scallops on limestone from Rough Sike, UK; (a) flow is from the top of the image to the bottom (B) flow is from the top of the image to the bottom (C) flow is from right to left. Flow direction indicated by the yellow arrow.

The cross-sectional morphology of scallops is typically characterised by a steep downward face (upstream end) and a more gradual face sloping back up in the direction of flow (Figure 2) (Bretz, 1942; Cooper, 2018; Curl, 1974; Faulkner, 2013; Ford and Williams, 2007; Gradziński, 2002). Because of this asymmetry, scallops preserve the direction of flow over the surface, meaning scallop orientation is a valuable indicator for understanding historic flow pathways in karst hydrology (Bögli, 1980). Scallops undergo a developmental period; however, existing literature has yet to provide estimates regarding the temporal scale necessary for this process. Previous research has shown, there is an inverse relationship between the scallop length (defined as the distance between the two scallop crests in the direction of flow) and the flow velocity of the fluid that created them (Blumberg and Curl, 1974; Charlton, 2003; Cooper, 2018; Curl, 1966; Ford and Williams, 2007; Goodchild and Ford, 1971; Hall, 2019; Hammer *et al.*, 2011; Springer and Hall, 2020); where shorter scallop lengths indicate faster flow velocity, and larger scallop lengths indicate slower flow velocity. Therefore, scallop morphology can be used to interpret paleo-flow velocity and direction, as well as providing valuable insights into the dominant erosional processes occurring within the channel at that time.

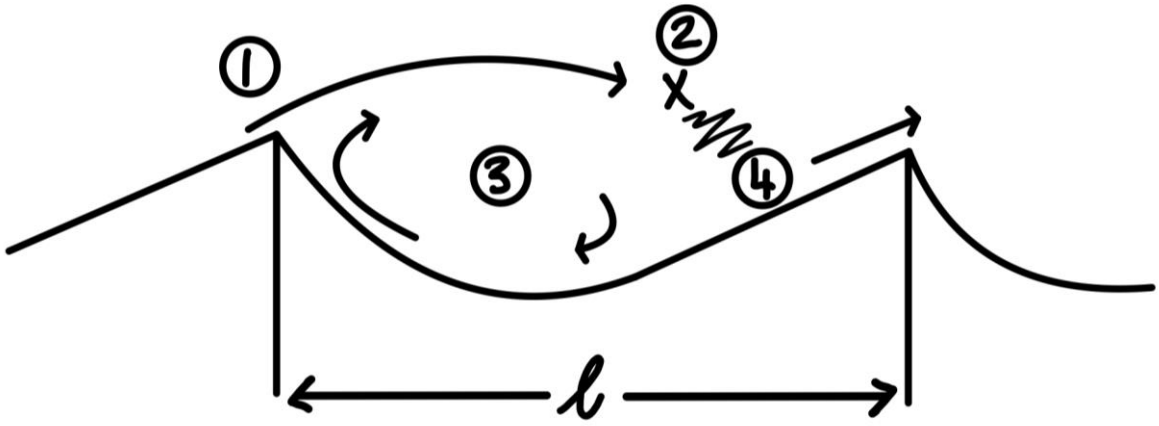

Figure 2: Schematic diagram (not to scale) showing “fluid motion in the vicinity of a scallop. Point 1: flow separation at the crest. Point 2: transition of laminar shear layer to turbulence. Point 3: recirculating flow in the lee eddy. Point 4: jet reattachment region” (Curl, 1974). l is the scallop length.

Cave scallops have a typical length between 0.05 and 0.2 m (up to 2 m), a width-to-length ratio of 2:1 and a length-to-amplitude ratio of 4-8:1 (Ford and Williams, 2007;

Santanatoglia, 2023). Previous work on scallops in caves revealed that scallop length measurements from an assemblage of scallops typically follow a unimodal, log-normal distribution (Charlton, 2003; Faulkner, 2013; Ford and Williams, 2007; Hall, 2019; Springer and Hall, 2020). However, the statistical distribution of scallop lengths from open river channels is yet to be determined (see Figure 3). Charlton (2003) suggested that if scallops follow this unimodal, log-normal distribution, but there is variability in discharge and velocity over time, there may be a scallop dominant discharge that these scallops represent. This would be the discharge at which the dissolutional erosion rate is greatest.

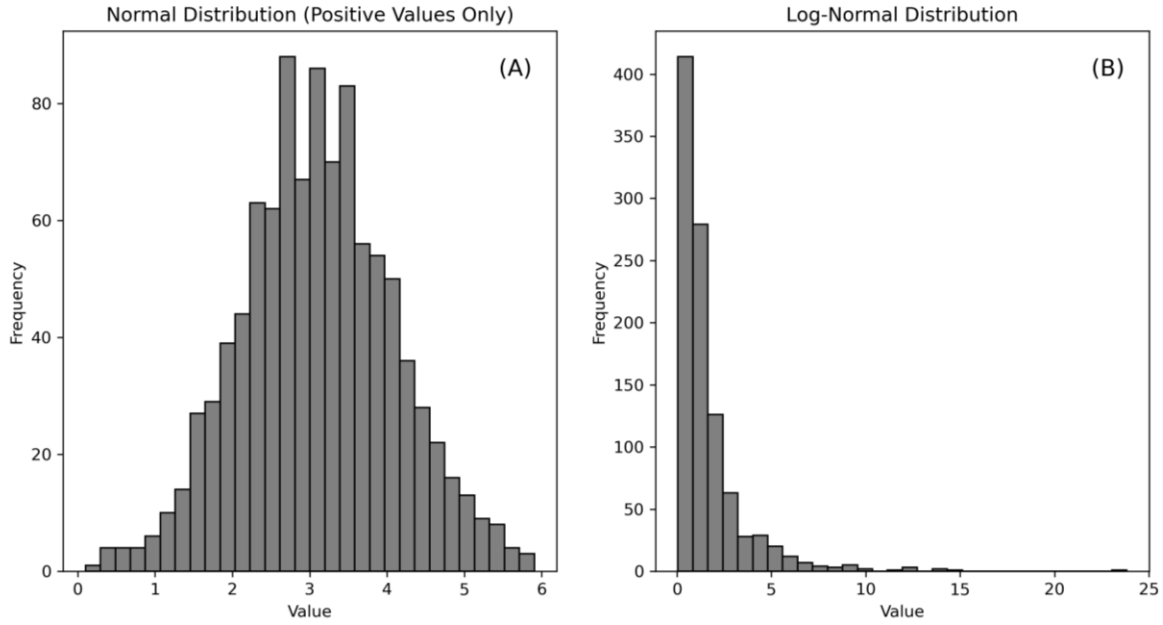

Figure 3: An example of a (A) normal distribution (positive values only), and a (B) log-normal distribution.

This study aims to investigate the distribution of scallops on limestone bedrock surfaces in open river channels, analyse their length and orientation patterns, and explore how channel features and flow conditions influence their formation and microtopography. To address this aim, the study is guided by the following research questions:

- RQ1: What is the spatial distribution of scallops at Trout Beck and Rough Sike?
- RQ2: To what extent do scallop lengths vary between rivers and height within a river?

- RQ3: How does scallop length and abundance relate to stream power?
- RQ4: What is the statistical distribution of scallop lengths?
- RQ5: How are scallops oriented and what is their statistical distribution?
- RQ6: How long does it take for scallops to develop?

1. Literature review

The aim of this brief literature review is to evaluate and summarise the current understanding of bedrock scallops, focusing on scallop morphology and development. An overview of the dissolution process in limestone will be introduced, alongside a summary of the original theory of scallop development in caves. Following this, scallop development in cave systems will be compared to open bedrock channels and factors influencing scallop development such as abrasion by sediment, flow velocity, and channel morphology will be examined. Finally, the statistical distributions of scallop lengths and methods of characterising them will be outlined.

1.1. Limestone (carbonate) dissolution processes

Carbonate rocks such as limestone can facilitate endemic bedforms produced by dissolution (e.g., scallops) (Richardson and Carling, 2005). Scallops develop from the dissolution of calcium carbonate ($CaCo_3$), the principal component of limestone. Dissolution of calcium carbonate occurs primarily due to the reaction with carbonic acid (H_2CO_3) present in the water. Carbonic acid is created when atmospheric carbon dioxide (CO_2) dissolves in water (H_2O) (Equation 1) (Bögli, 1980; Ryb *et al.*, 2014).

$$H_2O + CO_2 \rightleftharpoons H_2CO_3 \quad (1)$$

Once formed, the carbonic acid dissociates, allowing the calcium carbonate to react with the carbonic acid, forming calcium ions (Ca^{2+}) and bicarbonate ions (HCO_3^-) in water (Johnson *et al.*, 2017).

$$CaCO_3(s) + H_2CO_3 \rightarrow Ca^{2+}(aq) + 2HCO_3^- \quad (2)$$

The concentration of dissolved CO_2 in the water can vary due many factors including the water temperature, atmospheric CO_2 concentration, and the rate of water flow and mixing (Cole and Prairie, 2014). Covington *et al.* (2015) suggests that dissolution will occur at a greater rate in instances where mechanical erosion is limited (e.g. lack of sediment), the water is chemically unsaturated (e.g. upstream geology is non-carbonate), and in conditions where extreme flow events are limited.

1.2. Scallop formation and morphology

Curl (1966, 1974) and Blumberg and Curl (1974) proposed a theory of scallop development (in reference to scallops in limestone surface streams and caves) in which local flow separation caused by surface irregularities generates a jet (see Figure 2). This jet reattaches to the surface in a localised region, resulting in a greater rate of dissolution at that point (Cooper, 2018; Curl, 1974; Ford and Williams, 2007; Lundberg, 2019). In the case of limestone-water scallops, Curl's (1966, 1974) theory suggests that the increased localised rate of calcium carbonate dissolution, compared to dissolution through diffusion in the boundary layer (layer of fluid close to the bedrock surface in which viscous rather than turbulent forces dominate), is what drives the formation and development of the scallops. An inverse relationship between the scallop length and flow velocity was first proposed by Curl (1966) through a theoretical dimensional analysis. This relationship has since been shown in experimental flume work simulating scallop formation on a plaster surface under variable water flow velocities by Goodchild and Ford (1971), Blumberg and Curl (1974), and Villien et al. (2001, 2005). Claudin et al. (2017) suggest that as the flow interacts with altered bed topography, it causes erosion or sediment transport, leading to further surface modifications. Villien et al. (2005) produced scallops experimentally in plaster, showing how an initially flat surface gradually develops into a fully formed scalloped pattern over time.

Unit stream power (UPS, Ω) is a measure of a measure of the rate of energy expenditure of the water per unit area (Yang and Stall, 1974). Dingle et al. (in review) calculated the 10-year unit stream power, which is associated with a discharge event having a 10-year return period, for various cross-sections in Trout Beck and Rough Sike. However, for this analysis, the focus is not on the return period, but rather on the relative magnitude of the value and its relationship to high- or low-energy sections of the channel. The unit stream power was calculated using the equation:

$$\Omega = \frac{\rho g Q S}{w}$$

where ρ is the fluid density (kg m^{-3}), g is the gravitational acceleration (m s^{-2}), Q is the discharge (m^3 s^{-1}), S is the slope, and w is the channel width (m). Scallop length would be expected to be related to the relative energy conditions within a study

reach, with higher unit stream power generally associated with higher flow velocities and, consequently, smaller scallop lengths.

Cave scallops have been used as indicators of paleo-flow direction and velocity due to their asymmetry under unidirectional flow conditions and the established relationship between the scallop length and flow velocity (Bretz, 1942; Checkley and Faulkner, 2014; Coleman, 1945; Droin, 2021; Kicińska *et al.*, 2017; Maxson, 1940; Simms and Hunt, 2007; Skoglund and Lauritzen, 2005; Springer and Hall, 2020; Woodward and Sasowsky, 2009). Non-directional scallops develop where a prominent unidirectional flow is not present, such as surfaces in slack water or upstream faces of boulders (Richardson and Carling, 2005).

While scallops from surface streams develop under open-channel, free-surface conditions (exposed to the atmosphere), cave scallops form in two distinct zones: the phreatic zone (beneath the water table), where the cave conduit is filled with water, and no air is present (e.g., Faulkner, 2022; Gradziński, 2002; Hall, 2019; Lundberg *et al.*, 2017), or the vadose zone (the area between the earth surface and the water table) where both air and water are present (e.g., Checkley and Faulkner, 2014; Murphy and Moseley 2012). The temporal aspect of scallop development is not well-explored, and the development period of scallops is rarely addressed in the existing literature. However, long-term dissolution rates have been calculated at Rough Sike and Trout Beck, with rates of 0.98 mm yr^{-1} and 0.58 mm yr^{-1} respectfully (Dingle *et al., in review*).

Cave scallop lengths are thought to typically follow a unimodal, log-normal distribution (Charlton, 2003; Faulkner, 2013; Ford and Williams, 2007; Hall, 2019; Springer and Hall, 2020). Hall (2019) expands on the statistical distribution of cave scallop lengths through analysis of 1,756 cave scallops, finding that lower sample sizes of scallops (minimum of n = 30) are typically distributed normally or log-normally, whereas larger groups of scallops (n = 100) are typically distributed log-normally. Springer and Hall (2020) sampled 60 sets of scallops across three caves with sample sizes ranging from 30 – 40, finding that 57 out of the 60 sets of scallops sampled were classified as log-normal ($p > 0.05$). The normality and modality of scallops from open river channels is yet to be determined. Understanding the distribution of scallop length measurements within an assemblage is valuable for

determining whether the scallops represent one or multiple flows, while ensuring the summary statistic of the dataset, such as the Sauter mean, accurately represent the data.

Scallops in open bedrock channels have been documented by Coleman (1945) in surface channels in Ireland, and by Richardson and Carling (2005) at four sites, including Sleightholme Beck (limestone open bedrock channel). Coleman (1945) noted that cave scallops are better developed in terms of their sharpness and individuality than scallops found within surface channels, suggesting that sub-aerial weathering of exposed scallops occurring in surface channels when the active flow in the channel is low may affect their development. Richardson and Carling (2005) proposed that “high velocity and/or highly turbulent flow” is essential for the formation of distinct scallop assemblages in open bedrock channels, however no studies have been conducted to test this hypothesis. They classified scallops from open bedrock channels into two main forms, ‘directional’ and ‘non-directional’ scallops Figure 4. Directional scallops are further divided into ‘three-dimensional’ (unordered and *en echelon* arrangements), ‘intermediate’, ‘two-dimensional’, and ‘turreted’ scallops (Richardson and Carling, 2005).

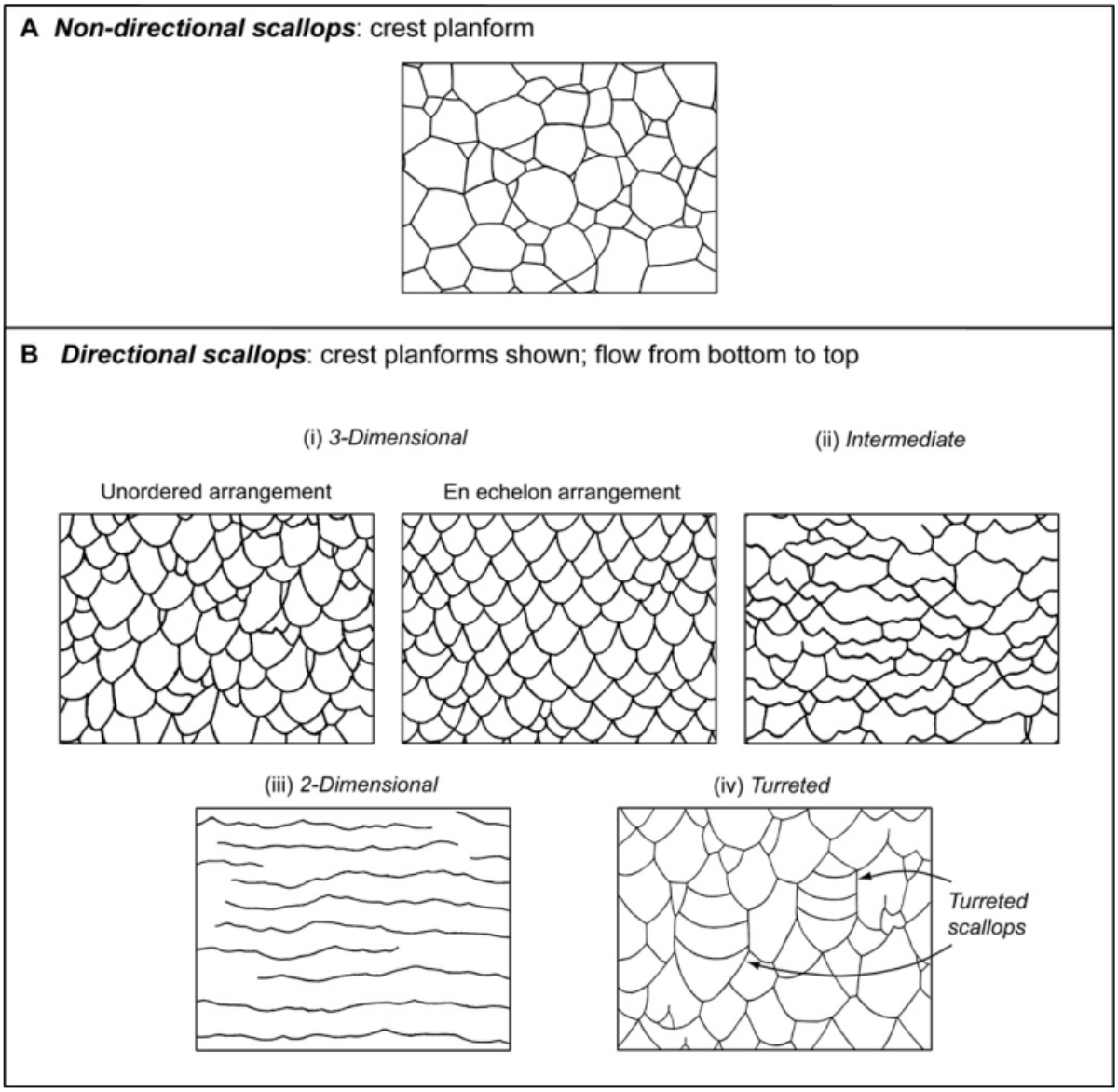

Figure 4: Crest planform view of (A) non-directional, and (B) directional scallop forms. Directional scallops are divided further into (i) three-dimensional, (ii) intermediate, (iii) two-dimensional, and (iv) turreted scallops. (Richardson and Carling, 2005).

1.3. Impact of sediment dynamics on scallop morphology

The role of sediment in the development and modification of scallops has been examined previously in relation to cave scallops. Curl (1966) suggested that if the scallop morphology is to be stable, the rate of removal of rock at the scallop crest and depression must be equal; if this balance is not met, the scallops may either deepen or the surface may move toward planation. Introducing sediment load could

interfere with this balance, as sediment will preferentially cover the concavity of the scallop, causing solution rates at the scallop crests to be greater than at the base, leading to the removal of the sculpted features (Goodchild and Ford, 1971). Curl (1966) also hypothesized that both abrasion in high energy flows with large sediment loads and weathering on the scalloped surfaces may preferentially weaken the crests, again causing the removal of the scalloped features. Faulkner (2013) highlights the key balance between having adequate flow velocity to produce full turbulence and support scallop formation, but not too great so that sediment is frequently transported, causing abrasion and the removal of the scalloped forms. Faulkner (2013) observed that in caves, scallop lengths decrease with increasing flow velocity to a limit of 3 ms^{-1}, where abrasion then dominates over chemical dissolution, and scallops reach a minimum size of c. 0.01 m before disappearing. Ford and Williams (2007) highlighted that at high flow velocities, abrasion from suspended sand can result in the development of elongated, polished features similar to flute markings. Abrasion may be a contributing factor to the modification of scallops, as mentioned by Bortel (2021), Cooper (2018), Hall (2019), and Bögli (1980), however, there is no evidence to indicate that abrasion is the main factor driving scallop development; instead, abrasion may alter the morphology of pre-existing scallop forms.

1.4. Calculating summary statistics for scallop length measurements

Material properties such as insoluble inclusions within the rock (e.g. fossils in limestone) or air bubbles may cause variability in local dissolution rates alongside the creation of more initial vortices, potentially developing scallops of smaller lengths (Curl, 1974; Ford and Williams, 2007; Goodchild and Ford, 1971). These smaller scallops may inherently not be representative of the primary flow dynamics near the surface. Within scallop assemblages, there may also be incomplete scallop forms that develop from scallop overlapping (Curl, 1974). Both processes can skew the scallop distribution to smaller sizes, therefore, a ‘Sauter mean’ is typically used to characterise scallop length, which reduces the importance of smaller lengths in the calculation of the mean. Springer and Hall (2020) find through resampling 100 scallop lengths using Monte Carlo simulations that if the arithmetic mean is used instead of the Sauter mean, the calculated discharges from the arithmetic mean length would be biased towards larger values. The Sauter mean is also typically

used instead of the arithmetic mean which has equal weighting but can be skewed by outliers, or geometric mean which is less skewed by outliers but can favour smaller values

The Sauter mean scallop length (L_{32}) can be calculated as:

$$L_{32} = \frac{\Sigma l_i^3}{\Sigma l_i^2} \quad (3)$$

where l_i is the length of the i^{th} scallop, calculated as the crest-to-crest length of the scallop in the direction of flow (Lauritzen, 1982; Springer and Hall, 2020). The standard deviation of the Sauter mean scallop length (S_{32}) can be calculated as:

$$S_{32} \approx \left[\frac{13}{n(n-1)} \sum_{i=1}^{n} \left(\ln L_i - \overline{\ln L_\iota}\right)^2\right]^{0.5} \quad (4)$$

where n is the number of samples, and L_i is the length of the i^{th} scallop in the dataset (Lauritzen, 1982; Springer and Hall, 2020). The arithmetic mean of scallop lengths has also been used by a range of authors (e.g., Despain *et al.*, 2016; Gale, 1984; Goodchild and Ford, 1971) and is calculated as:

$$\bar{L} = \frac{\Sigma \mathrm{x}}{n} \quad (5)$$

where $\bar{L}$ is the mean scallop length, x are the scallop length values, and n is the number of samples. However, Springer and Hall (2020) argue for the use of the Sauter mean as the original 'universal constants' of Re^* (scallop Reynold's number) and B_L (roughness constant) used within scallop derived velocity calculations were derived by Blumberg and Curl (1974) from experimental flume measured velocities, in which the Sauter mean was used.

In summary, the orientation and length of scallops are valuable indicators of flow dynamics in both cave and surface channels, however research on scallops in surface channels remains limited, leaving the variables that influence their formation and characteristics poorly understood.

2. Field Site

2.1. Moor House

Scallops have rarely been reported in open river channels (Section 1.2), with the majority of the existing literature focusing on scalloping in cave systems. Furthermore, there has been no quantitative measurement of scallop length or orientations for scallops found in surface channels. To evaluate the distribution and morphology of scallops found within river channels, a study site with abundant and accessible scalloping is required. Trout Beck and Rough Sike are perennial bedrock rivers located in the Moor House National Nature Reserve (Moor House NNR, 54.69° N, -2.38° E, Figure 5) that have evidence of scalloping on some of the limestone bedrock surfaces within the channel. The Moor House NNR ranges in elevation from 848 – 535 m (DEIMS-SDR, 2023). The Trout Beck study reach is approximately 230 m long, with elevations ranging from 553 - 547 m. The Rough Sike study reach is approximately 125 m long, with elevations ranging from 560 - 552 m. Table 1 includes low water surface slope values for various cross sections along Trout Beck and Rough Sike, with average slope values for the study reaches of 0.021 and 0.047 respectively. Trout Beck and Rough Sike have drainage areas of 8.3 and 1.2 km^2 respectively (see Figure 5).

Table 1: Low flow water surface slope and 10-year Unit Stream Power for cross-sections (from Dingle et al., in review) at Rough Sike and Trout Beck.

Cross-section ID (Dingle et al., in review)	**Low flow water surface slope (m/m)***	**10 yr Unit Stream Power (USP) (W m^{-2})**
Rough Sike (RS)		
RS1	0.022	109
RS2	0.082	706
RS3	0.048	328
RS4	0.069	651
RS5	0.015	57
Average	0.047	370
Trout Beck (TB)		
TB1	0.041	754

TB2	0.002	47
TB3	0.028	789
TB4	0.019	426
TB5	0.017	411
TB6	0.016	385
Average	0.021	469

Both rivers are mixed bedrock-alluvial rivers (Sharma, 2016; Turowski *et al.*, 2008), however the study sections of Trout Beck and Rough Sike are primarily bedrock-bound, with some sections that are have a thin covering of alluvium on the bedrock surface (bedrock-confined) (Figure 6). Smith (2004) classified Trout Beck in sections based upon the amount of bedrock, finding that 81% of Trout Beck was alluvial, 13% was semi-alluvial, and 5% was bare bedrock.

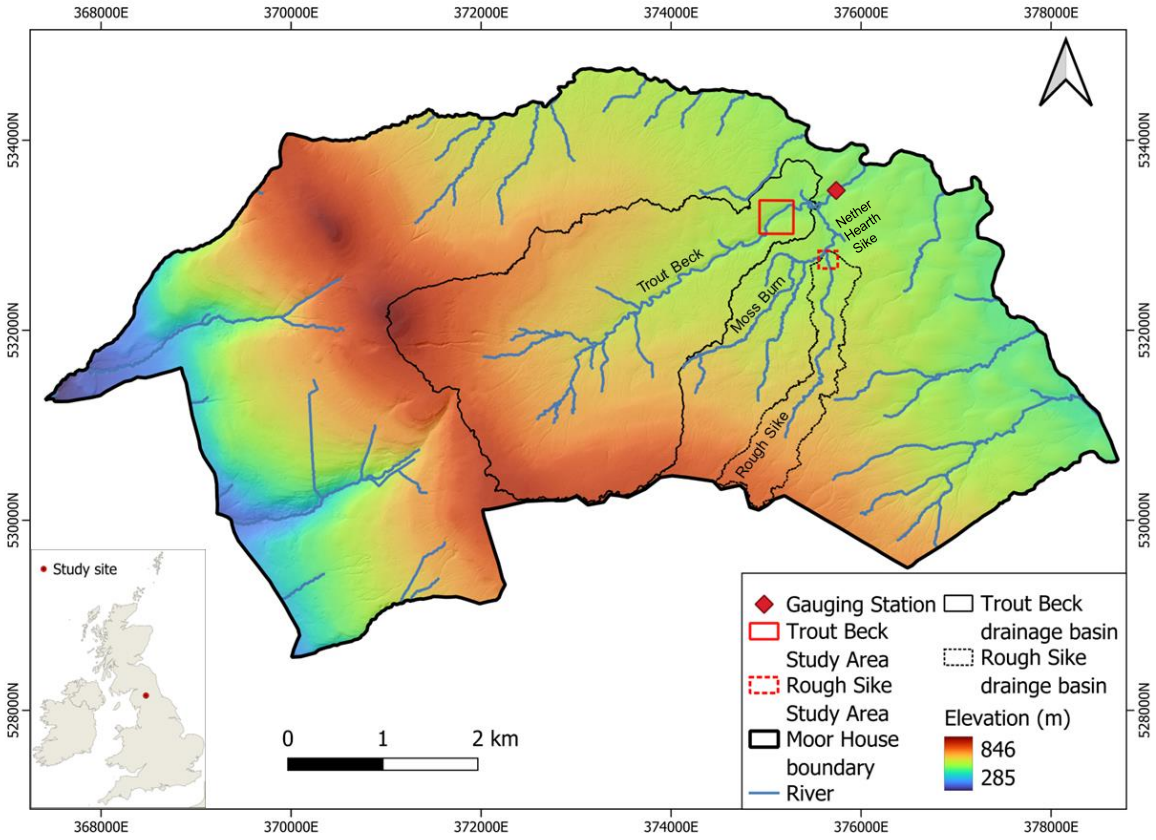

Figure 5: Elevation of Moor House. 2021, 1 m National Lidar Programme DTM [Accessed through Defra Survey Data Download. 11/03/2021]. Trout Beck drainage basin calculated above the confluence with Nether Hearth Sike. Rough Sike

drainage basin calculated above the confluence with Moss Burn. British National Grid – Grid square: NY.

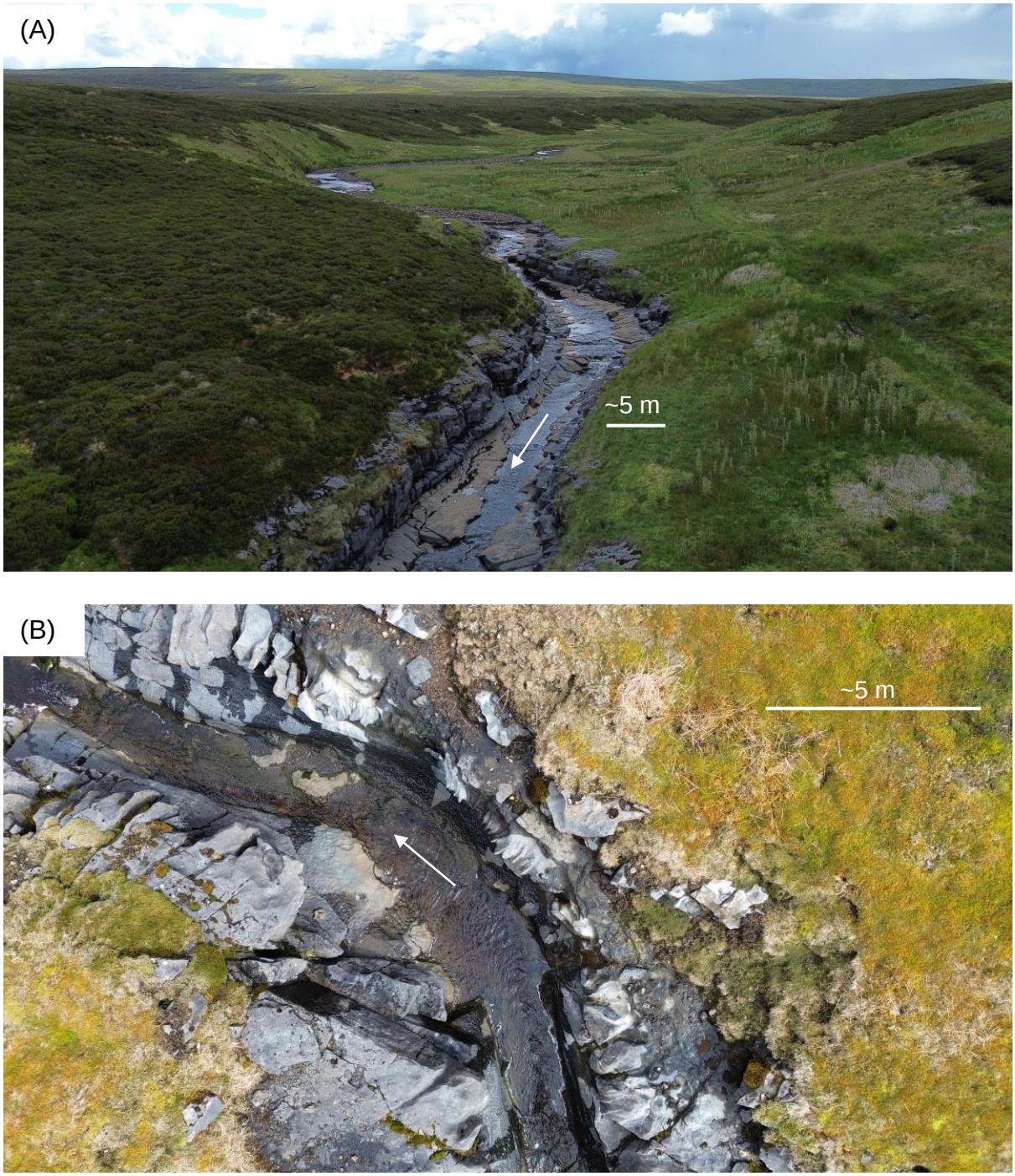

Figure 6: (A) Oblique drone photograph of part of the Trout Beck bedrock study reach, (B) planform drone photograph of a bedrock section of the Rough Sike study

reach. Drone photographs taken by Dr Elizabeth Dingle. White arrow indicates direction of flow. Approximate scale (~5 m) indicated by the white line.

Upstream and downstream of the main bedrock sections at Trout Beck and Rough Sike, the rivers are primarily alluvial, with only small, isolated areas of exposed bedrock observable (< 10 m). The surrounding land cover is mainly blanket peat (90% coverage, 1-2 m deep) due to the clay-rich deposits over the majority of the underlying bedrock providing an impermeable surface (Evans *et al.*, 1999). The pH within the river channels at Moor House NNR is on average 6.2, however this varies significantly with changes in discharge (ECN, 2024).

Convective rainfall in the summer and snow melt in the winter results in relatively large annual totals of precipitation at Moor House (mean total annual rainfall between 1994 - 1997 of 2071 mm, Evans *et al.*, 1999). Evans et al. (1999) describe the climate at Moor House as ‘sub-arctic oceanic’. Figure 7 highlights the annual variability in average daily river level from the Environment Agency gauging station at Trout Beck, with a mean daily average level of 0.22 m (~2013 – 2024). Sharma (2016) estimated the maximum, mean and minimum discharge values between 1991-2015, resulting in values of 14.2, 0.61, and 0.01 $m^3 s^{-1}$ in turn. Both Trout Beck and Rough Sike have a flashy hydrological regime (Evans *et al.*, 1999; Smith, 2004). The drainage area calculated above the Trout Beck gauging station is 11.5 km^2; the corresponding discharges for the Trout Beck and Rough Sike study reaches will be expected to be lower than the calculated discharges for the Trout Beck gauging station due to the smaller drainage areas (8.3 and 1.2 km^2 respectively) (Sharma, 2016).

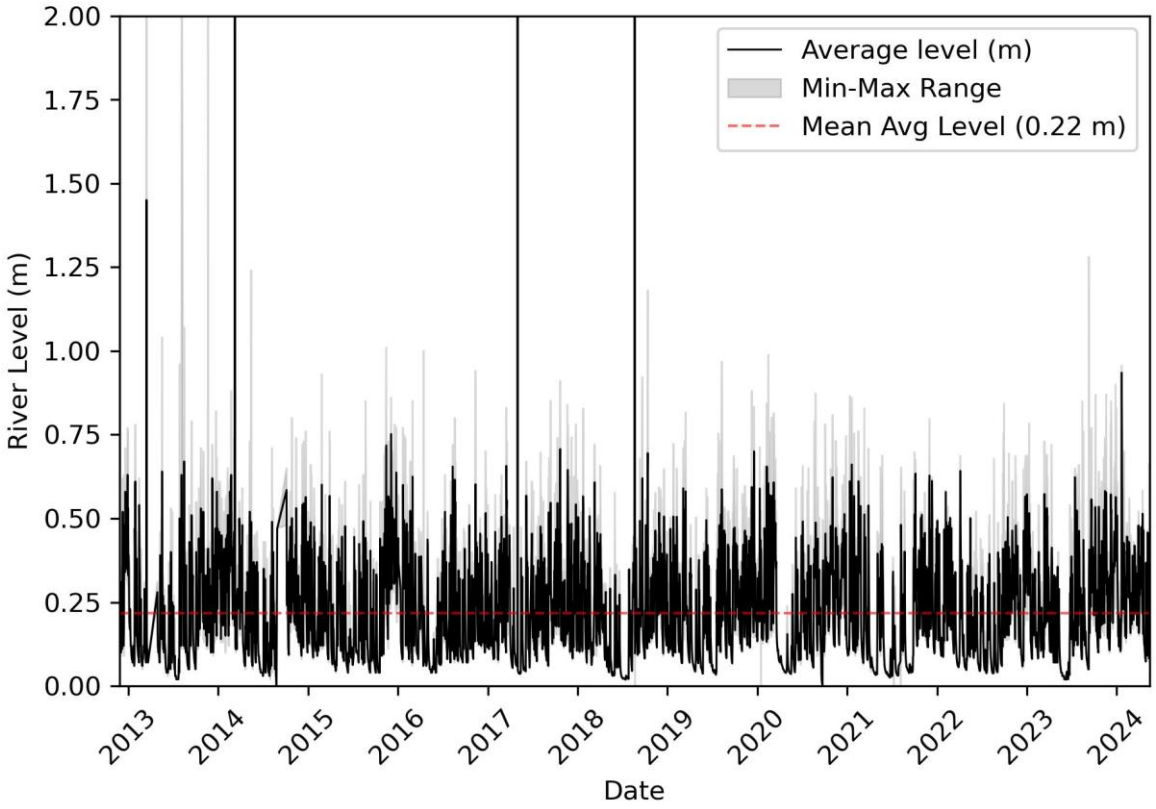

Figure 7: Average daily river level (m) from the Trout Beck River gauging station (EA location F3509). River level constrained to 2 m; some values may be truncated. Data downloaded from: https://riverlevels.uk/trout-beck-moorhouse.

2.2. Geology of Trout Beck and Rough Sike

The simplified bedrock geology of the Trout Beck and Rough Sike drainage basins can be viewed in Figure 8 to provide context for the spatial distribution of observed scalloping. The geological group will be investigated as a potential controlling factor on the development of scalloping. The exposed bedrock section at the most upstream point of the Trout Beck study reach is part of the Tynebottom Limestone Cyclothem (Figure 9), where the bedrock is dark fossiliferous limestone (compound corals such as *Lithostrotion* and *Lonsdaleia* are common (Johnson and Dunham, 1963)). Above the Tynebottom Limestone is a layer of shales (Tynebottom Plate), these shales can be observed just upstream of the Trout Beck study reach on the bank of the river and are notable sources of sediment. The Tynebottom Limestone Cyclothem extends from the most upstream section of the Trout Beck study reach, above the primary knickpoint and upstream for approximately 150 m. The rest of the

Trout Beck study reach downstream of the knickpoint is the Alston Formation, formed typically of cyclothymic sequences of “bioclastic limestones, sandstones, mudstones, siltstones and rare coals” (BGS, 2024: 1).

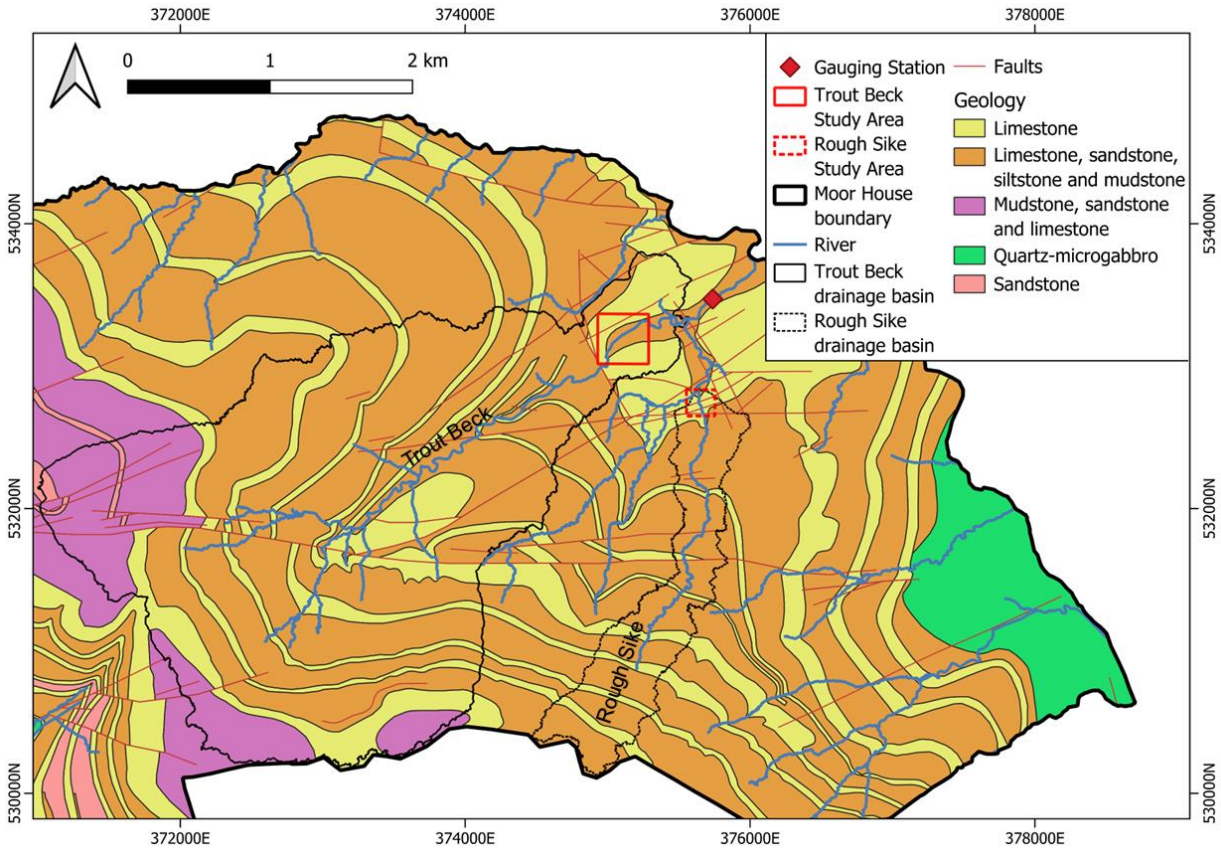

Figure 8: Simplified bedrock geology (1:50 000) of the Trout Beck and Rough Sike drainage basins at Moor House. Geological Map Data BSG © UKRI 2024. British National Grid – Grid square: NY.

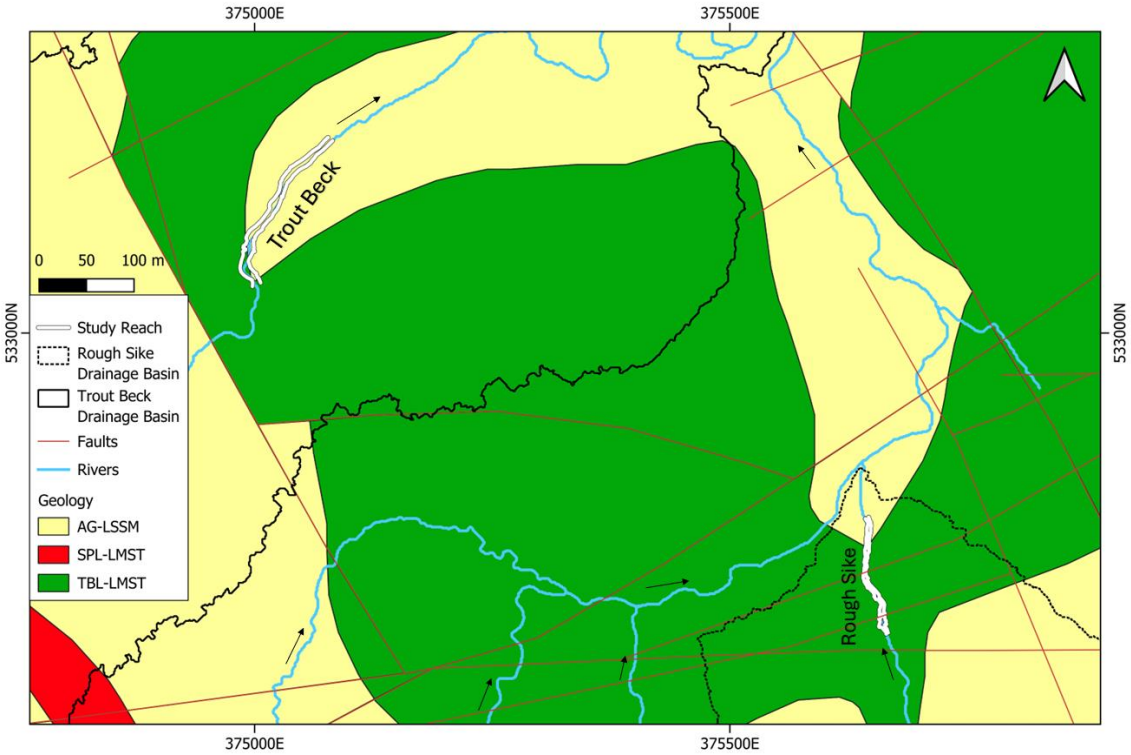

Figure 9: Detailed geology (1:50 000) of the Trout Beck and Rough Sike study reaches. AG-LSSM: Alston Formation (Limestone, sandstone, siltstone, mudstone); SPL-LMST: Single Post Limestone (Limestone); TBL-LMST: Tynebottom Limestone (Limestone). Geological Map Data BSG © UKRI 2024. British National Grid – Grid square: NY. Flow direction of the rivers indicated by the black arrows to the left of the channels.

The exposed bedrock at Rough Sike is primarily part of the Tynebottom limestone member and the most downstream part of the bedrock study reach leads into the Alston formation, comprised of limestone, sandstone siltstone and mudstone. The Alston formation continues downstream, where the bedrock reaches leads into a more alluvial, meandering channel. Upstream of the bedrock study reach, the Tynebottom limestone member continues, until it changes also to the Alston formation.

2.3. Trout Beck and Rough Sike channel morphology and features

The most upstream section of the Trout Beck study reach is semi-alluvial, with large coarse grained sediment bars, leading into a bedrock section just upstream of the knickpoint. The knickpoint is approximately 3 m in height and leads into the main

bedrock gorge section. The bedrock gorge eventually leads into a bedrock-constrained section with pool and boulder-riffle sequences, which in turn leads into an alluvial reach further downstream where the study site finishes. The average median grain size across the bedrock section of Trout Beck is 63 mm, as measured by Sharma (2016). No grain size data is available for the Rough Sike reach. Potholes are observed on some of the bedrock benches at Trout Beck (Figure 10a), supporting the idea that abrasion occurs frequently within the bedrock section of the channel; no significant potholes are present on the bedrock surfaces at Rough Sike. Both Trout Beck and Rough Sike have evidence of vertical ridges and decantation runnels (on the channel boundary walls), caused by dissolution by runoff from the adjacent peat (Figure 10b, c).

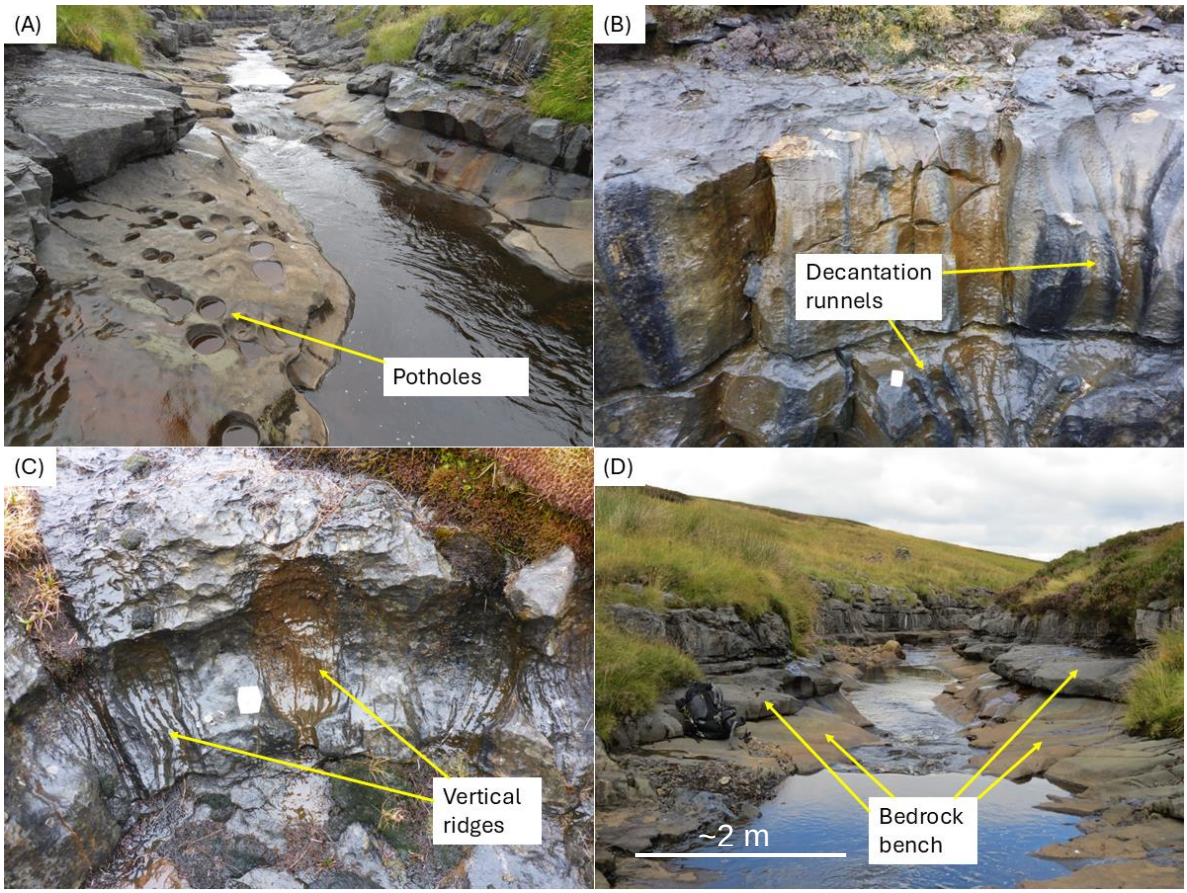

Figure 10: (A) Potholes at Trout Beck (potholes of approximately 10 cm diameter) (B) decantation runnels at Rough Sike, and (C) vertical ridges at Rough Sike, and (D) bedrock benches at Trout Beck. The white cube is 3 cm x 3 cm x 3 cm.

Closely upstream of the Rough Sike study reach is a relatively flat, low energy section with some alluvium present, leading into a knickpoint where the bedrock

study site begins. Below the knickpoint is a pool, leading toward another small knickpoint and the beginning of the main bedrock gorge section. This gorge section includes some large (~1 m^3+) boulders alongside smaller knickpoints. Downstream of the gorge is also several small knickpoints, finally leading to a pool and the start of a meandering alluvial reach where Rough Sike continues and joins with Trout Beck.

The channel width of the bedrock study sites at Trout Beck and Rough Sike range from approximately 5.5 – 7 m, and 2.4 – 6 m respectively. The maximum height of the channels at Trout Beck and Rough Sike are approximately 3 m and 1.5 m respectively. Bedrock benches (Figure 10) are observed along most of the bedrock study reaches.

3. Methodology

The purpose of this methodology section is to outline the process for investigating scallop distribution in free-surface river channels, evaluating morphological factors influencing their distribution and microtopography, and analysing scallop lengths and orientations. The methodology will firstly detail the process of evaluating the spatial distribution of scallops, linking their distribution to the local geology and elevation profiles of the channels. Then, approach used to compare and evaluate the length of the scallops at Trout Beck and Rough Sike will be introduced. Following this, the process for analysing the relationship between scallop length and height above the low water surface in the channels will be explained. This is followed by the analysis used to investigate the statistical distribution of the scallop length measurements from each site. Lastly, the methodology will cover the steps to test the relationship between the scallop orientation and position within the channel, alongside the approach for investigating the modality of the scallop orientation distributions.

3.1. What is the spatial distribution of scallops at Trout Beck and Rough Sike?

Scallops observed within the study reaches of Trout Beck and Rough Sike were grouped into contiguous assemblages (sites). These sites were then mapped using a planform, orthomosaic image of the study reaches, allowing the scallop distributions to be related to channel features. To identify any evidence of scalloping outside of the main study sites, walkover surveys approximately 1 km upstream and downstream of the study sites were conducted. Only the presence of scalloping was recorded, with no measurements of specific morphological features, such as scallop length or height above the channel, being taken. Identifying if scalloping occurs outside of the main study reaches will help to determine whether the processes or geology within the main study regions are key factors influencing the development of scallops.

To provide broader context, the drainage areas and elevation profiles of the two study rivers were created using the 2021, 1 m National Lidar Programme DTM. Firstly, the ‘Fill Sinks (Wang & Liu)’ tool from SAGA was applied. Secondly, the ‘Strahler Order terrain analysis’ tool was applied to delineate the rivers. Then, the ‘Channel network and drainage basins’ tool was applied to classify the river network.

Finally, a point shapefile was created at the location above which the drainage area above is to be calculated for Trout Beck and Rough Sike; then the ‘upslope area’ tool was applied, delineating the drainage area. The elevation profiles for the Trout Beck and Rough Sike rivers were created by using the ‘points along geometry’ tool (every 1 m) for the extracted sample sections of the two rivers. Once the points were created, the raster analysis ‘sample raster values’ tool was applied, retrieving the elevation data from the DEM for every point along the river (every 1 m). The elevation profiles of Trout Beck and Rough Sike provide the opportunity to link the locations of notable scalloping to changes in elevation within the surrounding area. The location of any observed scalloping was also linked to the underlying bedrock geology, derived from the 1:50 000 geological data from the British Geological Survey.

3.2. To what extent do scallop length vary between rivers and height within a river?

Within the bedrock reaches of Rough Sike and Trout Beck, ground-based photographs were taken of each prominent scallop assemblage. Each photograph included a reference scale and contextual information on the approximate flow direction of the river at each site (Figure 11). The scallop length is measured as the longest distance between the scallop crests in the estimated direction of flow (Figure 12). All identifiable directional scallops were sampled, regardless of their classification (e.g. 3-dimensional, intermediate) or ‘completeness’ as suggested by Springer and Hall (2020). The data were analysed in QGIS, where line shapefile attributes were created for the length of individual scallops measured in the site photographs. Initial scallop length attributes were transformed into scaled lengths (centimetres) using the reference scale in each photograph. This conversion factor was applied to each of the nondimensional scallop length values to determine their length in centimetres. Checkley and Faulkner (2014) previously used a similar approach to measure the length of scallops, however they used printed photographs and manually measured the scallop lengths.

Figure 11: An example of a scalloped site. The arrows indicate the direction of the scallops and length of the arrow indicates the scallop length. The arrow at the bottom of the photograph over the water approximates the primary flow direction of the river at this location, this was identified visually from the photographs in context with the SfM orthomosaic image. The line on the ruler allows the dimensionless length values

to be related to metric units. The rule for scale is 0.62 m. Photographs taken with an iPhone 12 Pro, 4032 x 3024 pixels.

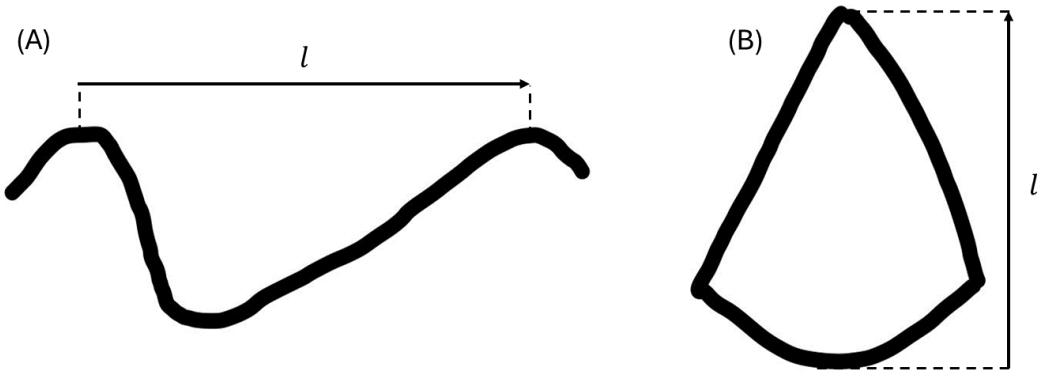

Figure 12: The length of an idealised scallop in an (A) cross-sectional, and (B) planform view. Not to scale.

This method of photographing the scallops to measure the scallop length is quick and simple to implement in the field. This is valuable for this study site as the scallops are often only accessible by wading in the active flow of the channel, limiting the use of more complex approaches such as Structure from Motion (Cooper, 2018; Droin, 2021) and 3D terrestrial laser scanning (Lundberg *et al.*, 2017) which have been previously used to measure the length of scallops in finer detail. Another method that has been used to measure scallop length in the field is simply using a ruler and manually measuring each scallop (Hall, 2019; Springer and Wohl, 2002), however for large samples this method would be time consuming. Distortion due to the perspective of the photograph could cause inaccuracy in the measurements, therefore images were taken orthogonal to the scalloped surface, and multiple photographs were taken if the assemblage extended over a large area. The data from the individual photographs are classed as sub-samples, which collate together to form a site (Figure 13). In cases where the sub-sample photographs overlapped and included some of the same scallops, care was taken to ensure that each scallop was sampled only once, thereby preventing the inclusion of duplicate scallops. Not all sites consist of sub-samples as some only required one photograph.

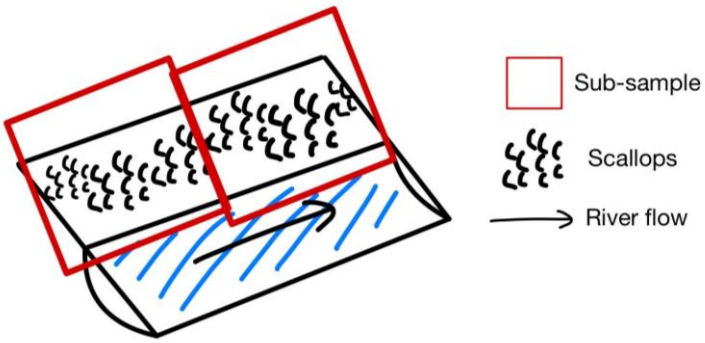

Figure 13: An example of sub-sample photograph extents for sampling of a scallop assemblage on a bedrock bench next to active flow in the channel. In this example, two sub-samples are taken to cover a contiguous scallop assemblage, or scallop 'site'.

To test for inaccuracies caused by measuring scallop lengths from a photograph with an included scale, a 1 cm length at the upper and lower section of the scale was compared to the average of the whole length to determine the approximate deviation across the image. Table 1 shows the variability in the 1 cm sample in six photographs, showing an average deviation between -10.0% and +13.7% when compared to the 1 cm value averaged from the reference scale included in the photograph. There is a maximum positive deviation of +22.1% and a minimum negative deviation of -15.2% in these samples. For further analysis the scallop length data will be rounded to the nearest 0.2 cm.

Table 2: Variability in a 1 cm sample from the upper and lower sections of the reference scale included in a random sample of photographs used to measure scallop length.

Random sample number	**Lower sample difference from the averaged reference scale (%)**	**Upper sample difference from the averaged reference scale (%)**
1	-2.1	8.8
2	-15.2	22.1
3	-14.0	18.3
4	-10.2	10.3
5	-9.7	11.8

Random sample number	Lower sample difference from the averaged reference scale (%)	Upper sample difference from the averaged reference scale (%)
6	-8.7	11.1
Mean	-10.0	13.7

Gale (1984) and Woodward and Sasowsky (2009) suggest a minimum of 25 scallop length measurements for each assemblage, however Hall (2019) argues that a minimum of 30 should be used as smaller sample sizes cause greatly increased variability and range in calculated Sauter mean lengths. Hall (2019) also states that inconsistent sample sizes may cause issues when comparing sites due to variability in the range of error of Sauter mean lengths. This study analysed all easily identifiable directional scallops within each assemblage and therefore has variable sample sizes. The scallop length sample sizes for each location at Rough Sike and Trout Beck ranged from 35-879, and 30-265 respectively, and with mean sample sizes of 260 and 108 respectively. Therefore, despite the variability in sample size, the large mean sample sizes in this study minimise error caused by the inconsistent sample sizes and even the smallest samples exceed the minimum data requirements specified by previous authors.

To test whether Trout Beck and Rough Sike have statistically different arithmetic mean scallop length values, a Welch's T-test (for samples with unequal variances) was performed. The null hypothesis claims that there is no significant difference between the arithmetic mean scallop length at Trout Beck and Rough Sike. A significance level of 0.05 was chosen.

To identify possible relationships between the scallop morphology and height of the scalloped surface within the channel, the height range for the scalloped sites were measured at both Trout Beck and Rough Sike. The height was calculated as the vertical distance above the water surface on the day of data collection (8th July 2024), which was a day of low flow in the channel (Figure 14). The distance above the low flow water surface was chosen over the channel bed surface as the channel bed topography is locally more variable (e.g., deep pools). The water surface varies with stage; however, all height measurements were taken on one day. The Trout

Beck at Moor House gauging station recorded an average daily river level of 0.08 m on 8th July 2024, which is much lower than the mean average river level of 0.22 m as highlighted in Figure 7. The lower (H2) and upper (H1) boundary of the scalloped bedrock surface was measured, providing a range of heights which the scalloped surface extends across (Figure 14). For the analysis relating the height of the scalloped site to the Sauter mean scallop length, the mean height ($\overline{H}$) of the range was used.

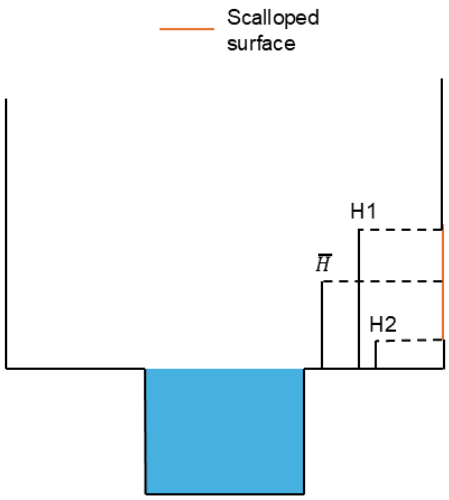

Figure 14: An example cross-section highlighting the height above the water surface measurements. The maximum (H1), minimum (H2), and mean ($\overline{H}$) height of the scalloped site above the low water surface is identified.

To test the significance of relationship between the Sauter mean scallop length and mean height of the scalloped surface above the water surface, Ordinary Least Squares (OLS) regression analysis, including a T-test in regression was applied (Seabold and Perktold, 2010). This tests if the gradient of the linear relationship is different from zero, with the null hypothesis stating that coefficient of the relationship is zero, therefore the mean height of the scalloped surface above the water has no influence on the Sauter mean scallop length of the scallop group. The alternative hypothesis is the opposite, where there is a significant relationship present.

3.3. How does scallop length and abundance relate to stream power?

The relationship between the Sauter mean length and abundance of scallops and its location in higher or lower energy sections of the channel was explored by analysing the USP. Dingle et al. (in review) sampled six cross-sections at Trout Beck, and five

at Rough Sike within the study reach, calculating USP for each cross-section. For each assemblage, Sauter mean scallop length values and the number of sampled scallops were linked to their corresponding USP values based on the nearest measured location. The Pearson's correlation coefficient and a linear regression model was used to assess the significance and relationship between USP and Sauter mean scallop length and abundance. The number of sampled scallops (abundance) is used as an indicator of how favourable the location is for the development and preservation of scallops.

3.4. What is the statistical distribution of scallop lengths?

Once the scallop length data had been grouped into sites, the statistical distribution of the scallop length values can be tested to determine if the data follows the expected log-normal distribution suggested in the literature from cave scallop length data (Charlton, 2003; Faulkner, 2013; Ford and Williams, 2007). Understanding if the surface stream scallops also follow the log-normal distribution expected in cave scallop assemblages will provide insight into whether cave and surface stream scallops are similar in their development. If the scallops do not follow this expected log-normal distribution, it could be suggested that other processes present only surface stream systems may be altering the distribution of scallop lengths within an assemblage.

The Shapiro-Wilk test is used to determine the normality of a dataset, resulting in two key statistics, the Shapiro-Wilk Statistic and the P-value. The closer the Shapiro-Wilk Statistic is to one, the more normally the data is distributed. The P-value refers to the probability of the null hypothesis being true, which in this application is that the data is from a normally distributed population ($\alpha = 0.05$). If the P-value is greater than 0.05, the data is classified as normally distributed, if the P-value is less than 0.05, the data is not normally distributed. To test for the normality of the data, the Shapiro-Wilk test was applied to all scallop length datasets for each site across Trout Beck and Rough Sike. The Shapiro-Wilk test was also rerun once a $\log_{10}(x)$ transformation had been applied to the original scallop length data to test if the original data is log-normally distributed.

Kernel Density Estimation (KDE) creates a probability density function which smooths the data and provides a visual interpretation of the density of the dataset.

This method of visual analysis is not influenced by the bin size like histograms are (Scikit Learn, 2024). The number of peaks detected within the upper and lower 5th percentile of the scallop length and Log_{10} transformed scallop length data distribution are also calculated. Alongside this, the number of peaks above the 50th percentile of the KDE values was calculated, identifying the main peaks in the dataset. The number of peaks in the KDE provides an estimation of the modality of the data, where a unimodal dataset has one peak, a bimodal dataset has two peaks, and a multimodal dataset has three or more peaks.

3.5. How are scallops oriented and what is their statistical distribution?

Scallops typically have a cross-sectional morphology characterised by a steep downward face (upstream end) and a more gradual face sloping back up in the direction of flow (Figure 2). The orientation of the scallops at Trout Beck and Rough Sike were determined through visual analysis of photographs. Automated scallop orientation approaches such as those by Droin (2021) can quickly classify scallop orientation, however, this approach requires a Structure from Motion (SfM) model of the surface and the results are variable in their accuracy. The scallop orientations were often measured from sloping or curved surfaces, therefore the 2D representation used in this analysis may result in some inaccuracies in the exact scallop orientation. Figure 11 shows an example site with arrows indicating the orientations of the scallops. The approximate local downstream flow direction was also identified at each sub-sample.

The scallop orientations are normalised relative to two main directions: the circular mean orientation (mean of angular data that accounts for the data wrapping around a circle, e.g., 0° and 360° are equal), and the approximate local primary flow direction of the river. This firstly involves the conversion of the raw orientation data from degrees into radians. The scallop orientations are then normalised by subtracting either the downstream flow orientation or the circular mean orientation (depending on the reference) from the raw scallop orientations. These adjusted orientations are then normalised by adding 2π radians to ensure the angles are positive, then applying modulo 2π radians to constrain the angles in the range – π to π, and then finally subtracting π to centre the data again. This process results in

scallop orientations normalised relative to either the circular mean direction (θ_C), or scallop orientations normalised relative to the approximate downstream flow direction (θ_F).

To analyse the distribution of scallop orientations, the θ_C values are used. Kernel Density Estimate (KDE) plots are created for each site by grouping the θ_C values from each sub-sample into the respective sites. The KDE plots are centred around the circular mean of the scallop orientations. Descriptive statistics of the scallop orientation distributions are provided, including the circular standard deviation and range. Peaks in the KDE are also detected, identifying if the distribution of scallop orientations follow a unimodal, bimodal or multimodal distribution. This provides an approximation if the scallops are all oriented in a single primary direction, or if they are preserving flows from two or more primary directions.

To analyse the θ_F values, the circular mean of the normalised scallop orientations ($\overline{\theta_F}$) are calculated for each individual sub-sample. The $\overline{\theta_F}$ values will then be compared across all sites for Trout Beck and Rough Sike, alongside identifying whether they are situated on the left or right bank of the channel. This will identify if the scallop orientations are deviated relative to the downstream flow direction of the channel due to the topography of the channel margins.

3.6. How long does it take for scallops to develop?

Long-term dissolution rates of 0.98 mm yr^{-1} and 0.58 mm yr^{-1} have been reported for Rough Sike and Trout Beck respectively (Dingle *et al., in review*), therefore the approximate formation time of scallops can be estimated using a model that applies a linear dissolution rate uniformly across a surface area. A half ellipsoid will be used as a simple representation of a scallop shape, with a length-to-width ratio of 2:1, and a length-to-depth ratio of 4:1 (Ford and Williams, 2007; Santanatoglia, 2023). The formation period for scallops of length 1 cm, 5 cm, and 20 cm, and 200 cm will be calculated, assuming a constant rate of dissolution overtime. The formation period will be calculated separately for Rough Sike and Trout Beck, due to their differing long-term dissolution rates.

4. Results

4.1. Introduction

The results section aims to present and describe the findings of this study. First, the spatial distribution of the scallops will be identified and linked to the local geology and channel profiles. Next, the scallop length data from Trout Beck and Rough Sike will be analysed and compared, identifying any differences between the morphology of the scallops from each site. The relationship between the scallop length and the height of the scallops above the low water surface in the channel will then be explored. This will be followed by the analysis of the normality and modality of the statistical distributions of scallop length measurements from Trout Beck and Rough Sike, evaluating if the scallop length distributions follow a typical distribution in open river channel environments. Finally, the scallop orientation will be analysed, linking their orientation to the position of the scallops within the channel, then identifying the modality of the statistical distributions.

4.2. What is the spatial distribution of scallops at Trout Beck and Rough Sike?

The Trout Beck study reach is approximately 1280 m^2, with a 460 m^2 of exposed bedrock during low flow conditions, and 140 m^2 of exposed sediment within the channel. At Rough Sike, the study reach is approximately 400 m^2, with approximately 260 m^2 of exposed bedrock during low flow conditions, and 5 m^2 of exposed sediment within the channel. Calculating the average scallop density for each study area by dividing the number of sampled scallops by the exposed bedrock reveals an approximate value of 2.6 scallops per m^2 at Trout Beck, and 47.9 scallops per m^2 at Rough Sike. The percentage sediment coverage of the study reaches for Trout Beck and Rough Sike is approximately 10.9%, and 1.3% respectively.

The elevation profiles of Trout Beck and Rough Sike can be viewed in Figure 15 and Figure 16, alongside the position of the main study reaches. At Trout Beck, no significant scalloping was observed upstream or downstream of the study region. At Rough Sike, scalloping is present upstream of the study reach, with examples of scallops found over 1 km upstream, but no evidence of scalloping was located downstream. The scalloping upstream of the bedrock study reach is primarily

concentrated within the Single Post Limestone (SPL-LMST), situated between the Alston formation both upstream and downstream of this section.

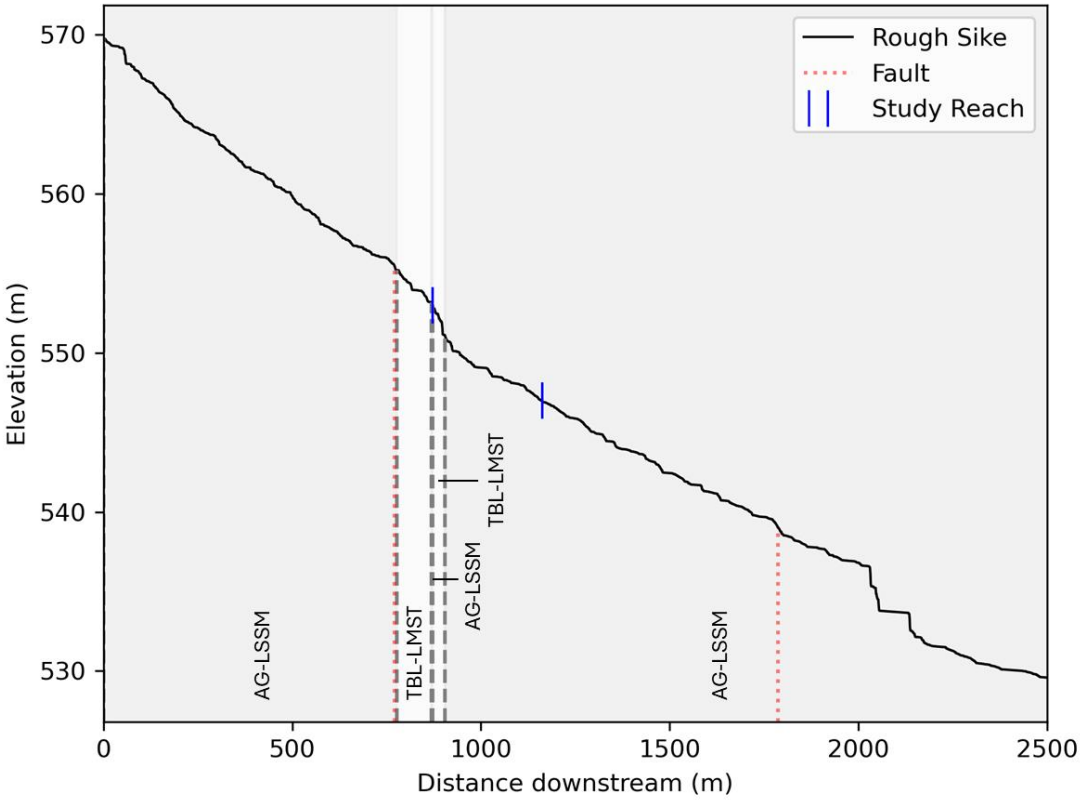

Figure 15: Elevation profile of Trout Beck. Local geology and fault lines indicated, alongside evidence of scalloping within the reach. AG-LSSM: Alston formation - limestone, sandstone, siltstone and mudstone, TBL-LMST: Tynebottom limestone member – limestone. The elevation profile highlights the river elevation

approximately 900 m upstream, and 1,300 m downstream of the study reach. The main study reach is located between the two blue lines.

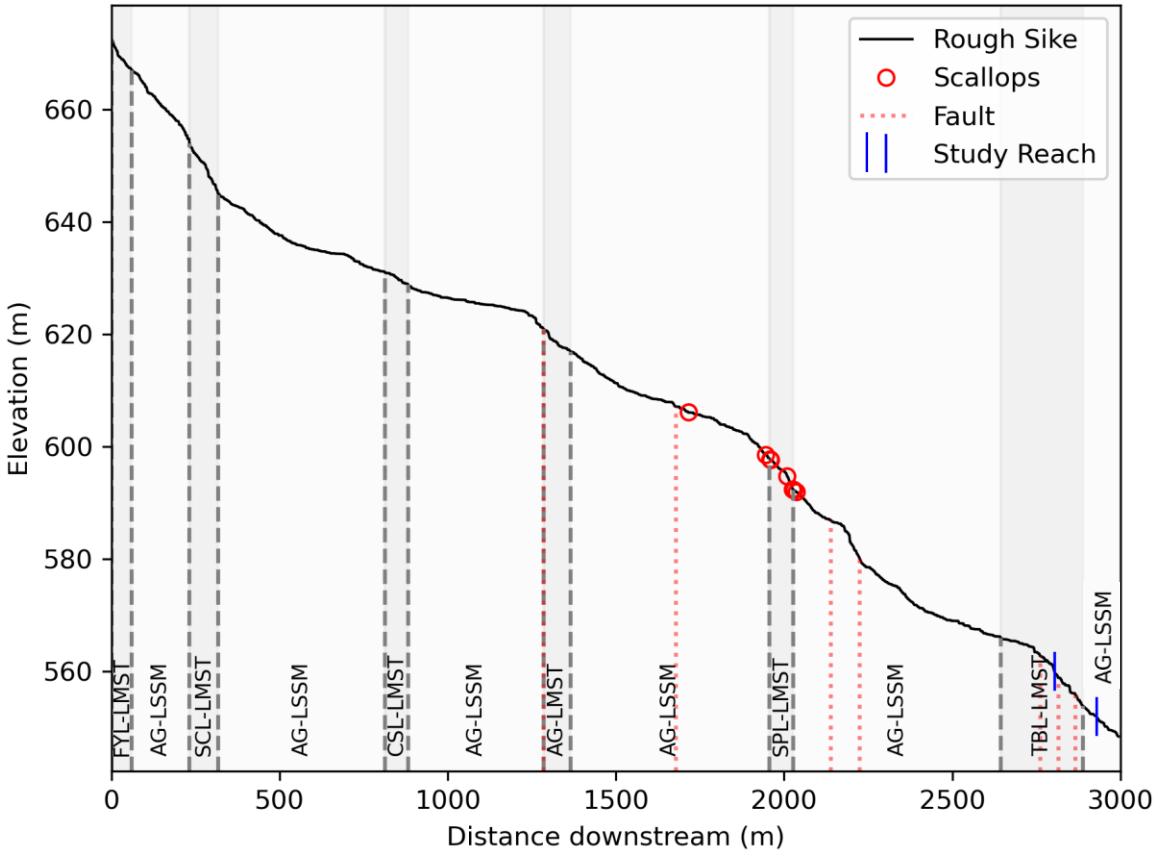

Figure 16: Elevation profile of Rough Sike. Local geology and fault lines indicated, alongside evidence of scalloping within the reach. FYL-LMST: Five yard limestone member – limestone, AG-LSSM: Alston formation - limestone, sandstone, siltstone and mudstone, CSL-LMST: Cockleshell limestone – limestone, AG-LSSM: Alston formation - limestone, sandstone, siltstone and mudstone, AG-LMST: Alston formation – limestone, AG-LSSM: Alston formation - limestone, sandstone, siltstone and mudstone, SPL-LMST: Single post limestone – limestone, AG-LSSM: Alston formation - limestone, sandstone, siltstone and mudstone, TBL-LMST: Tynebottom limestone member – limestone. The elevation profile highlights the river elevation approximately 2,800 m upstream, and 100 m downstream of the study reach. The main study reach is located between the two blue lines.

Extensive scalloping was observed at Rough Sike over the entire study reach, with 12,456 scallops sampled for this study. These were sampled from 48 sites across

the study reach, as can be seen Figure 17. Scallop assemblages at Rough Sike tend to develop more extensively in high energy sections of the channel, such as around knickpoints (e.g., Site 48) or narrow gorge sections. Lower energy sections, such as areas around pools in the channel, tend show less frequent scalloping. For example, sites 14 and 15 are located at a step in the channel, which is followed by a pool downstream with no scalloping observed; this is followed by sites 12 and 13 just downstream of the pool where scalloping is then observed again.

At Trout Beck, scalloping is also present within the study reach, however scallops were observed less frequently (1,185 sampled scallops), and the scallop assemblages were more widely dispersed across the study reach (Figure 18). Despite having large, exposed limestone bedrock surfaces within the study reach (~460 m^2), most of these surfaces are without evidence of extensive scalloping. Instead, evidence of dissolution within the channel is primarily seen in the vertical ridges and decantation runnels located in the upper geological units of the channel walls; these features are developed by dissolution from water draining from the surrounding area into the channel. 11 sites with well-developed scalloping were primarily focused within the main bedrock gorge section of the channel, and just upstream of the primary, large knickpoint.

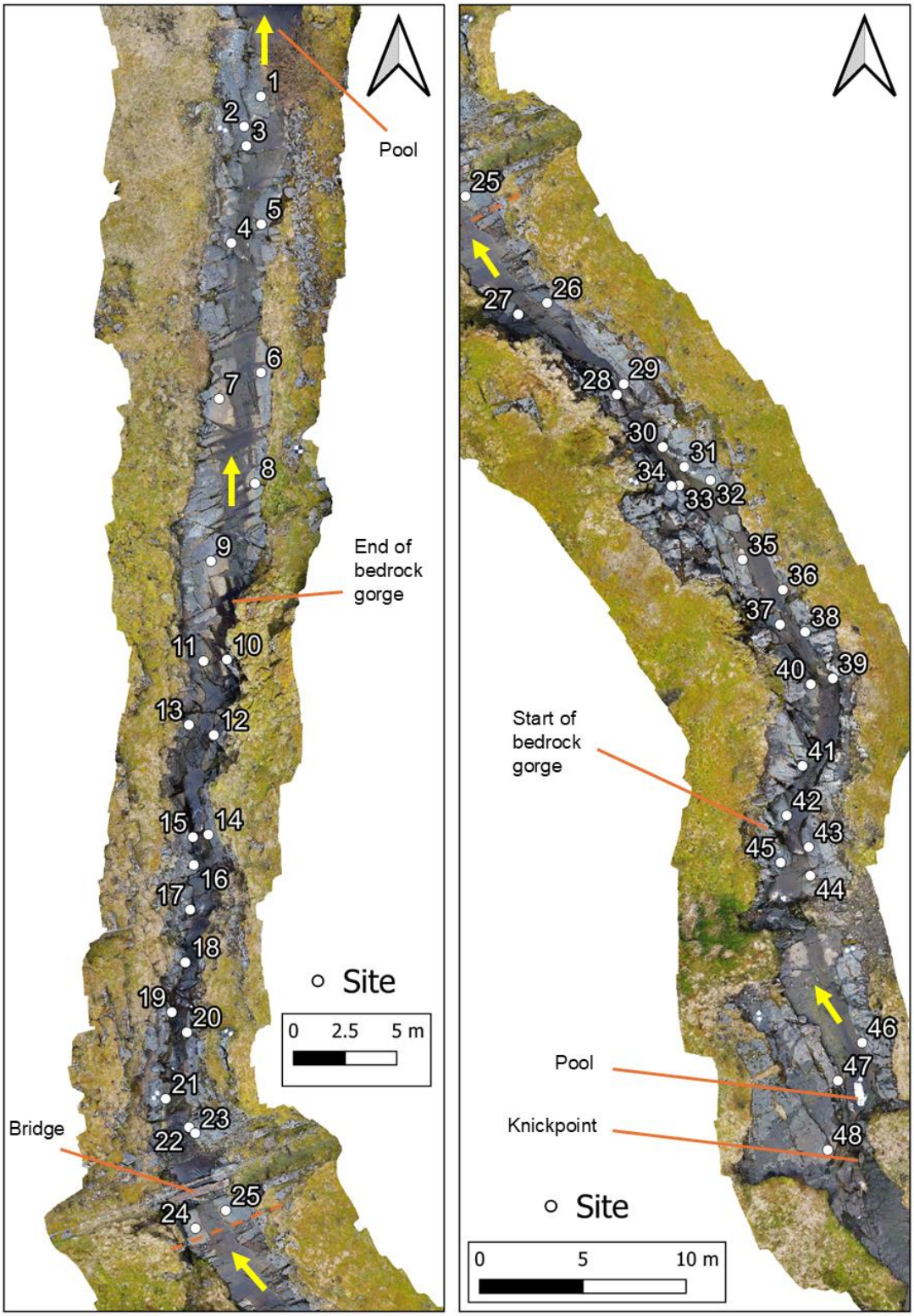

Figure 17: Study reach of Rough Sike, showing the locations of scalloped sample sites and key channel features. The dashed orange line highlights a common location between the continuation of the two sections of the reach. Flow direction indicated by the yellow arrow.

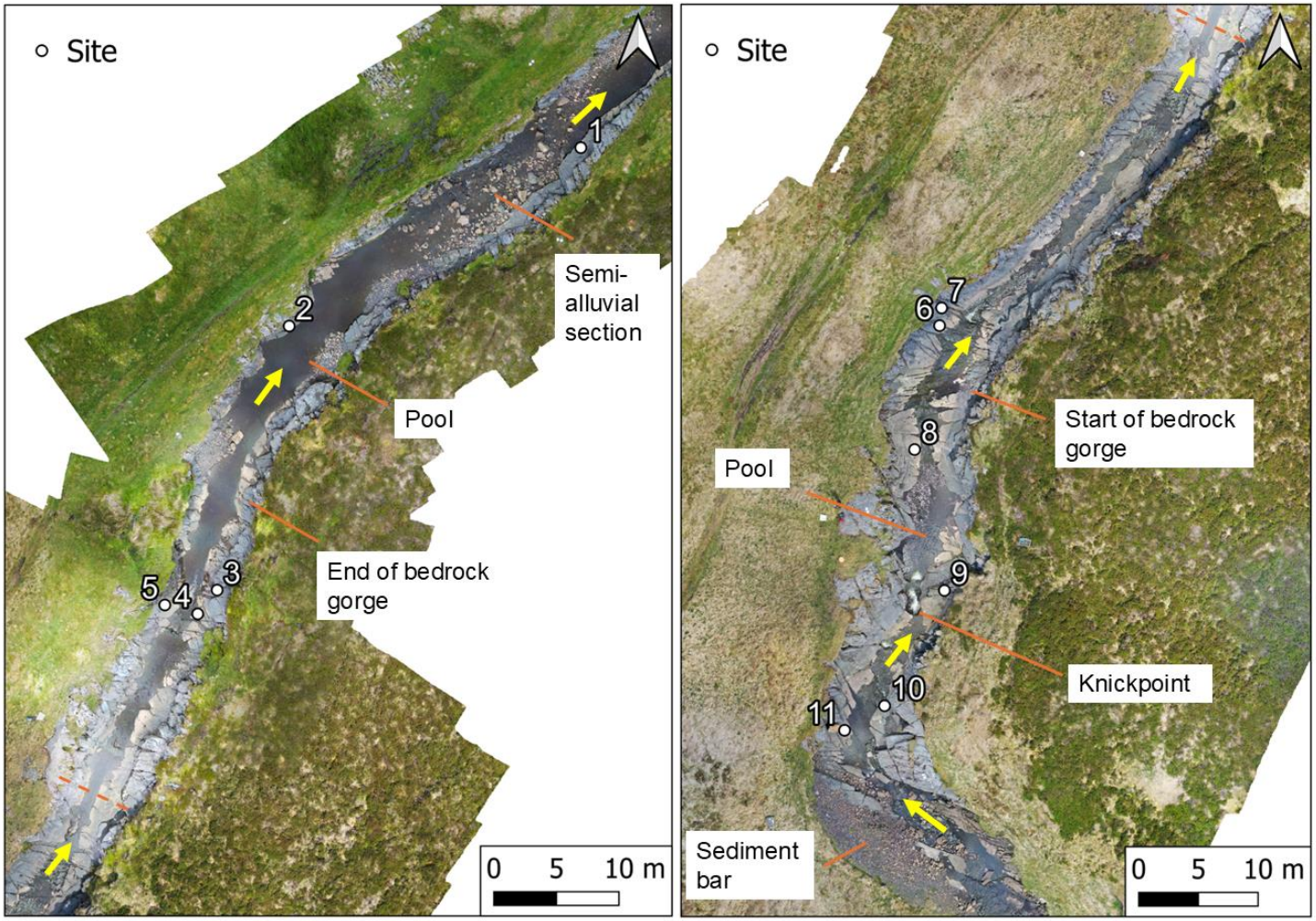

Figure 18: Study reach of Trout Beck, showing the locations of scalloped sample sites and various channel features. The dashed orange line highlights a common location between the two sections of the study reach. Flow direction indicated by the yellow arrow.

4.3. To what extent do scallop length vary between rivers and height within a river?

4.3.1. Scallop length variability between rivers

At Rough Sike, the number of scallops sampled at each site ranged from 38 – 879 with a mean count of 260 (SD = 208.6). At Trout Beck, the number of scallops sampled ranged from 30 – 265, with a mean count of 108 (SD = 73.2). The average across all mean scallop length calculations at Rough Sike was 2.4 cm (SD = 0.9). The average Sauter mean scallop length, which is typically used over the arithmetic mean for scallop analysis, across all sample sites at Rough Sike was 3.1 cm (S_{32} = 0.2). The coefficient of variation (standard deviation/mean) was also calculated as a percentage for both the arithmetic mean and Sauter mean at each sample site. For the arithmetic mean, the average across all sites was 36.9%. The coefficient of variation describes the level of dispersion around the mean of the data, with larger percentages indicating more dispersion.

At Trout Beck, the average across all mean scallop length calculations was 3.6 cm (SD = 1.5), with an average standard deviation of 1.5 across every site. The coefficient of variation for Trout Beck scallop length measurements was 43.6%. The average Sauter mean scallop length at Trout Beck was 5.1 cm (S_{32} = 0.2). A detailed view of the spatial distribution of sites alongside the corresponding Sauter mean scallop length can be seen in Figure 19 for Rough Sike and Figure 20 for Trout Beck. A simplified reach scale view of the channels with the corresponding Sauter mean scallop length values and sediment stores can be seen in Figure 21 and Figure 22. Table 3 shows the summary statistics describing the scallop length datasets for Trout Beck and Rough Sike (Tables A1 and A2 show the individual site calculations).

Table 3: Summary statistics of the Trout Beck and Rough Sike scallop length measurements. Average values calculated from the original site summaries shown in Tables A1 and A2.

	Trout Beck	**Rough Sike**
Average Number of scallops measured	108	260

	Trout Beck	Rough Sike
Average Mean scallop length (cm)	3.6	2.4
Average Standard deviation	1.5	0.9
Average Coefficient of variation (%)	43.6	36.9
Average Sauter mean scallop length (cm)	5.1	3.1
Average Sauter mean standard deviation (S_{32})	0.2	0.2

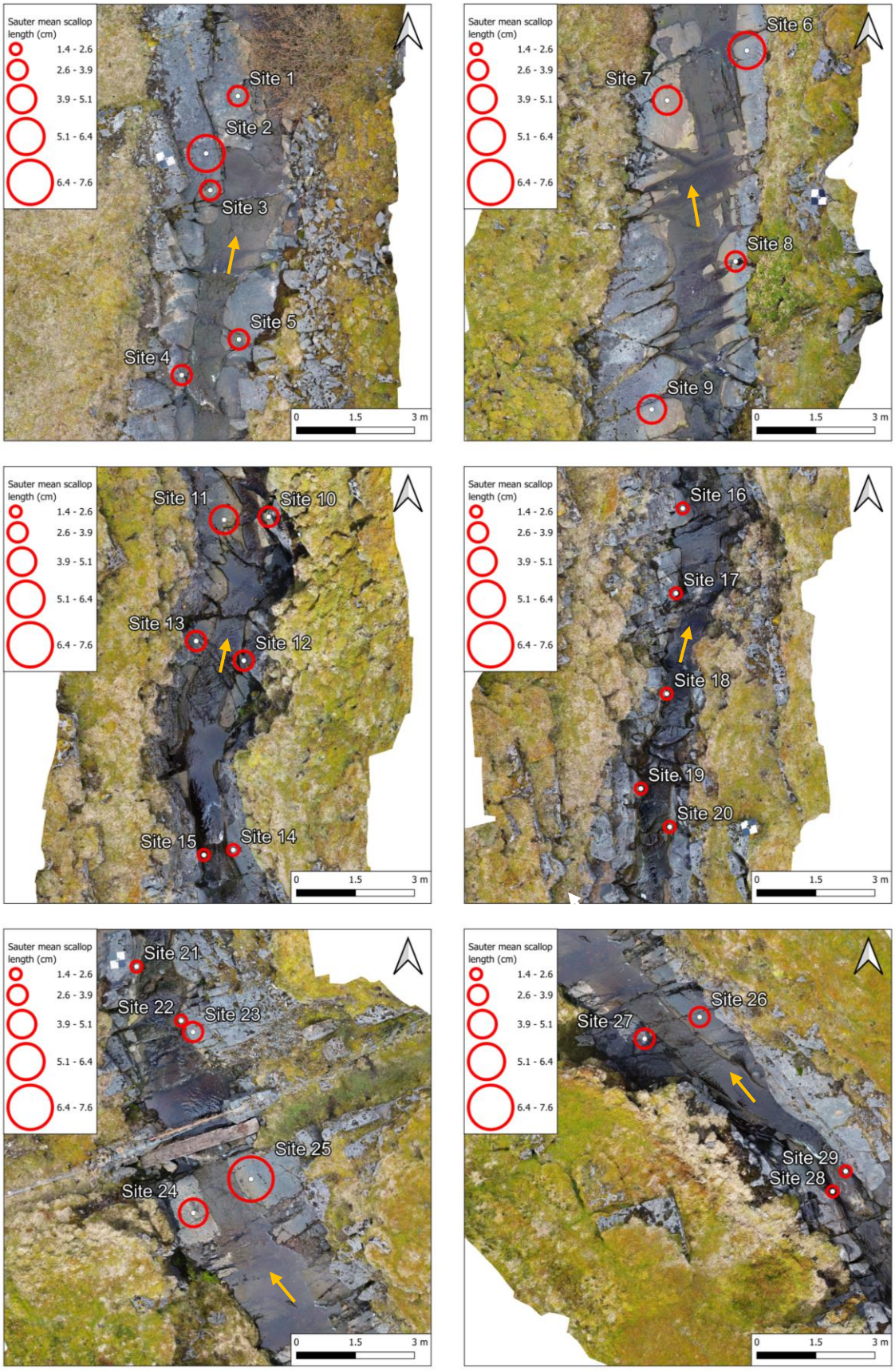
Sauter mean scallop length (cm)
1.4 - 2.6
2.6 - 3.9
3.9 - 5.1
5.1 - 6.4
6.4 - 7.6
Site 1
Site 2
Site 3
Site 4
Site 5
Site 6
Site 7
Site 8
Site 9
Site 10
Site 11
Site 12
Site 13
Site 14
Site 15
Site 16
Site 17
Site 18
Site 19
Site 20
Site 21
Site 22
Site 23
Site 24
Site 25
Site 26
Site 27
Site 28
Site 29
0
1.5
3 m

(continued)

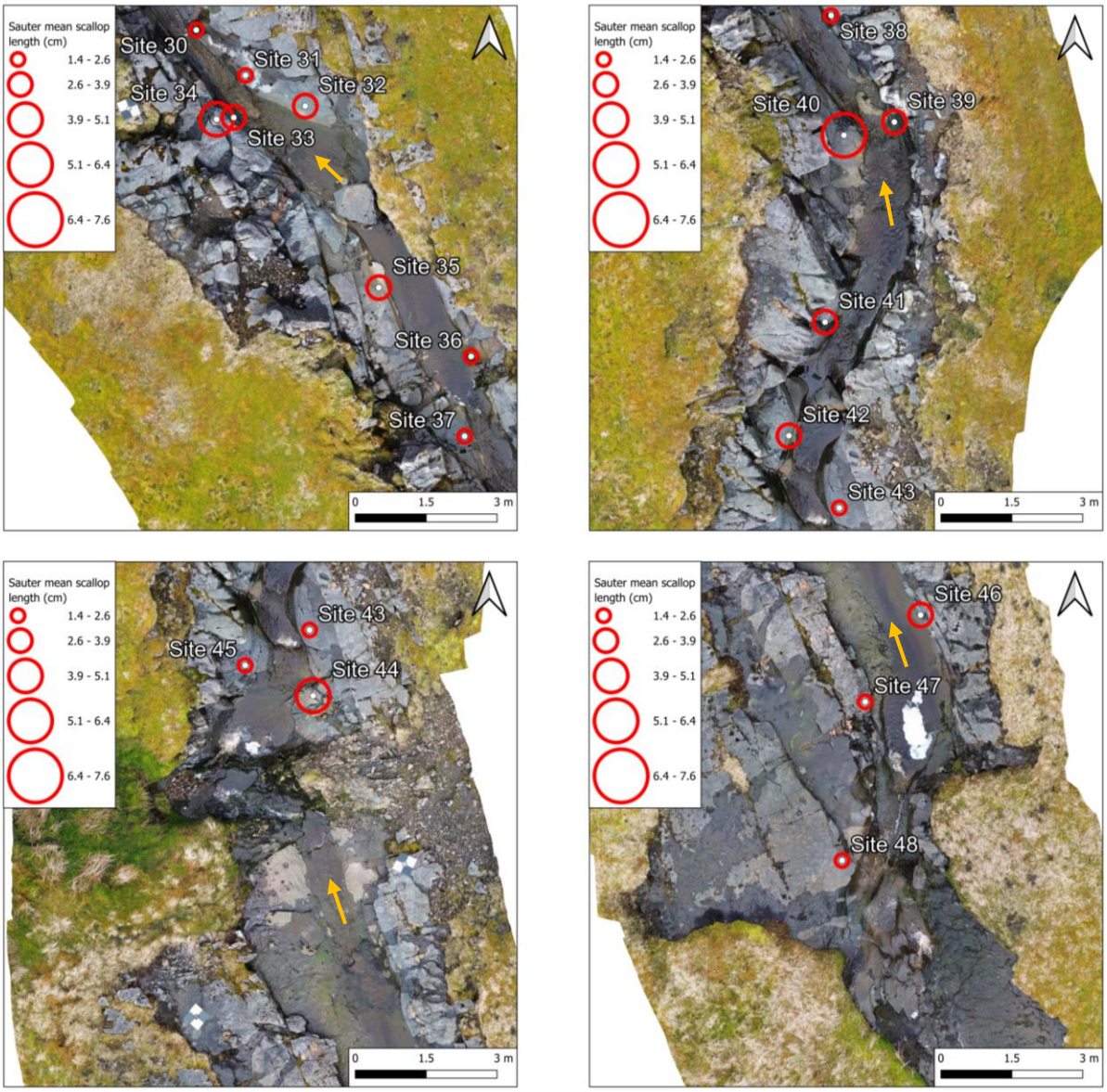

Figure 19: Visualisation of the Sauter mean scallop length (cm) values for each site at Rough Sike. Flow direction is indicated by the yellow arrow.

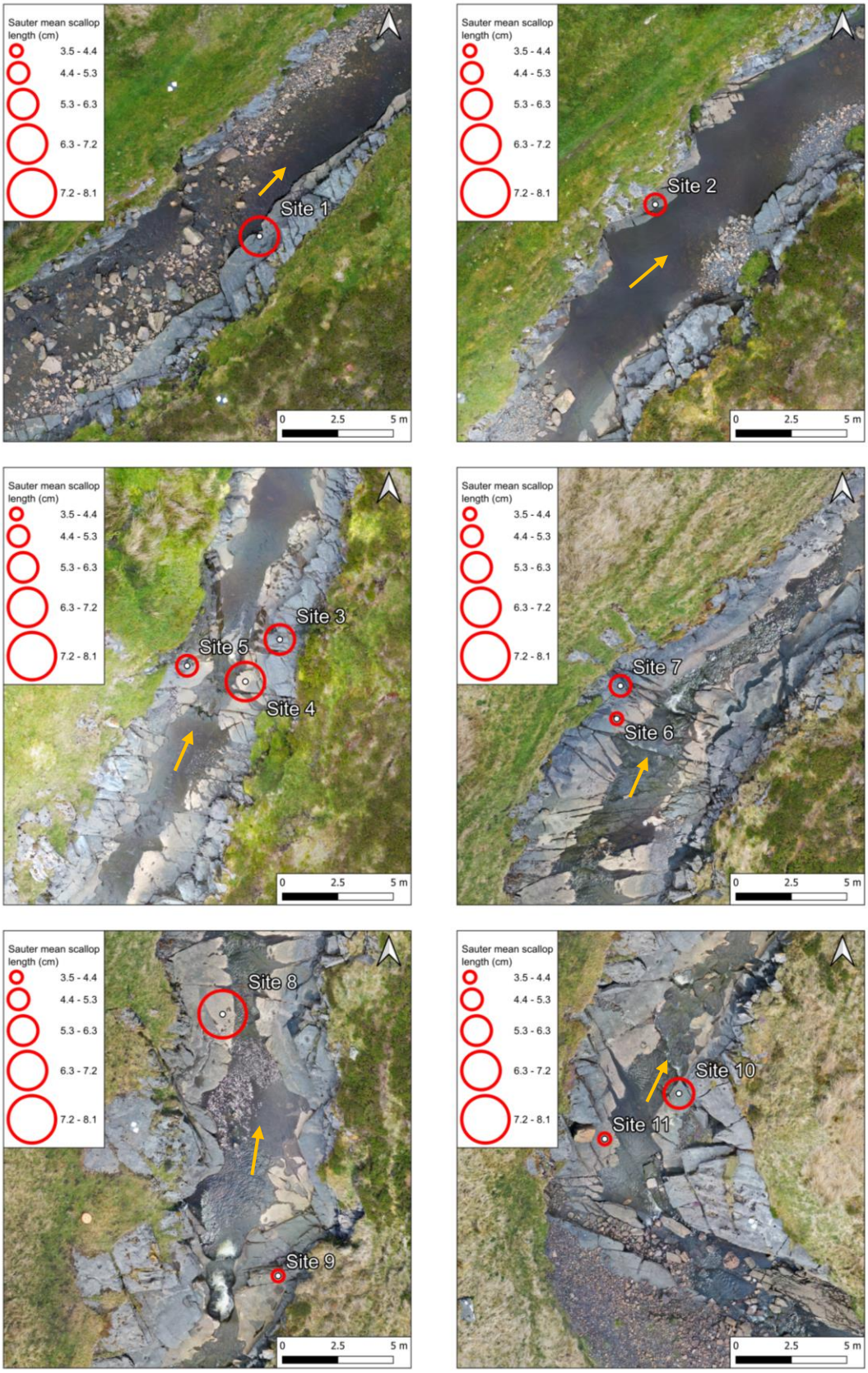

Figure 20: Visualisation of the Sauter mean scallop length (cm) values for each site at Trout Beck.

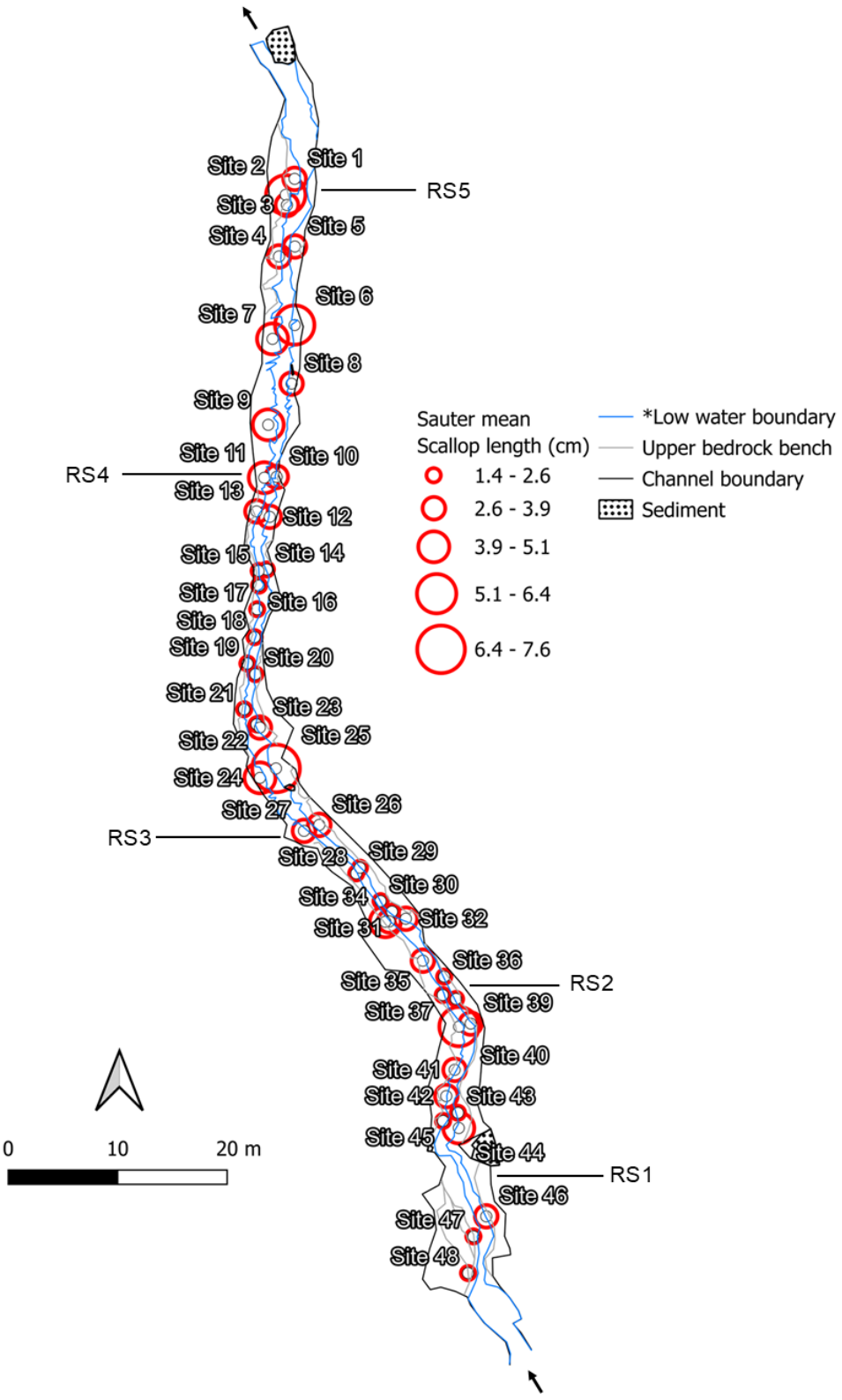

Figure 21: Sketch of Rough Sike identifying the sample sites, sediment within the channel, and the Sauter mean scallop length for each site. RS1-5 refer to the location of cross-sections sampled by Dingle et al. (in review). *The low water level is

the water level identified from the orthomosaic on day with relatively low flow in the channel. Flow direction is indicated by the black arrow.

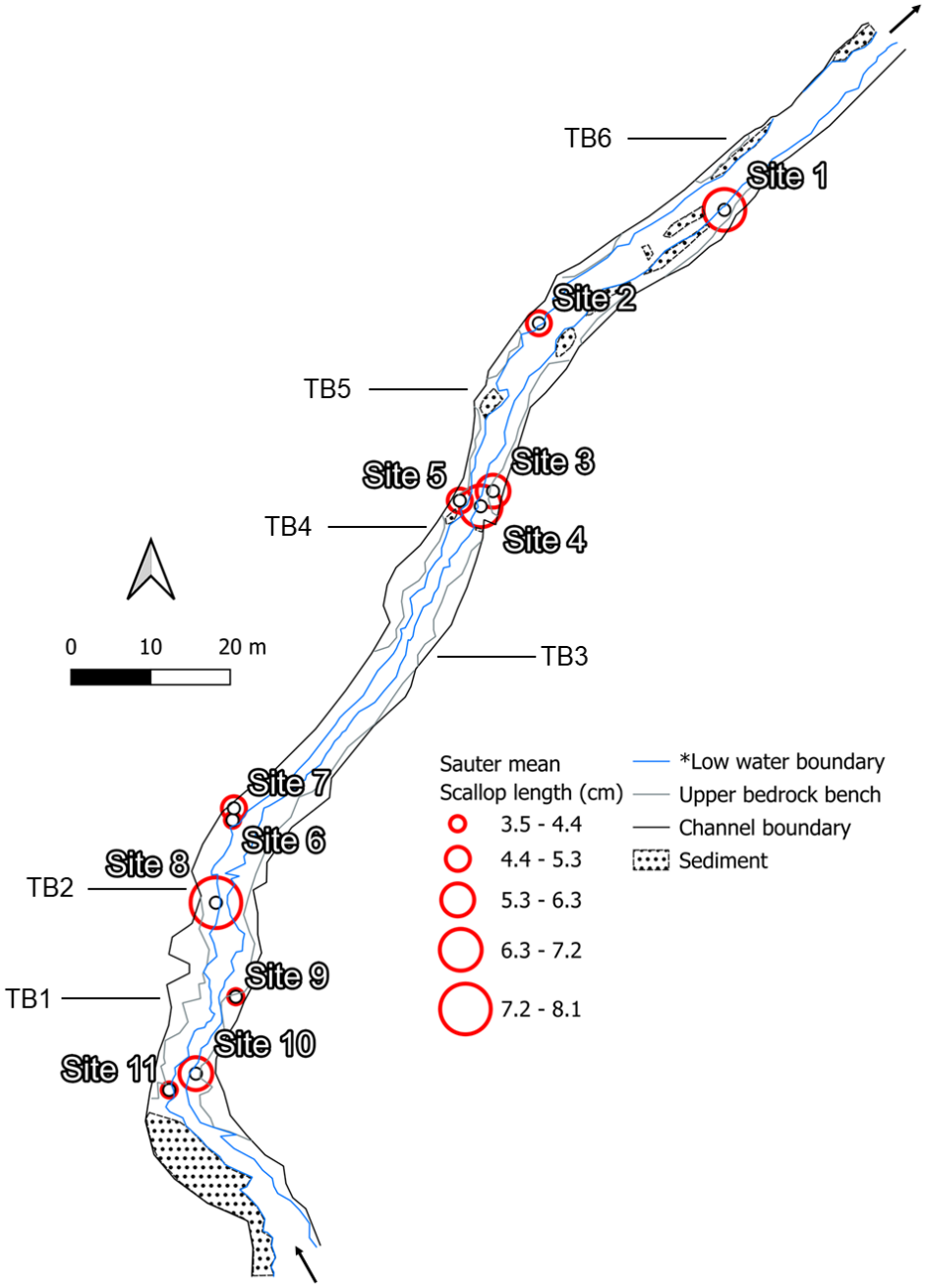

Figure 22: Sketch of Trout Beck identifying the sample sites, sediment within the channel, and the Sauter mean scallop length for each site. RS1-5 refer to the location of cross-sections sampled by Dingle et al. (in review). *The low water level is

the water level identified from the orthomosaic on day with relatively low flow in the channel.

Rough Sike has an overall range in Sauter mean scallop lengths of 6.2 cm compared to 4.6 cm at Trout Beck. However, Rough Sike has a smaller interquartile range (IQR) of 1.3 cm, compared to an IQR of 2.8 cm at Trout Beck. This is shown in the box and whisker plot in Figure 23 showing the tighter data spread at Rough Sike, apart from outliers at 5.5 cm and 7.8 cm. The scallops at Rough Sike ranged in length from 0.4 – 16 cm, and at Trout Beck the range of scallop lengths was 0.6 - 14.4 cm.

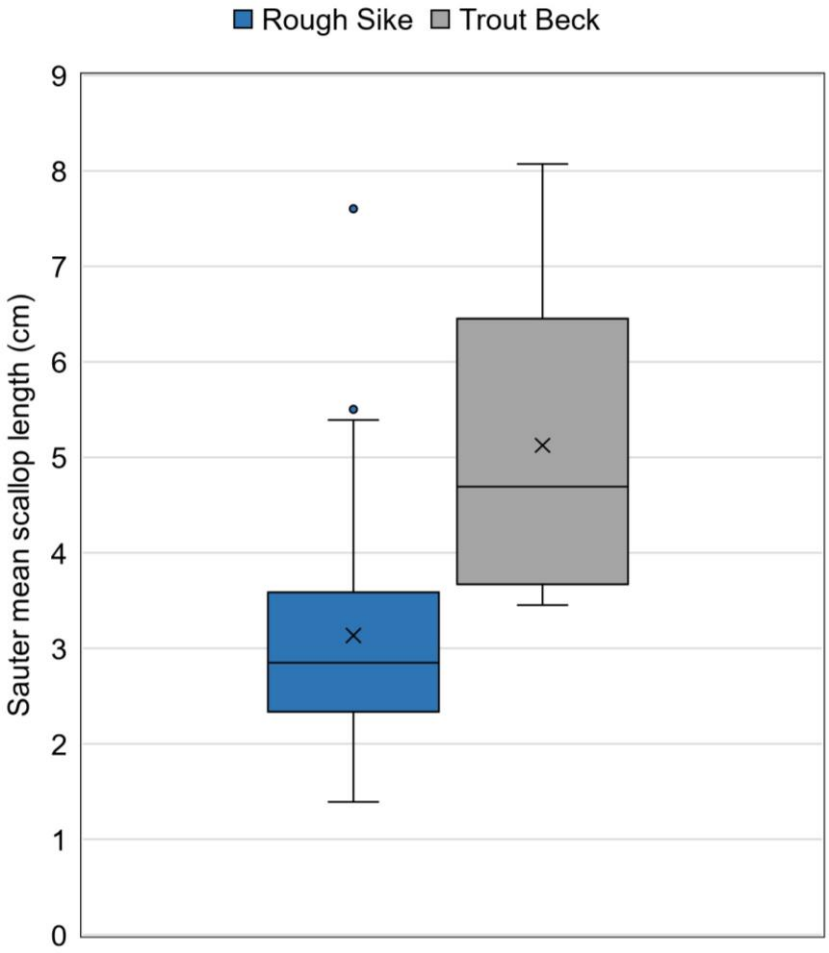

Figure 23: Sauter mean scallop length from each sample site at Rough Sike (n = 48 sample locations, 12,456 scallops sampled) and Trout Beck (n = 11 sample locations, 1,185 scallops sampled). ‘X’ identifies the mean value, the boxes identify

the upper and lower quartiles, and the tails highlight the maximum and minimum values excluding outliers; the outliers are identified by dots.

Figure 24 shows the distribution of all scallop length measurement across all sites at Trout Beck and Rough Sike. The histogram for Trout Beck reveals a significant peak around the scallop length of 2 - 4 cm, with a steady drop off as the scallop length increases. Rough Sike has a more defined peak at approximately 1.5 – 2 cm, with a sharp decrease in frequency as the scallop length increases. The smaller grouping of scallop length measurements at Rough Sike is identified also through the standard deviation of the calculated mean values (SD = 0.9 at Rough Sike, SD = 1.1 at Trout Beck). Calculating the mean scallop length of all combined scallop measurements resulted in a mean value of 3.5 cm (SD = 1.9) at Trout Beck, and 2.31 cm (SD = 1.2) at Rough Sike. Calculating the Sauter mean scallop length of all measurements resulted in a Sauter mean scallop length of 5.7 cm (S_{32} = 0.05, 2 d.p) at Trout Beck, and 3.7 cm (S_{32} = 0.02, 2 d.p) at Rough Sike.

A Welch's T-test was performed on the combined datasets of scallop lengths from Trout Beck and Rough Sike to determine whether the datasets have statistically different or equal arithmetic means. The difference in mean scallop length between Trout Beck and Rough Sike was statistically significant (t = 20.44; p = 1.59 e-80) at the 0.05 significance level (95% confidence level). This p-value is much smaller than the p-value threshold of 0.05 and suggests that the observed difference did not occur at random.

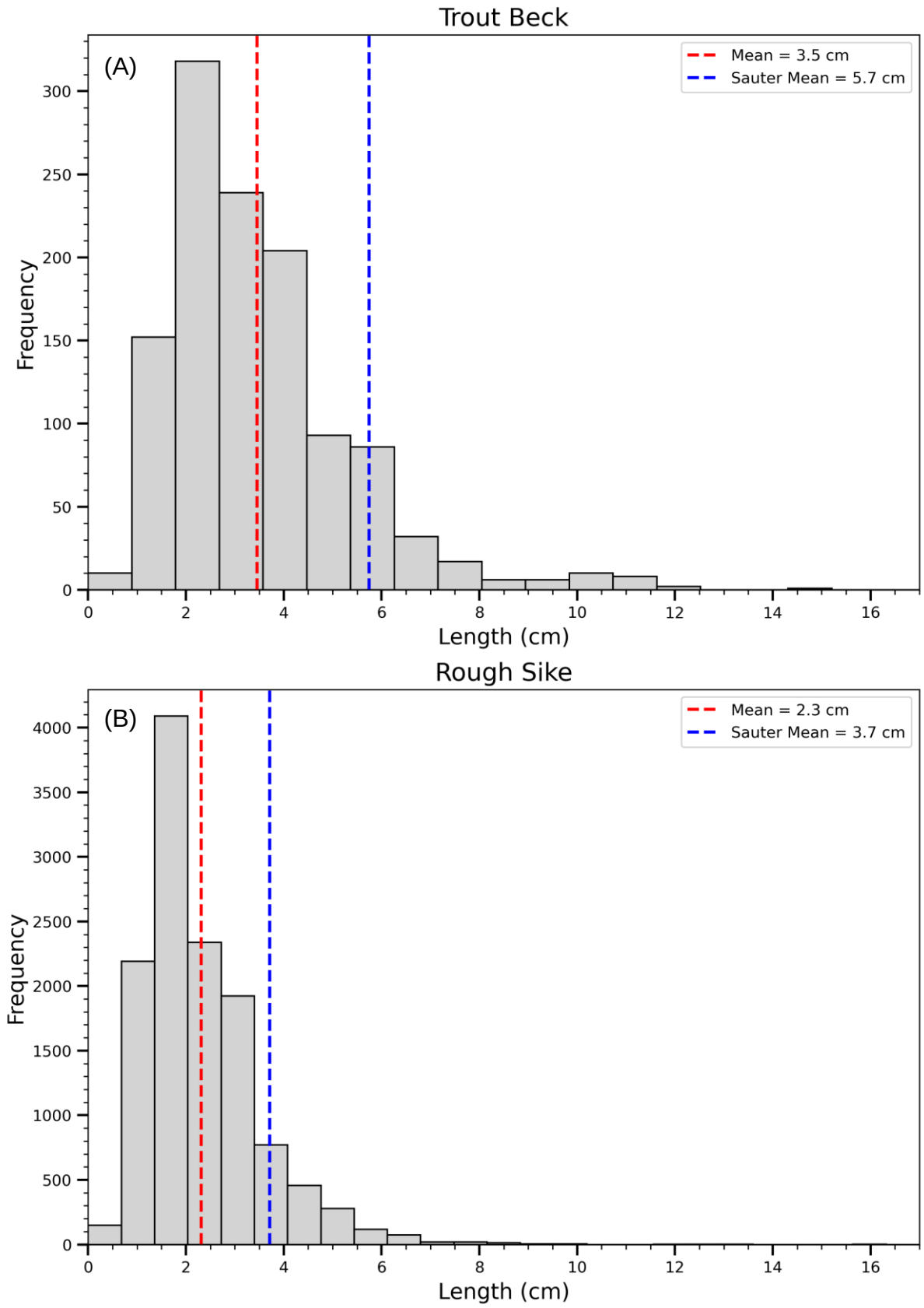

Figure 24: Histogram of scallop length measurements for all sites at (A) Trout Beck and (B) Rough Sike.

4.3.2. Scallop length variability with height in the channel

The relationship between the Sauter mean scallop length and the mean height of the scalloped surface above the low water surface was investigated. The ‘water surface’ is classified as the water level on the day which the day of data collection (8th July 2024), which was a day of relatively low flow in the channel. At Trout Beck, there is a negative relationship ($y = -1.14x + 5.88$) between scallop length and the height above the water surface, indicated by the negative gradient of -1.14 (Figure 25a). This suggests that as height of the scalloped surface increases above the water surface, the Sauter mean scallop length tends to decrease. The coefficient of determination (R^2) for the linear regression line at Trout Beck was 0.12, identifying that only 12% of the variance in the Sauter mean scallop length is explained by the change in mean height of the scalloped surface above the water surface. At Rough Sike (Figure 25b), the gradient of the linear regression line was steeper, with a value of -3.08, and the R^2 value was similar, with a value of 0.11, also indicating a weak linear relationship between the Sauter mean scallop length and mean height of the scalloped surface above the water surface.

The linear regression analysis tests the significance of the relationship using a T-test in regression. The resultant P-value of the test at Trout Beck was 0.29 (T = -1.13), which is greater than 0.05, therefore the null hypothesis can not be rejected, and the relationship between the Sauter mean scallop length and mean height of the scalloped surface above the water surface is not statistically significant. At Rough Sike, the P-value was 0.02 (T = -2.36), providing evidence that there is a statistically significant relationship between the Sauter mean scallop length and mean height of the scalloped surface above the low water surface at Rough Sike.

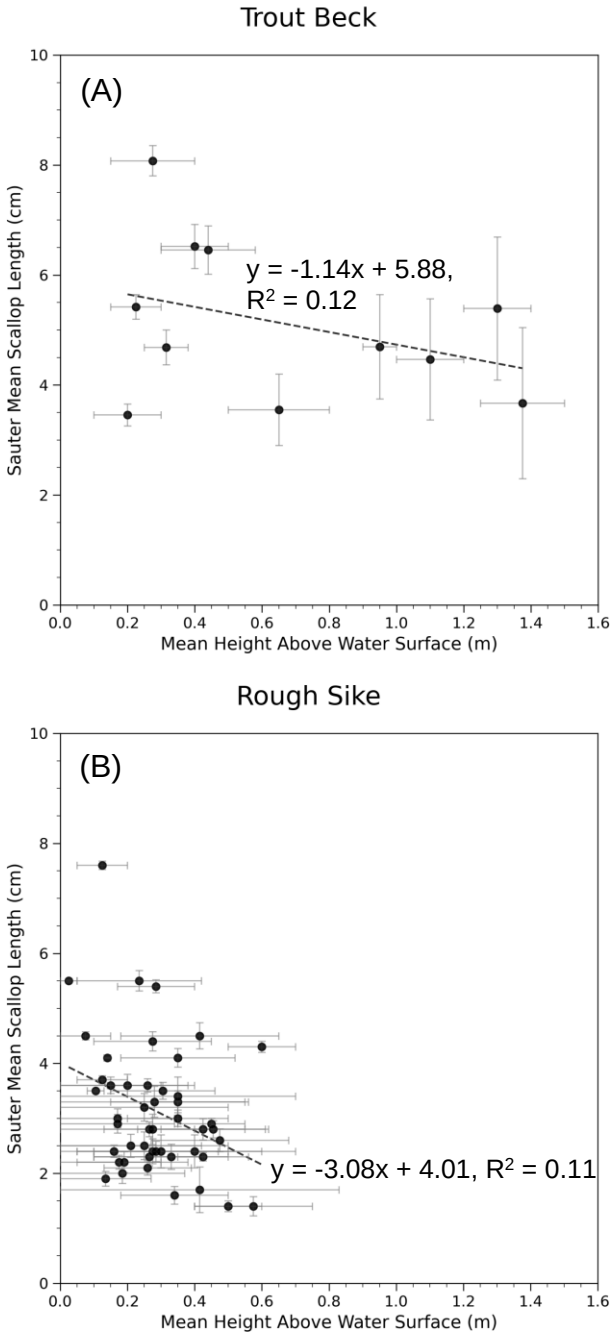

Figure 25: Relationship between the height above the water surface (m) and the Sauter-mean scallop length (cm) at (A) Trout Beck and (B) Rough Sike. Sauter-mean scallop length error bars (vertical) identify the S_{32} (Sauter mean scallop length standard deviation) and the mean height above the water surface error bars (horizontal) indicate the maximum and minimum heights that the scalloped surface extends across.

4.4. How does scallop length and abundance relate to stream power?

Table 1 includes the low flow water surface slope and 10-year unit stream power for the sampled cross-sections by Dingle et al. (in review) at Rough Sike and Trout Beck. Table C1 summarises the nearest cross-section sampled by Dingle et al. (in review) to each sample site at Trout Beck and Rough Sike, and Figure 26 and Figure 27 visualise the relationship between the scallop abundance and unit stream power values at Trout Beck and Rough Sike respectively. The Pearson's correlation coefficient of 0.53 at Trout Beck suggests that there is a positive relationship between USP and the number of scallops within an assemblage and the relationship is not statistically significant at the 0.05 significance level (P value = 0.09). The R^2 of 0.28 indicates that 28% of the variability in scallop abundance is explained by unit stream power, suggesting other variables may be contributing significantly to the scallop abundance. The slope of the linear trendline of 0.14 indicates an increase in scallop abundance as unit stream power increases at Trout Beck. At Rough Sike, the Pearson's correlation coefficient of -0.11 suggests a weak negative relationship between the number of sampled scallops and unit stream power, contrary to the positive correlation observed at Trout Beck. This relationship is also not significant however (P value = 0.46). The slope of the linear trendline (m = -0.09) also suggests that the scallop abundance decreases with an increase in stream power. At Rough Sike, the R^2 of 0.01 highlights that only 1% of the variability in scallop abundance is explained by unit stream power, therefore unit stream power is a very poor predictor of scallop abundance at this location.

Generally, when comparing the abundance of scalloping between the Trout Beck and Rough Sike, there is no clear link to average unit stream power within the study reaches. At Trout Beck, the average unit stream power was 489 W m^{-2}, and at Rough Sike the value was 370 W m^{-2}. The number of sampled scallops at Rough Sike was significantly higher (n = 12,456) when compared to Trout Beck (n = 1,185).

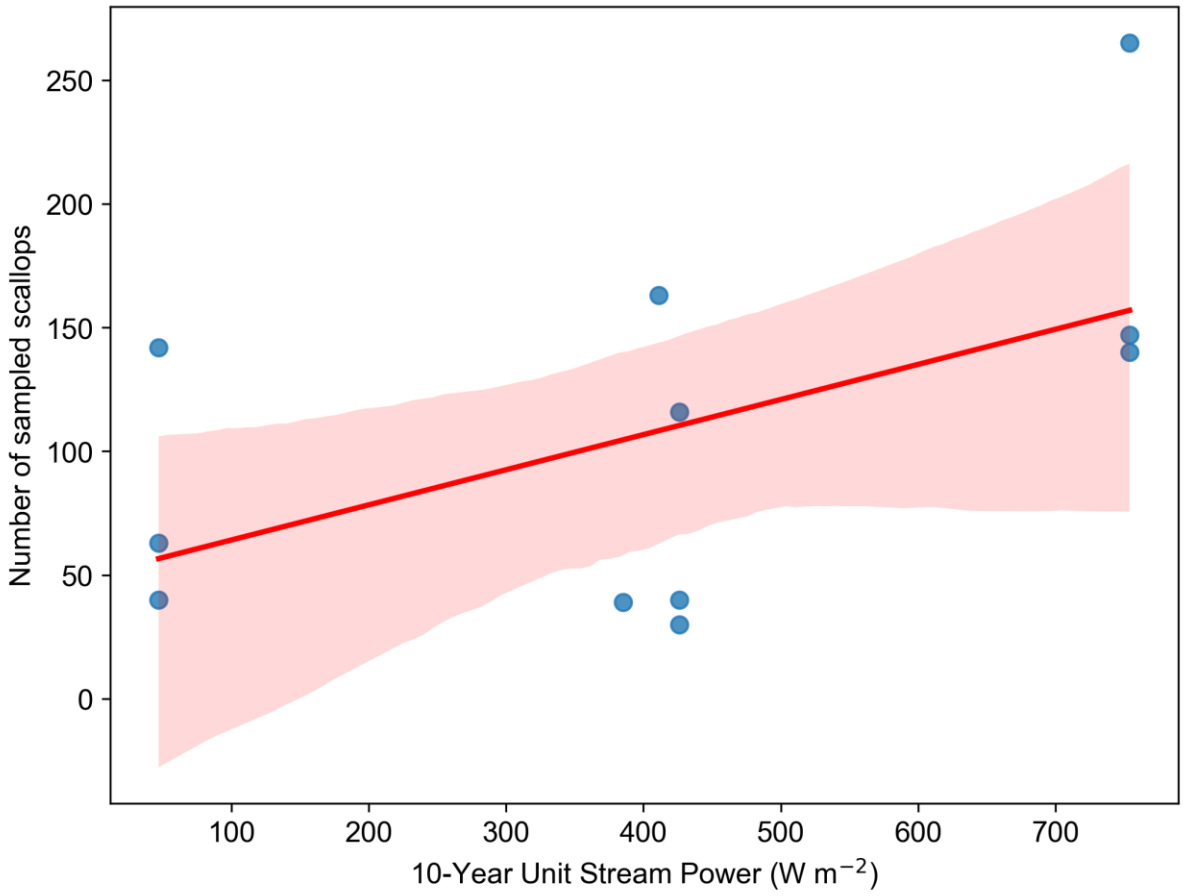

Figure 26: Relationship between the scallop abundance within an assemblage and the associated 10-year unit stream power for the closest available sample cross-

section by Dingle et al. (in review) at Trout Beck. y = 0.14x + 49.96, R^2 = 0.28. Red line is the linear trendline, red shaded region is the 95% confidence interval.

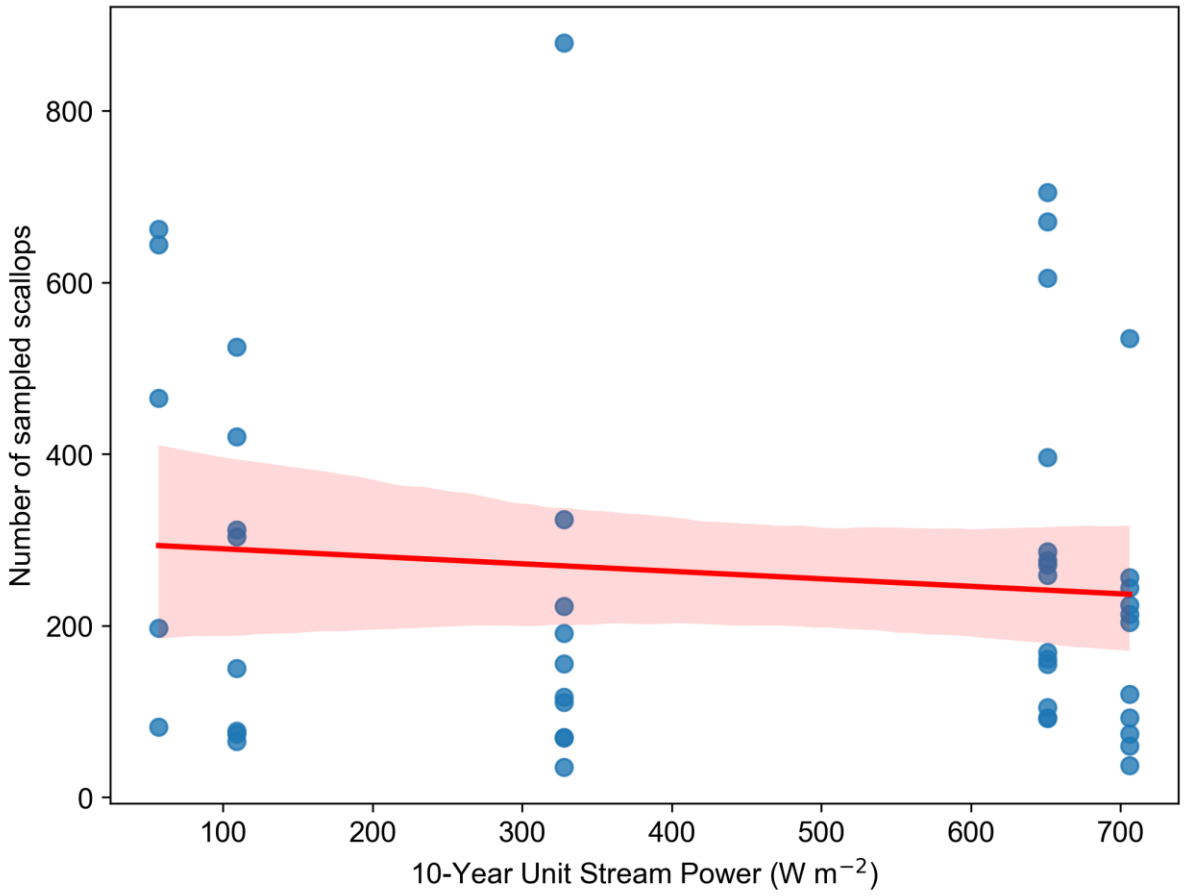

Figure 27: Relationship between the scallop abundance within an assemblage and the associated 10-year unit stream power for the closest available sample cross-section by Dingle et al. (in review) at Rough Sike. y = -0.09x + 298.34, R^2 = 0.01. Red line is the linear trendline, red shaded region is the 95% confidence interval.

The relationships between USP and the Sauter mean scallop lengths at Trout Beck and Rough Sike are visualised in Figure 28 and Figure 29 respectively.

The Pearson's correlation coefficient of -0.00 at Rough Sike suggests that there is no relationship between the USP and the Sauter mean scallop length. The relationship between the UPS and Sauter mean scallop length is not statistically significant at the 0.05 significance level (P value = 0.99). This is strong evidence that no relationship exists between the two variables at Rough Sike. The Pearson's correlation coefficient of -0.34 at Trout Beck suggests that there is a weak negative relationship between the USP and the Sauter mean scallop length. The relationship between the UPS and Sauter mean scallop length is not statistically significant at the 0.05 significance level (P value = 0.30). Five of the six unit stream power values were linked to scallop sample sites, with cross-section TB3 not being the nearest unit stream power location to any of the scallop sample sites. At Rough Sike, all unit stream power values were used.

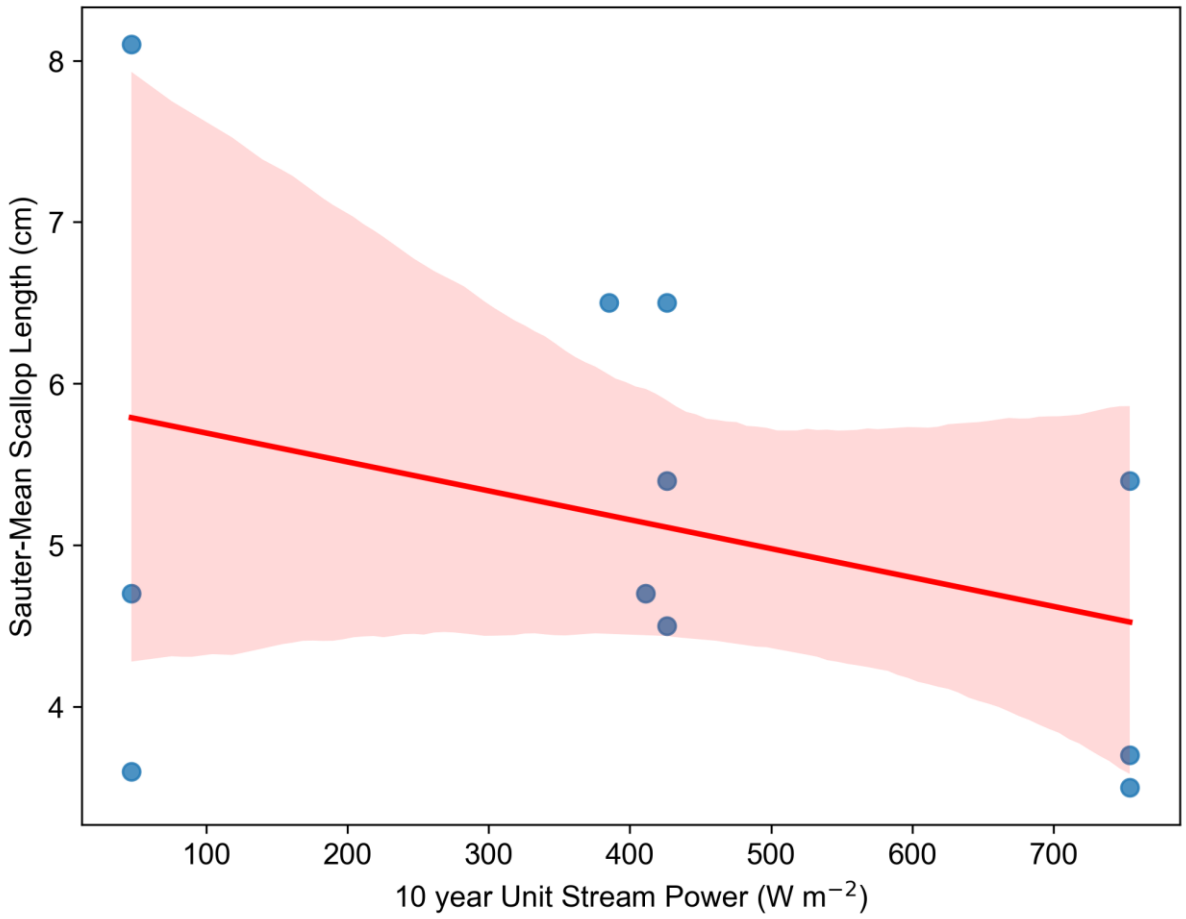

Figure 28: Relationship between the Sauter mean scallop length and the associated 10-year unit stream power for the closest available sample cross-section by Dingle et al. (in review) at Trout Beck. y = -0.00x + 5.87, R^2 = 0.12. Red line is the linear trendline, red shaded region is the 95% confidence interval.

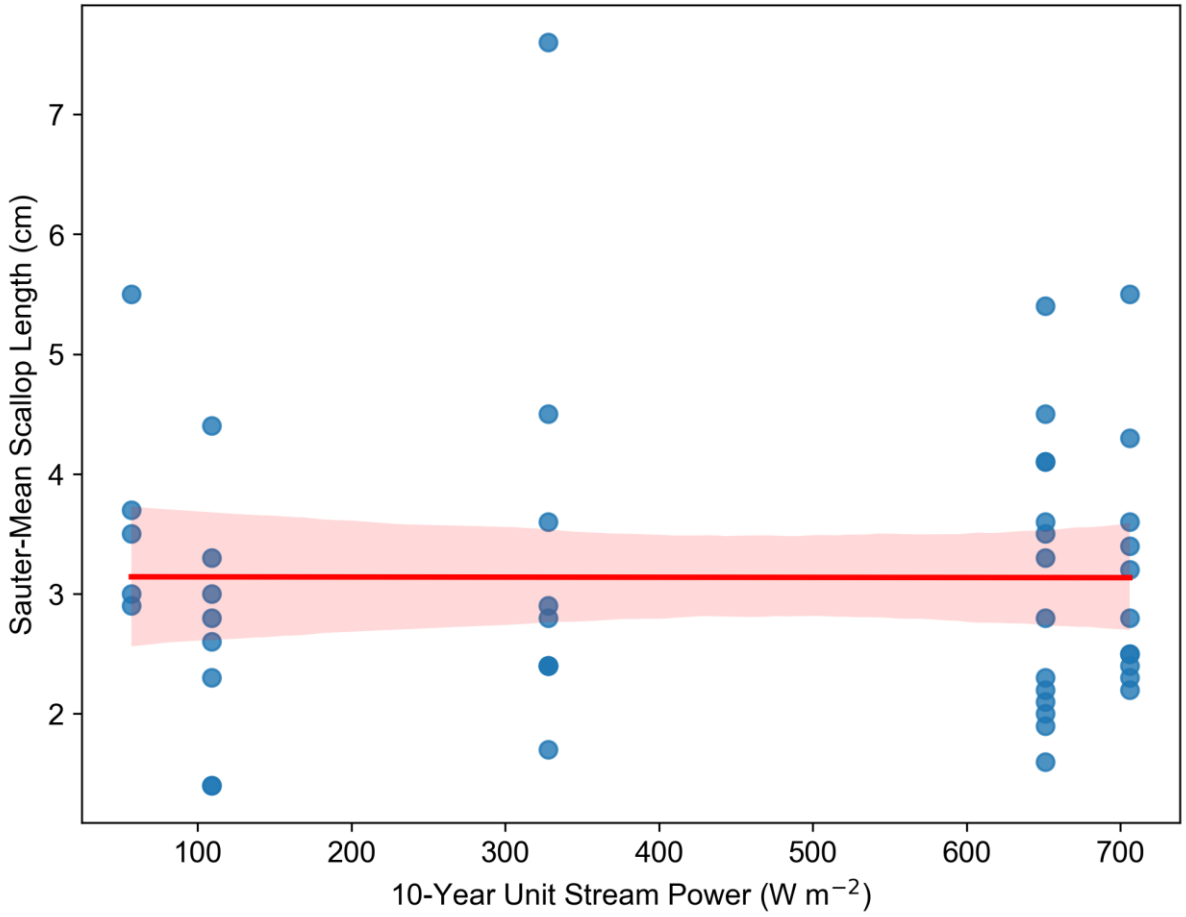

Figure 29: Relationship between the Sauter mean scallop length and the associated 10-year unit stream power for the closest available sample cross-section by Dingle et al. (in review) at Rough Sike. y = -0.00x + 3.14, R^2 = 0.00. Red line is the linear trendline, red shaded region is the 95% confidence interval.

4.5. What is the statistical distribution of scallop lengths?

4.5.1. Normality of scallop length distributions

The individual distribution and Shapiro-Wilk test results of each site both before and after the Log_{10} transformation can be viewed in Appendix B, and a summary of the results can be viewed in Table 4. Across all 11 sites that the scallop length was sampled at Trout Beck, only three had statistical distributions that can be considered normal (0.05 significance level). After applying a Log_{10} transformation to the original data, the Shapiro-Wilk test was rerun, resulting in nine out of the 11 new datasets to be considered normally distributed. The two sites (8 and 9) which were not normally distributed after the Log_{10} transformation had relatively large numbers of scallop length measurements, with counts of 142 and 265. However, sites 2, 3, 10 and 11

also had over 100 samples each and did result in normal distributions after the Log_{10} transformation. At Rough Sike, out of the 48 original scallop length datasets, three are considered normally distributed at the 0.05 significance level. After the Log_{10} transformation, 17 out of the 48 datasets were then classified as normally distributed. The average sample size of the datasets which were classified as normally distributed after the transformation was 116, compared to an average sample size of 338 for the resulting datasets which remained not-normally distributed. The average sample size of the three original datasets that were classified as normal before any transformation was 64.

Table 4: Summary of the Shapiro-Wilk test results, evaluating if the scallop length distributions are normally or not-normally distributed both before and after a Log_{10} transformation of the data.

	Normally distributed	**Non-normally distributed**
Rough Sike	3	45
Trout Beck	3	8
Rough Sike – Log_{10} transformed	17	31
Trout Beck – Log_{10} transformed	9	2

4.5.2. Modality of scallop length distributions

Evaluations of the modality of the scallop length data were derived from peak detection of Kernel Density Estimates. A unimodal dataset has one peak, a bimodal dataset has two peaks, and a multimodal dataset has three or more peaks. At Trout Beck, five sites were classed as unimodal, four were classed as bimodal, and two were classed as multimodal (11 sites total, Table 5, Table B3). At Trout Beck, six sites had peaks detected in the upper 5^{th} percentile of the data, and zero were detected in the lower 5th percentile. Not including peaks detected in the upper and lower 5^{th} percentile of the scallop length data changes this modality, with eight sites

then being classed as unimodal, three as bimodal, and zero as multimodal. There seems to be a prevalence of an increase in frequency in the relatively larger scallop length measurements within groups of scallops found in morphologically distinct locations at Trout Beck. After applying a Log_{10} transformation to the scallop length data, nine sites were classed as unimodal, two as bimodal, and zero as multimodal (Table B4). Only one peak was detected in the lower 5^{th} percentile of the Log_{10} transformed data, and zero peaks were detected in the upper 5th percentile. Removing the one peak in the lower 5th percentile changes the modality of the 11 sites to 10 sites being unimodal, and one site being bimodal. Only identifying peaks which fall above the 50^{th} percentile (median) of the KDE values provides an estimate of the number of 'large', or primary peaks in the dataset, disregarding smaller fluctuations in the density distribution. Applying this method to the scallop length data from Trout Beck reveals that 10 of the 11 datasets are now classified as unimodal, with one primary peak. Only one dataset, site 9, recorded two peaks above the 50^{th} percentile of the KDE values. After the Log_{10} transformation, all sites had only one primary peak, and would therefore be classified as unimodal.

Table 5: Summary of Trout Beck and Rough Sike modality analyses. The values indicate how many sites are unimodal, bimodal or multimodal.

	Unimodal	**Bimodal**	**Multimodal**
Rough Sike	29	15	4
Trout Beck	5	4	2
Rough Sike – excluding peaks in the upper and lower 5^{th} percentiles	47	1	0
Trout Beck – excluding peaks in the upper and lower 5^{th} percentiles	8	3	0

	Unimodal	Bimodal	Multimodal
Rough Sike – only including peaks above 50th percentile of KDE values	48	0	0
Trout Beck – only including peaks above 50th percentile of KDE values	10	1	0
Rough Sike - Log_{10} transformed	38	9	1
Trout Beck - Log_{10} transformed	9	2	0
Rough Sike - Log_{10} transformed, excluding peaks in the upper and lower 5th percentiles	45	3	0
Trout Beck - Log_{10} transformed, excluding peaks in the upper and lower 5th percentiles	10	1	0
Trout Beck - Log_{10} transformed, only including peaks above 50th percentile of KDE values	11	0	0
Rough Sike - Log_{10} transformed, only including peaks above 50th percentile of KDE values	46	2	0

The KDE at Rough Sike reveal similar trends in modality, with 29 sites being classed as unimodal, 15 as bimodal, and 4 as multimodal (48 sites total, Table B5). Six of the 48 sites at Rough Sike included peaks in the lower 5th percentile, and 21 sites included peaks in the upper 5th percentile. Not including the peaks in the upper and lower 5th percentiles, 47 sites were classified as unimodal, and only one site was

classified as bimodal. The trend of secondary or more peaks in the upper 5th percentile is also evident at Rough Sike. Rough Sike has on average a much greater number of scallop measurements at each site, increasing the confidence in the evaluated modality and other descriptive statistics of the scallop length distribution. After applying a Log_{10} transformation to the scallop length data, 38 sites were classed as unimodal, nine sites were classed as bimodal, and one site was classified as multimodal (Table B6). Six of the nine peaks in the upper and/or lower 5th percentile were detected in the lower 5th percentile, with the other three being detected in the upper 5th percentile of the Log_{10} transformed data. Recording only the peaks above the 50th percentile of the KDE values at Rough Sike reveals that all original scallop length datasets would then be classed as unimodal, with one distinct peak. Applying this also to the Log_{10} transformation data, 46 of the 48 sites would be classified as unimodal, with two sites (sites 12 and 14) being classified as binomial with two primary peaks.

4.6. How are scallops oriented and what is their statistical distribution?

4.6.1. Relationship between scallop orientation and location in the channel

The mean scallop orientation (degrees) relative to the primary flow direction is shown for all sub-sample sites (some sites have multiple sub-sample datasets) across Trout Beck and Rough Sike in Figure 30. The mean scallop orientation normalised to the flow is calculated for each sub-sample (photograph) within each site. Typically, the sub-sample sites which were located on the left bank of the river (if facing downstream and are indicated by the circles on Figure 30) have a positive mean scallop orientation. As the scallop orientations were normalised relative to the primary flow direction, positive deviations indicate scallops oriented toward the right bank, and negative orientations indicate scallops oriented toward the left bank. However, in cases where scallops were sampled on steep bedrock walls for example, they can not be oriented into the wall. On flat bedrock benches though, scallops can be oriented in any direction, therefore the morphological context of the site within the channel need to be considered when explaining the data.

At Rough Sike, only three of the 54 sub-sample sites which were located on the left bank had negative mean scallop orientations. Out of the 47 sub-sample sites which

were located on the right bank, only three had positive mean scallop orientations, with a maximum mean deviation of 4.5°. The average mean scallop orientation across all sub-sample sites at Rough Sike on the left bank was 31.5° (SD = 28.0), and from sub-sample sites on the right bank was -37.9° (SD = 22.9).

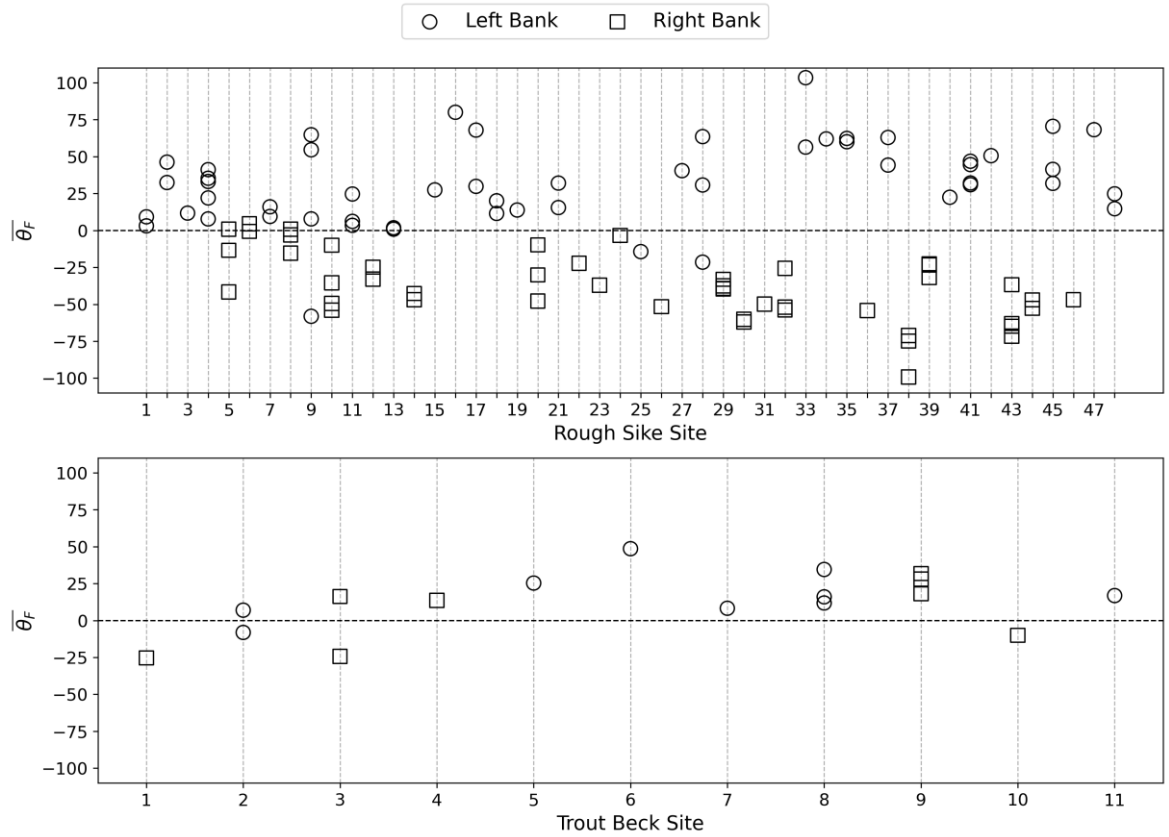

Figure 30: Mean scallop orientations (degrees) relative to the primary flow direction ($\overline{\theta_F}$) for each sub-sample across all sites at Rough Sike and Trout Beck. The circles and squares indicate whether the sample is located on the left or right bank of the river if facing downstream. A positive angle indicates a scallop orientation to the right of the primary flow direction of the river (towards the right bank) and negative indicates a scallop orientation to the left (towards the left bank).

At Trout Beck, one of the nine sub-samples on the left bank had negative mean scallop orientations, and five of the eight sub-sample sites on the right bank had positive mean scallop orientations. The average mean scallop orientation across all sub-sample sites at Trout Beck on the left bank was 17.8° (SD = 16.6), and from sub-sample sites on the right bank was 6.0° (SD = 22.7). The deviation from the mean was greater from the samples on the right bank, as indicated by the greater standard deviation.

To further highlight the pattern between scallop orientations on the left and right banks, all orientation measurements from the left and right banks were combined into separate groups. This distributions of scallop orientations on the left and right banks at Trout Beck are visible in Figure 31 (Table 6), with a calculated circular mean orientation of 17.8° (circular SD = 20.9°) for the scallops located on the left bank, and 4.1° (circular SD = 23.5°) for those on the right bank. At Rough Sike (Figure 32), the distinction of scallop orientations between the left and right bank is clearer, with circular mean orientations of 29.3° (circular SD = 33.6°) on the left bank, and -37.1° (circular SD = 28.5°) on the right bank.

Table 6: Summary of the mean scallop orientation calculations from scallops on the left and right bank. Identifies the difference between averaging the mean scallop orientation from the sub-samples from different banks and grouping all scallop orientation measurements from each bank into separate datasets and then calculating the circular mean.

	Trout Beck	**Rough Sike**
Average of mean scallop orientations calculated from sub-samples from the left bank	17.8°	31.5°
Average of mean scallop orientations calculated from sub-samples from the right bank	6.0°	-37.9°
Circular mean of all left bank scallop orientations	17.8°	29.3°
Circular mean of all right bank scallop orientations	4.1°	-37.1°

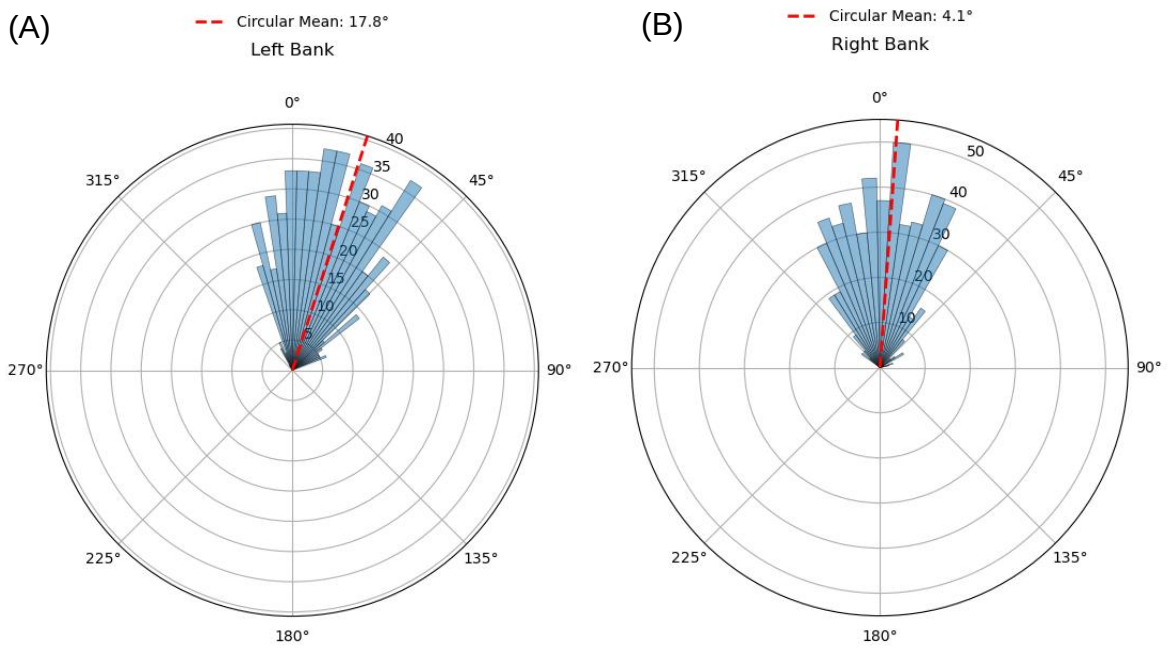

Figure 31: Rose plots showing the distribution of scallop orientations from the sites on the (A) left and (B) right bank of Trout Beck (if facing downstream). The scallops are normalised relative to the primary flow direction in the channel, so 0° is the primary flow direction, and a positive orientation indicates an orientation to the right, and a negative orientation indicates an orientation to the right of this flow.

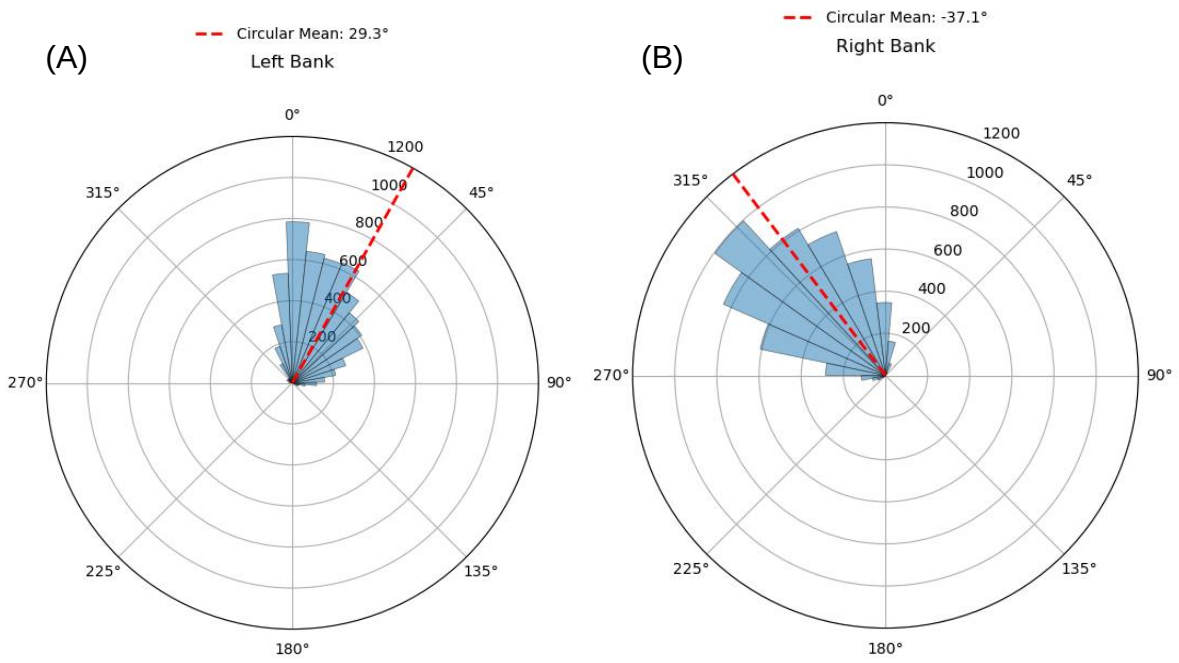

Figure 32: Rose plots showing the distribution of scallop orientations from the sites on the (A) left and (B) right bank of Rough Sike (if facing downstream). The scallops are normalised relative to the primary flow direction in the channel, therefore 0° here is the primary flow direction, and a positive orientation indicates an orientation to the right, and a negative orientation indicates an orientation to the right of this flow.

OLS linear regression analysis revealed that the mean surface angle has a significant influence on the absolute mean scallop orientation at Rough Sike, but not Trout Beck. The surface angles for each site can be viewed in Table 7 and Table 8. The Trout Beck data resulted in a P-value of 0.85, which is significantly greater than the 0.05 significance level; this is reflected in the R^2 value of 0.00, indicating that none of the variability in the absolute mean scallop orientation is explained by the mean surface angle (Figure 33a). At Rough Sike, the P-value from the OLS linear regression analysis was 0.001, much below the threshold significance level of 0.05, therefore the relationship is significant at this level. However, the R^2 value of 0.11 at Rough Sike is also not very large, suggesting that the relationship between the variables is relatively weak (Figure 33b). The standard error at Rough Sike was 0.11, and at Trout Beck it was 0.83, highlighting that the Rough Sike data fits the linear regression model more closely than the Trout Beck data. The relationships at Trout Beck and Rough Sike are both positive, suggesting an increase in surface angle

leads to an increase in the scallop orientation deviation from the primary flow in the channel.

Table 7: Surface angle and mean height above the low water surface of the scalloped sites at Trout Beck.

Site	Surface angle (degrees)	Mean height above low water surface (m)
1	13	0.44
2	10	0.32
3	9	1.30
4	6	0.40
5	11	1.10
6	10	0.65
7	15	0.95
8	12	0.28
9	17	1.38
10	17	0.23
11	17	0.20

Table 8: Surface angle and mean height above the low water surface of the scalloped sites at Rough Sike.

Site	Surface angle (degrees)	Mean height above low water surface (m)
1	11	0.11
2	10	0.45
3	11	0.03
4	22	0.17
5	26	0.13
6	14	0.29
7	4	0.14
8	12	0.31
9	13	0.35

Site	Surface angle (degrees)	Mean height above low water surface (m)
10	20	0.35
11	6	0.42
12	41	0.26
13	28	0.27
14	59	0.34
15	70	0.18
16	36	0.27
17	35	0.26
18	50	0.14
19	66	0.19
20	43	0.28
21	49	0.29
22	32	0.16
23	34	0.46
24	8	0.08
25	10	0.13
26	30	0.17
27	34	0.15
28	64	0.30
29	60	0.42
30	38	0.25
31	21	0.43
32	29	0.28
33	66	0.25
34	29	0.60
35	51	0.20
36	37	0.19
37	33	0.21
38	48	0.40
39	48	0.35
40	21	0.24

Site	Surface angle (degrees)	Mean height above low water surface (m)
41	83	0.28
42	86	0.43
43	41	0.48
44	20	0.28
45	33	0.33
46	51	0.35
47	44	0.58
48	43	0.50

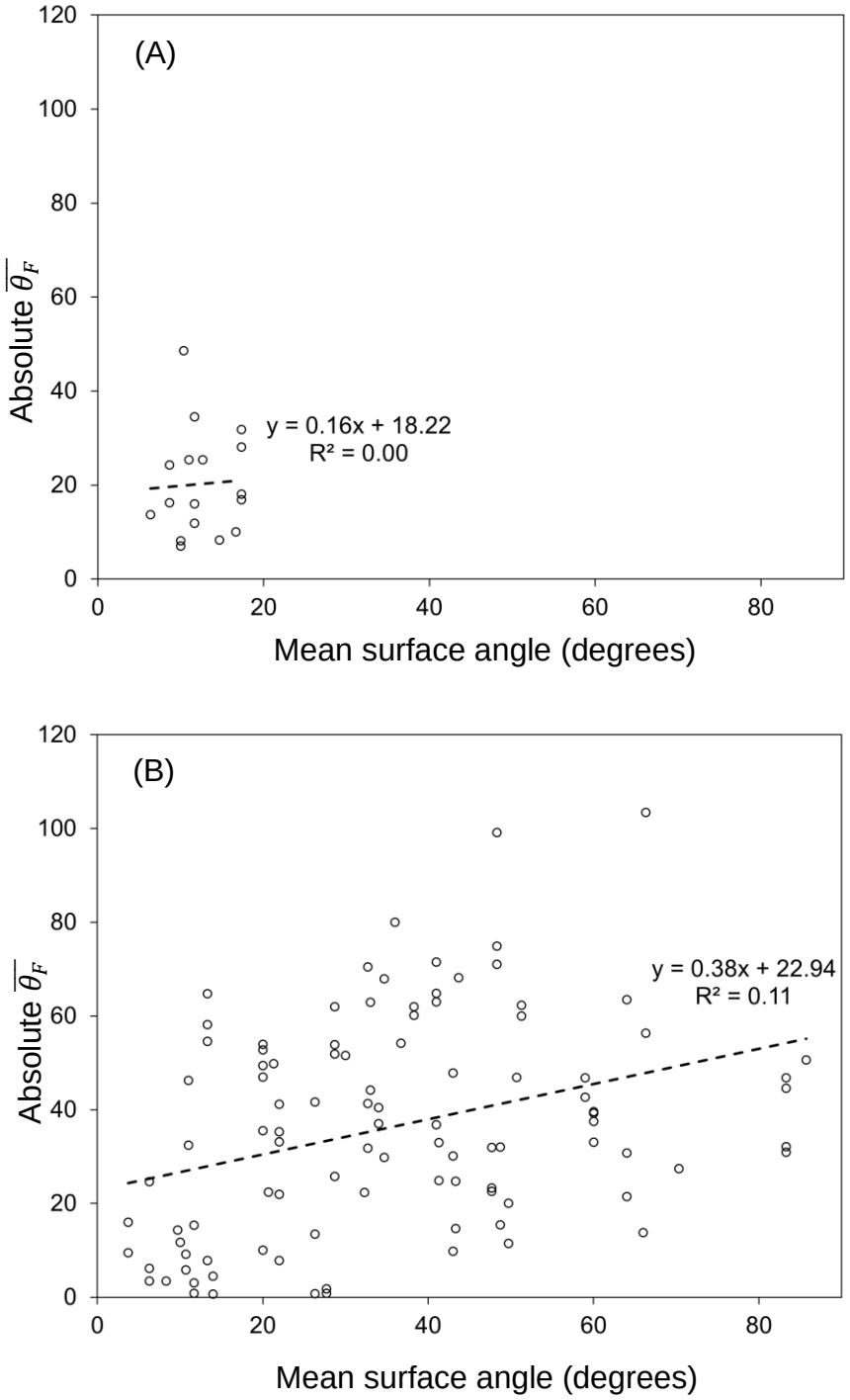

Figure 33: The relationship between the absolute mean scallop orientation relative to the flow direction ($\overline{\theta_F}$) and the mean surface angle at (A) Trout Beck and (B) Rough Sike.

4.6.2. Modality of scallop orientation distributions

Kernel Density Estimate plots can be seen in Figure 34 and Figure 35 for Trout Beck and Rough Sike sites respectively and the detailed summaries of the distributions

can be viewed in Tables C1 and C2. The KDE plots provide a visualisation of the distribution of scallop orientations relative to the circular mean orientation. Out of the 11 sites at Trout Beck, peak detection of the KDE lines identified eight sites with scallop orientations following a unimodal distribution, one site following a bimodal distribution, and two sites following a multimodal distribution (Table 9). At Rough Sike, 32 sites were identified with scallop orientations following a unimodal distribution, 15 sites following a bimodal distribution, and one site following a multimodal distribution. The mean circular standard deviation of scallop orientations, normalised relative to the to the circular mean (θ_C), was 16.2° for Trout Beck and 19.7° for Rough Sike. These circular standard deviation values are relatively low, suggesting that the data are fairly concentrated around the circular mean. The mean circular standard deviation for unimodal, bimodal and multimodal distributions at Trout Beck was 12.5°, 50.7°, and 13.9° respectively, while at Rough Sike it was 19.0°, 21.3°, and 19.5°. The range and Interquartile Range (IQR) of scallop orientations at Trout Beck was 76° and 21.1° respectively, whereas at Rough Sike the range was greater, with a range of 115° and an IQR of 25° respectively.

Table 9: Summary of the scallop orientation modality results.

	Unimodal	**Bimodal**	**Multimodal**
Rough Sike	32	15	1
Trout Beck	8	1	2

Applying a Chi-Squared test to test the relationship between the modality (unimodal, bimodal, or multimodal) of the scallop orientation distributions, and the scallop length distributions for each site revealed no significant relationship at the 0.05 significance level for Trout Beck (Chi-Squared statistic (x^2) = 5.1, p = 0.08) and Rough Sike (x^2 = 1.5, p = 0.8). This suggests that if the scallop length distribution is bimodal for example, this isn't always also correlated by two peaks in the modality of the scallop orientation distribution for the same assemblage.

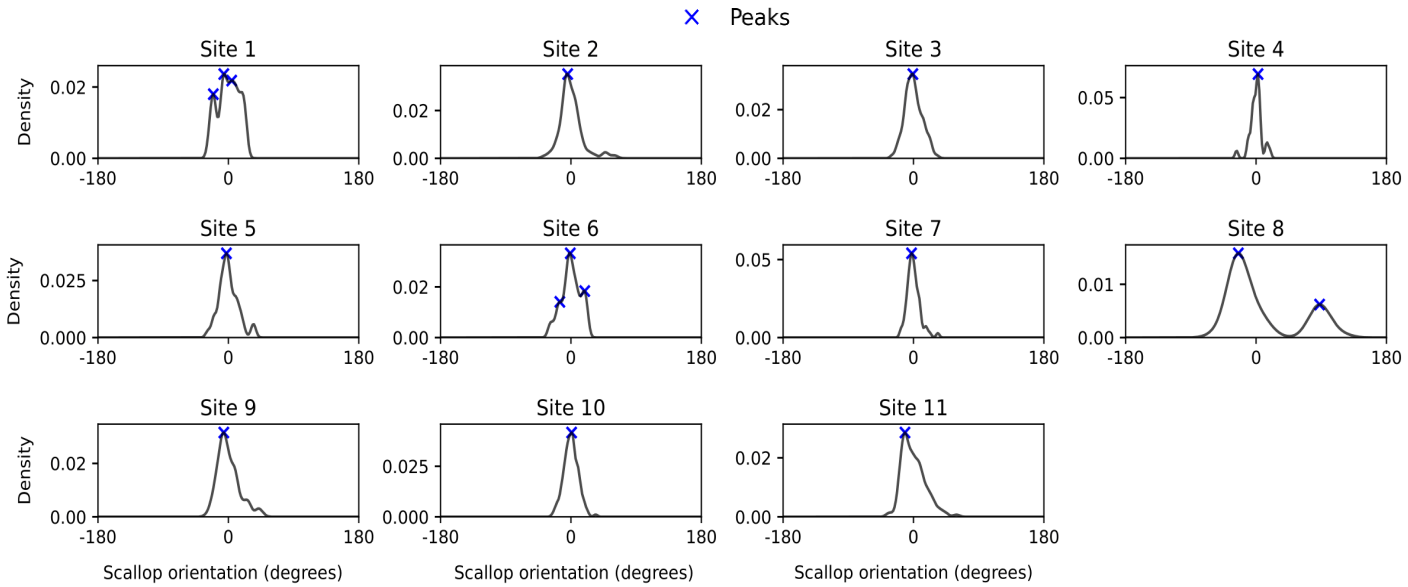

Figure 34: Kernel Density Estimation (KDE) plots showing the distribution of relative scallop orientations across all sites at Trout Beck. The scallop orientations are normalised to a relative 0-degree reference. Peaks in the KDE lines are noted by a blue cross. The orientations are centred around the mean circular mean scallop orientation for the respective sub-sample and are grouped into each site for analysis.

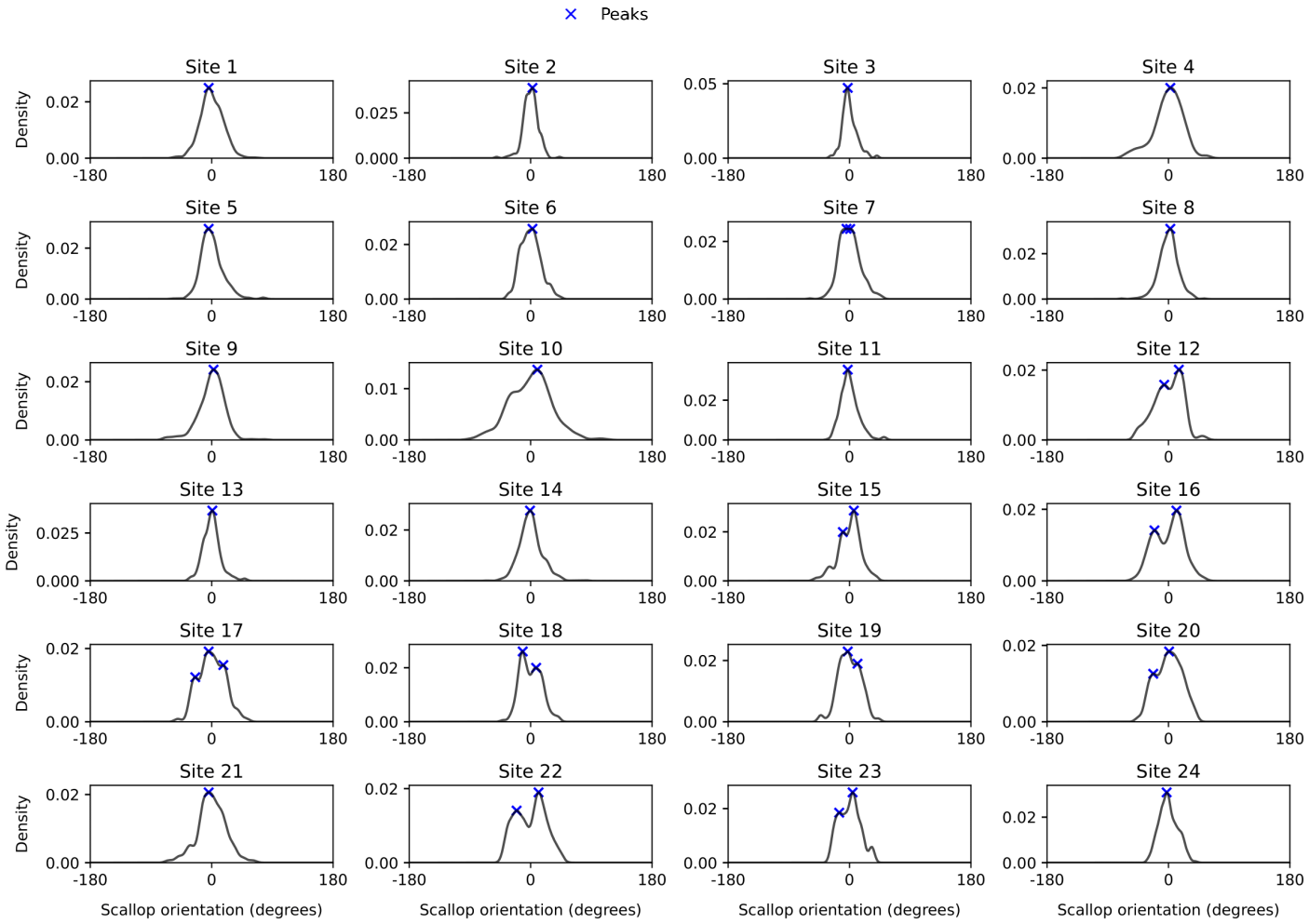
Peaks
Site 1
Site 2
Site 3
Site 4
Site 5
Site 6
Site 7
Site 8
Site 9
Site 10
Site 11
Site 12
Site 13
Site 14
Site 15
Site 16
Site 17
Site 18
Site 19
Site 20
Site 21
Site 22
Site 23
Site 24
Density
Scallop orientation (degrees)

(continued)

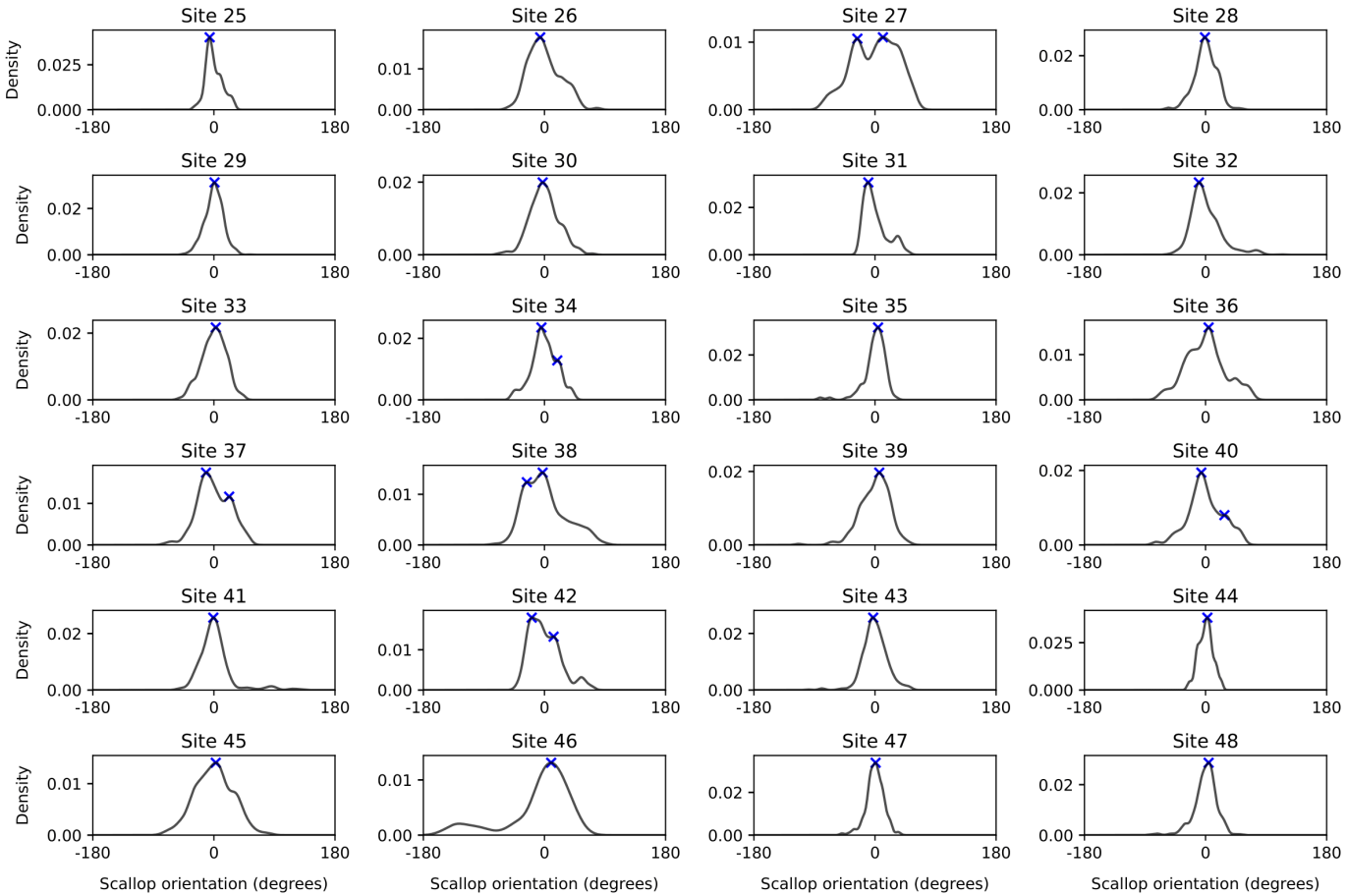

Figure 35: Kernel Density Estimation (KDE) plots showing the distribution of relative scallop orientations across all sites at Rough Sike. The scallop orientations are normalised to a relative 0-degree reference. Peaks in the KDE lines are noted by a blue cross. The orientations are centred around the mean circular mean scallop orientation for the respective sub-sample and are grouped into each site for analysis.

4.7. How long does it take for scallops to develop?

This first-order estimate of the scallop development period is based on long-term dissolution rates estimated by Dingle et al. (in review) of 0.98 mm yr^{-1} and 0.58 mm yr^{-1} for Rough Sike and Trout Beck respectively. A very small scallop of 1 cm is estimated to be developed between 0.9-1.4 years, depending on the dissolution rate used within the calculation. The scallop development periods for Rough Sike are shorter than Trout Beck for the same scallop size, due to the faster dissolution rate within the channel. A very large scallop of 200 cm, larger than any observed at Trout Beck and Rough Sike, is estimated to be developed between 170.1 and 287.4 years. A more representative scallop length for the scallops observed at these sites is a 5 cm scallop, estimated to be developed in 4.3 and 7.2 years at Rough Sike and Trout Beck respectively. provides a summary of the scallop formation period for each scallop size under the different dissolution rate conditions.

Table 10 provides a summary of the scallop formation period for each scallop size under the different dissolution rate conditions.

Table 10: Scallop formation period (years) for varying scallop lengths (cm) at Trout Beck and Rough Sike

Scallop length (cm)	Trout Beck (0.58 mm yr^{-1})	Rough Sike (0.98 mm yr^{-1})
1	1.4	0.9
5	7.2	4.3
20	14.4	8.5
200	287.4	170.1

5. Discussion

5.1. What is the spatial distribution of scallops at Trout Beck and Rough Sike?

At Rough Sike, the evidence of scalloping upstream of the bedrock study reach is primarily grouped in the change to the Single post limestone (SPL-LMST) between the Alston formation (AG-LSSM). Some of the scalloped surfaces upstream of Rough Sike were not in-situ (i.e. are on boulders and bedrock blocks), therefore it is possible that they may have originated from the Alston formation upstream and may have been transported to the Single post limestone section where they currently are observed. However, some of the observed scalloping was on the in-situ bedrock surfaces, therefore the Single post limestone is also conducive to scallop development. The Rough Sike main bedrock study reach with abundant scalloping is within the Tynebottom Limestone member (TBL-LMST), contrasting with the Trout Beck main bedrock study reach which is within the Alston formation (AG-LSSM). Therefore, it is possible that there is a lithological control on scalloping, as scalloping is significantly more abundant in Rough Sike (n = 12,456) than Trout Beck (n = 1,185). Scalloping was not present in the upstream or downstream walkover survey of Trout Beck, despite the bedrock geology being part of the same Alston formation where scalloping is observed within the main study reach. Upstream and downstream of both Trout Beck and Rough Sike, the rivers are primarily alluvial which limits the exposed of limestone bedrock units and therefore their potential observation.

Scalloping is observed on a range of limestone surfaces at both Trout Beck and Rough Sike, including heavily fossilised (typically compound corals) and non-fossilised limestone. Curl (1974) suggested that insoluble inclusions (e.g. fossils) may provide the surface required for smaller scalloping; however, no statistical comparisons have been tested in this study. This links to the defect theory of scallop development, for which it is suggested that scallop development is reliant initially upon a defect in the surface (Villien *et al.*, 2001, 2005).

The land cover surrounding both Trout Beck and Rough Sike is predominantly blanket peat (Evans *et al.*, 1999), which will likely increase rates of dissolution within the channels due to their low pH (more H^+ ions). Organic acids are formed by the

decomposition of organic material which makes up peat, lowering the pH of water which flows through the peatlands into the rivers (Evans *et al.*, 2016). The surrounding land cover in the area being peatland may be a driving factor for why scalloping is present in these two rivers.

Covington et al. (2015) noted that if the water causing dissolution and consequently the development of the scallops is undersaturated with respect to calcite, the rate of dissolution will increase, and if the water is saturated, the dissolution rate will decrease. The upstream geology of both Trout Beck and Rough Sike is primarily carbonate, therefore it may be expected that the water within the channel is already partially saturated with respect to calcite. Despite this, scalloping is prevalent both in Trout Beck and Rough Sike. This may be due to sediment covering the carbonate bedrock, protecting the bedrock from dissolution, as highlighted by Covington et al. (2015) and Farrant and Smart (2011). Upstream of the study reaches, the rivers are primarily alluvial, which may be a key factor allowing scallops to form at these locations as they are the first main exposed bedrock reaches in the area.

5.2. To what extent do scallop length vary between rivers and height within a river?

5.2.1. Scallop variability between rivers

This research provides the first detailed quantitative analysis of scallop length and orientation from scallops in surface channels outside of closed cave environments. The T-test result (t = 20.44; p = 1.59e-80) shows that Trout Beck and Rough Sike have statistically different mean scallop length values. Trout Beck has larger mean scallop lengths than Rough Sike, suggesting that they developed under slower flow velocities (Curl, 1974). There is currently no accurate flow velocity data for both Trout Beck and Rough Sike for the recent period to test whether this fits the present flow conditions. The number of scallops sampled from each site also varied, ranging from 38 – 879 with a mean count of 259.5 (SD = 208.6) at Rough Sike to a count of 30 – 265, with a mean count of 107.7 (SD = 73.2) at Trout Beck. This indicates that Rough Sike has a considerably greater number of scallops within the study reach, while at Trout Beck, scallops are less frequent.

Trout Beck has a more readily available sediment supply alongside greater sediment storage within the study reach (sediment coverage of Trout Beck and Rough Sike

study reaches is approximately 10.9%, and 1.3% respectively). Upstream of the Trout Beck study site are large sediment stores, such as the sediment bar viewed in Figure 18 and Figure 22. Rough Sike has limited sediment input and has a very small amount of sediment storage within the channel (1.3%). Scalloping is primarily a process controlled by dissolution in this environment, and frequent abrasion from the mobilisation of sediment may erode and inhibit scallop development. Curl (1966) and Goodchild and Ford (1971) both suggest that as the sediment load increases, scallops may begin to be filled with sediment and covered, reducing the development of these features. Curl (1966) also highlights the important balance between erosion at the base and crest of scallops, whereby if sediment fills to base, erosion will preferentially reduce the crest of the scallop, causing the eventual removal of the scallops. There is also a balance between having adequate flow velocity to produce the correct flow properties that is needed for scallop development, but not too large that any sediment within the channel is frequently entrained causing frequent abrasion and the mechanical removal of the scalloped surfaces (Faulkner, 2013). The percentage sediment coverage of the study reaches for Trout Beck and Rough Sike is approximately 10.9%, and 1.3% respectively, and the average scallop density is 2.6 scallops per m^2 at Trout Beck, and 47.9 scallops per m^2 at Rough Sike. Therefore, increased abrasion at Trout Beck due to the more readily available sediment coverage may be a contributing factor to the reduced scallop density by removing evidence of scalloping on the bedrock surfaces. No sediment was observed within the scallops at either site, however stores of sediment were present within both channels. Ford and Williams (2007) found through experimentation that abrasion may lead to elongation and polishing of scallops, leading to features more similar to flute markings. At Trout Beck, scallops typically have larger lengths (Sauter mean scallop length at Trout Beck and Rough Sike is 5.1 cm, and 3.1 cm respectively), which may be a result of more frequent abrasion within the channel elongating the scallops over time (Figure 36).

Figure 36: Example of scallops on limestone bedrock at (A) Trout Beck and (B) Rough Sike. Scale is indicated on the figures. Flow direction indicated by the orange arrow; flow is from the top to the bottom of the images.

5.2.2. Scallop variability with height in the channel

The relationship between the scallop length and the height of each scallop assemblage within the channels provides contextual information regarding the variability of scallop lengths at the cross-sectional scale of the river channel. In the bedrock channels at both Trout Beck and Rough Sike, a negative relationship was present between the Sauter mean scallop length and the height at which they were located above the sampled low water surface.

At Trout beck, this relationship was not significant, however at Rough Sike, where there were an increased number of sample sites and sampled scallops, the relationship was classified as statistically significant. This negative relationship implies that scallops located higher above the active flow in the channel are representing faster flow velocities. Vertical erosion within bedrock channels can lower the bed elevation over time (Hurst and Anderson, 2018), with lateral erosion of knickpoints, which are present in both reaches, typically driving this change. Therefore, scallops located higher within the channel may represent paleo-flow

conditions, which developed at a time where the exposed bedrock was at or near the channel bed. As a negative relationship was found between height above the low water surface and the Sauter mean scallop length, this may imply that the flow velocity within the channel when these scallops were developed may have been faster than the present flow conditions. Furthermore, as scallops are observed in the channels at a range of elevations up to ~0.8 m and ~1.5 m at Rough Sike and Trout Beck respectively, however scallop development is reliant upon the velocity in the vicinity of the boundary layer within the flow, the present hydrological regime and channel configuration may not be sufficient to develop scalloping at these heights within the channel.

5.3. What is the statistical distribution of scallop lengths?

5.3.1. Normality of scallop length distributions

This analysis of scallop length distributions from Trout Beck and Rough Sike provides a contrast to the typical log-normal distribution of scallop lengths observed in caves by Charlton (2003) and Springer and Hall (2020). While previous studies have documented the log-normal or normal distribution of cave scallop lengths, the results from this study instead suggest that scallops developed in open river channel conditions exhibit more variable distributions in length, and do not follow a strict log-normal or normal length distribution.

The results from this study indicate that scallops developed in open river channels do not follow the expected log-normal distribution in length measurements that cave scallops are expected to follow. This difference from the expected log-normal distribution may be attributed to the more variable and heterogeneous flow conditions within surface streams, likely resulting in the increased scallop length variability within individual assemblages. Cave environments may result in these more typical length distributions due to a more stable and often phreatic conditions which the scallops develop under. Whereas surface streams are subject to a range of variables which may drive this increased scallop length variability, such as extreme fluctuations in flow velocity, sediment load, and exposure to the atmospheric processes (e.g., weathering). Also, cave scallops develop under phreatic or vadose conditions, while surface stream scallops develop in open channel flow.

5.3.2. Modality of scallop length distributions

The automated peak detection of the Kernel Density Estimations provided valuable insight into the modality of the scallop length datasets. In previous studies, scallop length typically are found to follow a unimodal, log-normal distribution, leading to the idea that the scallops may instead represent a 'scallop dominant discharge', where the dissolutional erosion is greatest, and therefore produces the most morphological work in creating and modifying the scallops (Charlton, 2003; Lauritzen, 1989). This study finds that scallop lengths are also primarily unimodal, with one distinct primary peak in the scallop length distribution. This is identified through analysis of the peaks detected above the 50th percentile of the KDE values, revealing that at Trout Beck, 10 of the 11 sites, and at Rough Sike, 48 of the 49 sites were classified as unimodal once only these peaks were used. However, identifying peaks within the extremes of the data distributions (upper and lower 5th percentiles) revealed that many sites had smaller peaks at these extreme lengths. At Trout Beck, across the four sites where peaks were detected in the upper and/or lower 5th percentile of the data, all six peaks were detected in the upper 5th percentile. Across the 18 sites at Rough Sike where peaks were detected in the upper and/or lower 5th percentile of the data, all 22 peaks were detected in the upper 5th percentile. This suggests that multiple flow conditions may be preserved within a single assemblage, potentially representing the present flow conditions (main peak), alongside secondary flow patterns (peaks in upper/lower 5th percentiles).

5.4. How does scallop length relate to stream power?

As scallop length is inversely proportional to flow velocity (Curl, 1974), it would be expected that, as the unit stream power increases, flow velocity will increase. This is because $Q = vA$, where v is the flow velocity (m s^{-1}) and A is the cross-sectional area (m^2), and discharge is proportional to the unit stream power. The relationship between unit stream power and scallop abundance at Trout Beck and Rough Sike is contrasting, as at Trout Beck, a positive relationship is observed (Pearson's correlation coefficient = 0.53), where an increase in unit stream power leads to an increase in scallop abundance. However, at Rough Sike, a negative relationship is present (Pearson's correlation coefficient = -0.11). No significant relationships are observed at either river, and this may be because many factors may influence scallop abundance, and unit stream power is likely not a significant contributor to this. At Rough Sike, the very low R^2 of 0.01 suggests that unit stream power is a very

poor predictor of scallop abundance, compared to an R^2 of 0.28 at Trout Beck. Sample size may be a contributing factor to the difference in relationship, with Rough Sike having significantly greater scallop sites (48 compared to 11 at Trout Beck), however only has five USP values compared to six at Trout Beck. Scallop development is reliant upon various factors, and these may be influenced by changes in unit stream power. For example, a greater unit stream power may hinder scallop development as sediment transport may increase, causing more frequent abrasion, therefore hindering scallop development (Curl, 1966; Goodchild and Ford, 1971; Faulkner, 2013).

At Trout Beck, the Pearson correlation coefficient (-0.34) suggests a weak negative relationship between the USP and the Sauter mean scallop length, however the gradient of the linear trendline is -0.00, indicating a very weak or neutral relationship. Also, the relationship is not significant (P value = 0.30) at the 0.05 significance level, therefore this analysis does not provide sufficient evidence to support the idea that an increase in unit stream power would lead to a decrease in Sauter mean scallop length of an assemblage. At Rough Sike, the data show also show no significant relationship between the USP and the Sauter mean scallop length, with the linear trendline also having a gradient of -0.00, but with a R^2 value of 0.00 compared to a value of 0.12 at Trout Beck. The P values of the statistical testing of 0.99 at Rough Sike, and 0.30 at Trout Beck also support the conclusion that there is no significant relationship. This contradicts the expected relationship based on the theoretical relationships present between unit stream power, flow velocity, and Sauter mean scallop length.

The scallop length data were paired with the corresponding stream power values based on their nearest distance. However, only six unit stream power values were used in the analysis for Trout Beck, and five for Rough Sike, therefore, some sites may be located at a reasonable distance from the location where the unit stream power was calculated for; this may limit the accuracy and interpretations of the data. Additionally, Rough Sike included only five unit stream power values for this analysis, despite having 48 sampled scallop sites. To enhance the accuracy of data interpretation, more frequent unit stream power calculations would have provided a better understanding of the high and low energy sections of the reaches, and in turn,

a more accurate interpretation of the relationships between the scallop length and USP.

5.5. How are scallops oriented and what is their statistical distribution?

5.5.1. Relationship between scallop orientation and location in the channel

The orientation and location of the scallops within the channel can provide valuable insights into the flow dynamics and morphological development of scallops within these river channels. Figure 30 highlights the mean orientations of scallops relative to the primary flow direction at each location, alongside their relative positioning on either the left or right bank of the channel. The results show that at Rough Sike, the scallops were predominantly oriented in the direction towards the primary flow in the channel, rather than outwardly, towards the banks of the channel (Figure 31, Figure 32). However, at Trout Beck, the orientations were more variable, though the limited number of sites and scallops sampled from this river reduces the confidence in this relationship.

At Rough Sike, the pattern of scallop orientations being in the direction towards the active flow in the channel rather than the banks is likely due to the local morphology of the bedrock channel. Rough Sike is primarily a bedrock gorge, with some areas of more gradual inwardly sloping bedrock banks (see Figure 17). Therefore, the gravitational forces and topographic constraints within the gorge will typically direct the water flow back towards the primary flow direction of the channel. As scallops preserve the direction of the flow that modifies them, it would be expected that scallops located on the banks of a bedrock gorge would be typically oriented downstream, and slightly towards the centre of the channel. This is consistent with what is observed in the scallops at Rough Sike.

The data suggest that the morphological context of the scalloped location must be considered when inferring paleo-flow directions within a channel, as significant variability in scallop orientation can be driven by local scale topographic variability. This is also highlighted in the relationship identified at Rough Sike between the scallop orientation and surface angle, where an increase in surface angle resulted in an increase in the deviation of the scallop orientation from the primary flow direction.

5.5.2. Modality of the scallop orientation distributions

Scallop orientation distributions can provide valuable insight into the flow dynamics within river channels, as the scallops preserve the flow direction of the water that shapes the scallops (Bögli, 1980). Unimodal scallop orientation distributions were observed at eight of the 11 sites at Trout Beck, and 32 of the 48 sites at Rough Sike, indicating that scallop assemblages are generally orientated in a similar direction, likely representing the predominant flow direction across the surface. The low circular standard deviation values of 16.2 and 19.7 for scallop orientations at Trout Beck and Rough Sike, respectively, further supports this, suggesting that that most scallops within each assemblage closely align with the primary flow direction. At two sites in Trout Beck, and 16 sites at Rough Sike, more than one mode was detected in the orientation distributions. This may be representative of multiple flow directions across the bedrock surface, which could reflect heterogeneity of the flow dynamics at these sites.

When the modality (unimodal, bimodal, or multimodal) of the length and orientation distributions were examined using the Chi-squared test, no significant correlation was observed at either Trout Beck or Rough Sike. This suggests that while scallop assemblages may preserve multiple flow directions (more than one mode in the orientation distribution), this does not necessarily correlate to an equal number of modes in the scallop length distribution.

5.6. How long does it take for scallops to develop?

This first-order scallop formation model is simple and does represent the exact 3-dimensional shape of a scallop; instead, it approximates the shape using a half-ellipsoid. Furthermore, dissolution within scallops does not occur at a uniform rate across their shape, rather, certain areas experience concentrated dissolution, while others undergo less intense dissolution (Cooper, 2018; Curl, 1974; Ford and Williams, 2007; Lundberg, 2019). The highest observed scallops at Rough Sike and Trout Beck were recorded at 0.83 m and 1.5 m above the water surface, respectively, on the day of data collection. The simple formation time, derived from the dissolution rate calculations, applies specifically to periods when the scallops are submerged. However, this will greatly depend on the water level within the channel,

which can fluctuate seasonally (Evans *et al.,* 1999) and be influenced by various factors such as precipitation, temperature, and other environmental conditions.

Other variables, such as pH, temperature, and sediment dynamics within the channels may significantly influence the dissolution rate during the period of erosion. For example, Goodchild and Ford (1971) mention that if sediment were to cover the concavity of a scallop, this may reduce the dissolution rate at the base of the scallop compared to exposed areas of the scallop at the crest. This approach uses a dissolution rate derived from the limestone surfaces on which the scallops develop, offering a first-order estimate of the formation period for scallops in rivers, a calculation that has not been reported before.

6. Conclusion

This study presents the findings from a field-based study investigating bedrock scallop distribution and morphology in upland river channels. Trout Beck has significantly larger mean scallop lengths than Rough Sike, indicating that they developed due to a slower flow velocity (Curl, 1974). The Sauter mean scallop length at Trout Beck across all sites was 5.1 cm (S_{32} = 0.2) and at Rough Sike it was 3.1 cm (S_{32} = 0.2). The average scallop density at Trout Beck and Rough Sike was 2.6 scallops per m^2 and 47.9 scallops per m^2 respectively. Scalloping at Rough Sike is more abundant, and smaller in general than at Trout Beck. This may be because of the different geological group that the sites are primarily located within, or, due to the greater sediment coverage within the channel at Trout Beck (10.9% compared to 1.3% at Rough Sike), potentially removing evidence of scalloping through increased abrasion rates.

At both Trout Beck and Rough Sike, a negative relationship was present between the Sauter mean scallop length and the height at which they were located above the water surface, implying that scallops located higher above the active flow in the channel are representing faster flow velocities. Scallops located higher in the channel may be representing paleo-flows within the channel when the bed level was higher. The scallop length distributions from each site did not follow a typical normal or log-normal distribution, and did not exhibit a typical unimodal distribution, with evidence of multiple peaks within many scallop length distributions for individual sites at both Trout Beck and Rough Sike. This evidence differs from the typical scallop length distributions derived from cave scallop studies. This may be because of factors such as weathering and abrasion within surface channel environments modifying the scallop morphology.

Contrasting relationships were observed between USP and scallop abundance at Trout Beck and Rough Sike, with both positive and negative relationships observed at each site respectively. A weak negative and neutral relationship between the USP and the Sauter mean scallop length was observed at Trout Beck and Rough Sike respectively. No significant relationships were observed between the Sauter mean scallop length or scallop abundance and the USP at Trout Beck or Rough Sike.

At Rough Sike, the data indicate that scallops were generally oriented towards the centre of the channel, whereas at Trout Beck, their orientations were more variable. Additionally, the surface angle may also influence the scallop orientation; at Rough Sike a significant relationship was observed where an increase in surface angle resulted with an increase in scallop orientation deviation from the primary flow direction. This suggests that the morphological context of the scalloped location must be considered when inferring paleo-flow directions, as scallop orientation can vary with local scale topographic changes. Furthermore, analysis of the statistical distributions of the scallop orientations revealed variable in the modality, suggesting that individual scallop assemblages may preserve multiple flow pathways. However, no correlation was discovered between the modality of the scallop length and orientation distributions.

A first-order estimate of the scallop development timescales for a range of scallop sizes was generated under two different dissolution rates, providing the first such estimate for surface channel scallops on limestone surfaces.

7. Appendices

7.1. Appendix A: Scallop length

Table A1: Number of scallops measured, mean scallop length, standard deviation, coefficient of variation, and Sauter mean scallop length calculations from the sites at Trout Beck.

Site	Number of scallops measured	Mean scallop length (cm)	Standard deviation of mean	Coefficient of variation (%)	Sauter mean scallop length (cm)	Standard deviation of Sauter mean scallop lengths
1	39	5.3	1.7	32.0	6.5	0.2
2	163	3.6	1.4	39.7	4.7	0.2
3	116	3.6	1.7	46.0	5.4	0.2
4	30	5.8	1.5	25.5	6.5	0.2
5	40	3.5	1.3	37.9	4.5	0.3
6	40	2.9	1.0	35.8	3.6	0.3
7	63	3.2	1.6	49.0	4.7	0.3
8	142	3.2	2.8	87.5	8.1	0.2
9	265	2.1	1.2	56.5	3.7	0.2
10	147	3.8	1.7	43.9	5.4	0.2
11	140	3.1	0.8	25.5	3.5	0.1
Mean	**107.7**	**3.6**	**1.50**	**43.6**	**5.1**	**0.2**

Table A2: Number of scallops measured, mean scallop length, standard deviation, coefficient of variation, and Sauter mean scallop length calculations from the sites at Rough Sike.

Site	Number of scallops measured	Mean scallop length (cm)	Standard deviation	Coefficient of variation (%)	Sauter mean scallop length (cm)	Standard deviation of Sauter mean scallop lengths
1	644	2.4	1.1	43.9	3.5	0.1
2	197	4.0	1.8	45.3	5.5	0.2
3	82	2.2	0.8	37.6	2.9	0.2

Site	Number of scallops measured	Mean scallop length (cm)	Standard deviation	Coefficient of variation (%)	Sauter mean scallop length (cm)	Standard deviation of Sauter mean scallop lengths
4	662	2.4	0.8	34.6	3.0	0.1
5	465	2.9	1.0	36.2	3.7	0.1
6	155	4.2	1.5	36.7	5.4	0.2
7	605	3.1	1.1	35.4	4.1	0.1
8	396	3.0	0.9	31.5	3.5	0.1
9	671	3.1	1.2	39.7	4.1	0.1
10	286	2.5	1.0	39.2	3.3	0.1
11	276	3.4	1.4	40.6	4.5	0.1
12	161	2.7	1.0	37.2	3.6	0.2
13	271	2.3	0.8	33.4	2.8	0.1
14	705	1.3	0.4	31.4	1.6	0.1
15	93	1.8	0.6	30.2	2.2	0.2
16	259	1.8	0.6	34.1	2.3	0.1
17	105	1.8	0.5	26.9	2.1	0.2
18	169	1.5	0.5	35.5	1.9	0.2
19	92	1.7	0.5	31.2	2.0	0.2
20	223	2.0	0.6	28.9	2.4	0.1
21	117	1.9	0.7	37.2	2.4	0.2
22	70	1.9	0.7	36.1	2.4	0.2
23	35	2.3	0.8	35.4	2.8	0.3
24	191	3.7	1.2	32.3	4.5	0.1
25	111	5.3	2.4	45.8	7.6	0.2
26	156	2.5	0.7	30.0	2.9	0.1
27	69	2.8	1.1	38.0	3.6	0.2
28	324	1.8	0.7	38.0	2.4	0.1
29	879	1.3	0.5	35.1	1.7	0.1
30	213	1.9	0.7	39.7	2.5	0.2
31	120	1.9	0.6	32.3	2.3	0.2
32	535	2.2	0.8	37.2	2.8	0.1
33	204	2.4	1.0	40.6	3.2	0.2

Site	Number of scallops measured	Mean scallop length (cm)	Standard deviation	Coefficient of variation (%)	Sauter mean scallop length (cm)	Standard deviation of Sauter mean scallop lengths
34	60	2.9	1.4	48.1	4.3	0.3
35	93	2.8	1.0	37.1	3.6	0.2
36	37	1.8	0.6	32.9	2.2	0.2
37	256	2.0	0.7	36.7	2.5	0.1
38	224	1.9	0.7	37.6	2.4	0.1
39	244	2.3	1.1	47.3	3.4	0.2
40	74	3.8	1.6	43.0	5.5	0.2
41	312	2.5	1.0	41.0	3.3	0.1
42	74	2.3	0.8	33.5	2.8	0.2
43	420	2.0	0.7	36.7	2.6	0.1
44	65	3.5	1.3	36.5	4.4	0.2
45	525	1.6	0.7	44.0	2.3	0.1
46	77	2.0	0.9	45.8	3.0	0.2
47	150	1.1	0.4	34.0	1.4	0.2
48	304	1.2	0.4	30.8	1.4	0.1
Mean	**260**	**2.4**	**0.9**	**36.9**	**3.1**	**0.2**

7.2. Appendix B: Statistical distribution of scallop lengths

Table B1: Trout Beck scallop length Shapiro-Wilk test results before and after a Log_{10} transformation at Sites 1-11.

Site	Count	Shapiro-Wilk Statistic	P-value	Normality	Log_{10} Transformed Shapiro-Wilk Statistic	Log_{10} Transformed p-value	Log_{10} Transformed Normality
1	39	0.930	0.019	Not normal	0.958	0.148	Normal
2	163	0.958	7.32E-05	Not normal	0.988	0.175	Normal

Site	Count	Shapiro-Wilk Statistic	P-value	Normality	Log_{10} Transformed Shapiro-Wilk Statistic	Log_{10} Transformed p-value	Log_{10} Transformed Normality
3	116	0.855	2.70E-09	Not normal	0.986	0.277	Normal
4	30	0.941	0.096	Normal	0.977	0.754	Normal
5	40	0.904	0.002	Not normal	0.948	0.065	Normal
6	40	0.970	0.359	Normal	0.961	0.180	Normal
7	63	0.890	3.76E-05	Not normal	0.972	0.163	Normal
8	142	0.889	6.50E-09	Not normal	0.974	0.008	Not normal
9	265	0.787	2.58E-18	Not normal	0.960	1.05E-06	Not normal
10	147	0.903	2.46E-08	Not normal	0.992	0.613	Normal
11	140	0.982	0.064	Normal	0.982	0.069	Normal

Table B2: Rough Sike scallop length Shapiro-Wilk test results before and after a Log^{10} transformation at Sites 1-48.

Site	Count	Shapiro-Wilk Statistic	P-value	Normality	Log^{10} Transformed Shapiro-Wilk Statistic	Log^{10} Transformed p-value	Log^{10} Transformed Normality
1	644	0.946	1.52E-14	Not normal	0.988	3.07E-05	Not normal
2	197	0.965	8.40E-05	Not normal	0.977	0.002	Not normal
3	82	0.962	0.017	Not normal	0.983	0.347	Normal

Site	Count	Shapiro-Wilk Statistic	P-value	Normality	Log^{10} Transformed Shapiro-Wilk Statistic	Log^{10} Transformed p-value	Log^{10} Transformed Normality
4	662	0.952	8.19E-14	Not normal	0.990	2.30E-04	Not normal
5	465	0.922	8.94E-15	Not normal	0.992	0.016	Not normal
6	155	0.925	3.37E-07	Not normal	0.991	0.410	Normal
7	605	0.925	8.53E-17	Not normal	0.988	6.10E-05	Not normal
8	396	0.976	4.37E-06	Not normal	0.978	9.40E-06	Not normal
9	671	0.957	3.88E-13	Not normal	0.989	5.10E-05	Not normal
10	286	0.958	2.14E-07	Not normal	0.988	0.015	Not normal
11	276	0.967	5.74E-06	Not normal	0.984	0.003	Not normal
12	161	0.924	1.69E-07	Not normal	0.975	0.005	Not normal
13	271	0.968	8.78E-06	Not normal	0.985	0.007	Not normal
14	705	0.940	2.89E-16	Not normal	0.971	1.39E-10	Not normal
15	93	0.940	3.49E-04	Not normal	0.976	0.080	Normal
16	259	0.965	5.54E-06	Not normal	0.980	0.001	Not normal
17	105	0.961	0.004	Not normal	0.968	0.012	Not normal
18	169	0.950	1.00E-05	Not normal	0.974	0.003	Not normal

Site	Count	Shapiro-Wilk Statistic	P-value	Normality	Log^{10} Transformed Shapiro-Wilk Statistic	Log^{10} Transformed p-value	Log^{10} Transformed Normality
19	92	0.977	0.104	Normal	0.938	2.90E-04	Not normal
20	223	0.961	8.07E-06	Not normal	0.976	0.001	Not normal
21	117	0.949	2.22E-04	Not normal	0.965	0.004	Not normal
22	70	0.934	0.001	Not normal	0.956	0.015	Not normal
23	35	0.953	0.137	Normal	0.967	0.361	Normal
24	191	0.967	1.95E-04	Not normal	0.990	0.182	Normal
25	111	0.930	2.03E-05	Not normal	0.981	0.106	Normal
26	156	0.970	0.002	Not normal	0.979	0.015	Not normal
27	69	0.955	0.014	Not normal	0.983	0.466	Normal
28	324	0.943	6.97E-10	Not normal	0.981	3.19E-04	Not normal
29	879	0.911	2.74E-22	Not normal	0.968	6.93E-13	Not normal
30	213	0.937	5.75E-08	Not normal	0.987	0.044	Not normal
31	120	0.958	0.001	Not normal	0.975	0.025	Not normal
32	535	0.956	1.39E-11	Not normal	0.986	5.79E-05	Not normal
33	204	0.923	7.75E-09	Not normal	0.989	0.115	Normal
34	60	0.918	0.001	Not normal	0.981	0.457	Normal

Site	Count	Shapiro-Wilk Statistic	P-value	Normality	Log^{10} Transformed Shapiro-Wilk Statistic	Log^{10} Transformed p-value	Log^{10} Transformed Normality
35	93	0.918	2.08E-05	Not normal	0.987	0.506	Normal
36	37	0.938	0.040	Not normal	0.978	0.662	Normal
37	256	0.959	1.14E-06	Not normal	0.981	0.001	Not normal
38	224	0.933	1.33E-08	Not normal	0.980	0.003	Not normal
39	244	0.925	8.50E-10	Not normal	0.991	0.134	Normal
40	74	0.816	3.46E-08	Not normal	0.974	0.125	Normal
41	312	0.941	8.20E-10	Not normal	0.991	0.054	Normal
42	74	0.949	0.005	Not normal	0.974	0.122	Normal
43	420	0.922	6.16E-14	Not normal	0.989	0.003	Not normal
44	65	0.976	0.250	Normal	0.964	0.059	Normal
45	525	0.889	4.93E-19	Not normal	0.985	2.36E-05	Not normal
46	77	0.877	2.07E-06	Not normal	0.977	0.169	Normal
47	150	0.904	2.28E-08	Not normal	0.956	1.05E-04	Not normal
48	304	0.942	1.32E-09	Not normal	0.960	2.10E-07	Not normal

Table B3: The number of peaks in the KDE of the scallop length data from Trout Beck. The modality (unimodal, bimodal, or multimodal – as determined by the number of peaks), number of peaks in the upper and lower 5% of the data distribution, and the number of peaks above the 50th percentile of the KDE values is also noted.

Site	Number of Peaks	Modality	Peaks in Lower 5%	Peaks in Upper 5%	Peaks above the 50th percentile of the KDE values
1	2	Bimodal	0	1	1
2	1	Unimodal	0	0	1
3	3	Multimodal	0	2	1
4	1	Unimodal	0	0	1
5	2	Bimodal	0	0	1
6	1	Unimodal	0	0	1
7	1	Unimodal	0	0	1
8	2	Bimodal	0	0	1
9	4	Multimodal	0	2	2
10	2	Bimodal	0	1	1
11	1	Unimodal	0	0	1

Table B4: The number of peaks in the KDE of the Log_{10} transformed scallop length data from Trout Beck. The modality (unimodal, bimodal, or multimodal – as determined by the number of peaks), number of peaks in the upper and lower 5% of

the data distribution, and the number of peaks above the 50th percentile of the KDE values is also noted.

Site	Number of Peaks	Modality	Peaks in Lower 5%	Peaks in Upper 5%	Peaks in upper 50th percentile of KDE values
1	1	Unimodal	0	0	1
2	1	Unimodal	0	0	1
3	1	Unimodal	0	0	1
4	1	Unimodal	0	0	1
5	2	Bimodal	0	0	1
6	1	Unimodal	0	0	1
7	1	Unimodal	0	0	1
8	2	Bimodal	1	0	1
9	1	Unimodal	0	0	1
10	1	Unimodal	0	0	1
11	1	Unimodal	0	0	1

Table B5: The number of peaks in the KDE of the scallop length data from Rough Sike. The modality (unimodal, bimodal, or multimodal – as determined by the number of peaks), number of peaks in the upper and lower 5% of the data distribution, and the number of peaks above the 50th percentile of the KDE values is also noted.

Site	Number of Peaks	Modality	Peaks in Lower 5%	Peaks in Upper 5%	Peaks in upper 50th percentile of KDE values
1	1	Unimodal	0	0	1
2	1	Unimodal	0	0	1
3	1	Unimodal	0	0	1
4	1	Unimodal	0	0	1
5	2	Bimodal	0	1	1
6	2	Bimodal	0	1	1

Site	Number of Peaks	Modality	Peaks in Lower 5%	Peaks in Upper 5%	Peaks in upper 50th percentile of KDE values
7	1	Unimodal	0	0	1
8	2	Bimodal	0	1	1
9	2	Bimodal	0	1	1
10	1	Unimodal	0	0	1
11	1	Unimodal	0	0	1
12	3	Multimodal	0	2	1
13	1	Unimodal	0	0	1
14	1	Unimodal	0	0	1
15	1	Unimodal	0	0	1
16	1	Unimodal	0	0	1
17	1	Unimodal	0	0	1
18	1	Unimodal	0	0	1
19	1	Unimodal	0	0	1
20	1	Unimodal	0	0	1
21	2	Bimodal	0	1	1
22	1	Unimodal	0	0	1
23	1	Unimodal	0	0	1
24	1	Unimodal	0	0	1
25	3	Multimodal	0	2	1
26	1	Unimodal	0	0	1
27	1	Unimodal	0	0	1
28	2	Bimodal	0	1	1
29	3	Multimodal	0	2	1
30	1	Unimodal	0	0	1
31	1	Unimodal	0	0	1
32	1	Unimodal	0	0	1
33	1	Unimodal	0	0	1
34	1	Unimodal	0	0	1
35	2	Bimodal	0	1	1
36	1	Unimodal	0	0	1

Site	Number of Peaks	Modality	Peaks in Lower 5%	Peaks in Upper 5%	Peaks in upper 50th percentile of KDE values
37	2	Bimodal	0	1	1
38	2	Bimodal	0	1	1
39	1	Unimodal	0	0	1
40	1	Unimodal	0	0	1
41	2	Bimodal	0	1	1
42	2	Bimodal	0	0	1
43	3	Multimodal	0	2	1
44	1	Unimodal	0	0	1
45	2	Bimodal	0	1	1
46	2	Bimodal	0	1	1
47	2	Bimodal	0	1	1
48	2	Bimodal	0	1	1

Table B6: The number of peaks in the KDE of the Log_{10} transformed scallop length data from Rough Sike. The modality (unimodal, bimodal, or multimodal – as determined by the number of peaks), number of peaks in the upper and lower 5% of the data distribution, and the number of peaks above the 50th percentile of the KDE values is also noted.

Site	Number of Peaks	Modality	Peaks in Lower 5%	Peaks in Upper 5%	Peaks in upper 50th percentile of KDE values
1	1	Unimodal	0	0	1
2	1	Unimodal	0	0	1
3	1	Unimodal	0	0	1
4	2	Bimodal	1	0	1
5	1	Unimodal	0	0	1
6	1	Unimodal	0	0	1
7	2	Bimodal	0	1	1
8	1	Unimodal	0	0	1

Site	Number of Peaks	Modality	Peaks in Lower 5%	Peaks in Upper 5%	Peaks in upper 50th percentile of KDE values
9	1	Unimodal	0	0	1
10	1	Unimodal	0	0	1
11	1	Unimodal	0	0	1
12	2	Bimodal	0	0	2
13	1	Unimodal	0	0	1
14	4	Multimodal	1	1	2
15	1	Unimodal	0	0	1
16	1	Unimodal	0	0	1
17	1	Unimodal	0	0	1
18	1	Unimodal	0	0	1
19	2	Bimodal	1	0	1
20	2	Bimodal	1	0	1
21	2	Bimodal	1	0	1
22	1	Unimodal	0	0	1
23	1	Unimodal	0	0	1
24	1	Unimodal	0	0	1
25	1	Unimodal	0	0	1
26	1	Unimodal	0	0	1
27	1	Unimodal	0	0	1
28	1	Unimodal	0	0	1
29	2	Bimodal	1	0	1
30	1	Unimodal	0	0	1
31	1	Unimodal	0	0	1
32	1	Unimodal	0	0	1
33	1	Unimodal	0	0	1
34	1	Unimodal	0	0	1
35	1	Unimodal	0	0	1
36	1	Unimodal	0	0	1
37	1	Unimodal	0	0	1
38	1	Unimodal	0	0	1

Site	Number of Peaks	Modality	Peaks in Lower 5%	Peaks in Upper 5%	Peaks in upper 50th percentile of KDE values
39	1	Unimodal	0	0	1
40	2	Bimodal	0	1	1
41	1	Unimodal	0	0	1
42	1	Unimodal	0	0	1
43	1	Unimodal	0	0	1
44	1	Unimodal	0	0	1
45	1	Unimodal	0	0	1
46	1	Unimodal	0	0	1
47	1	Unimodal	0	0	1
48	2	Bimodal	0	0	1

(A)

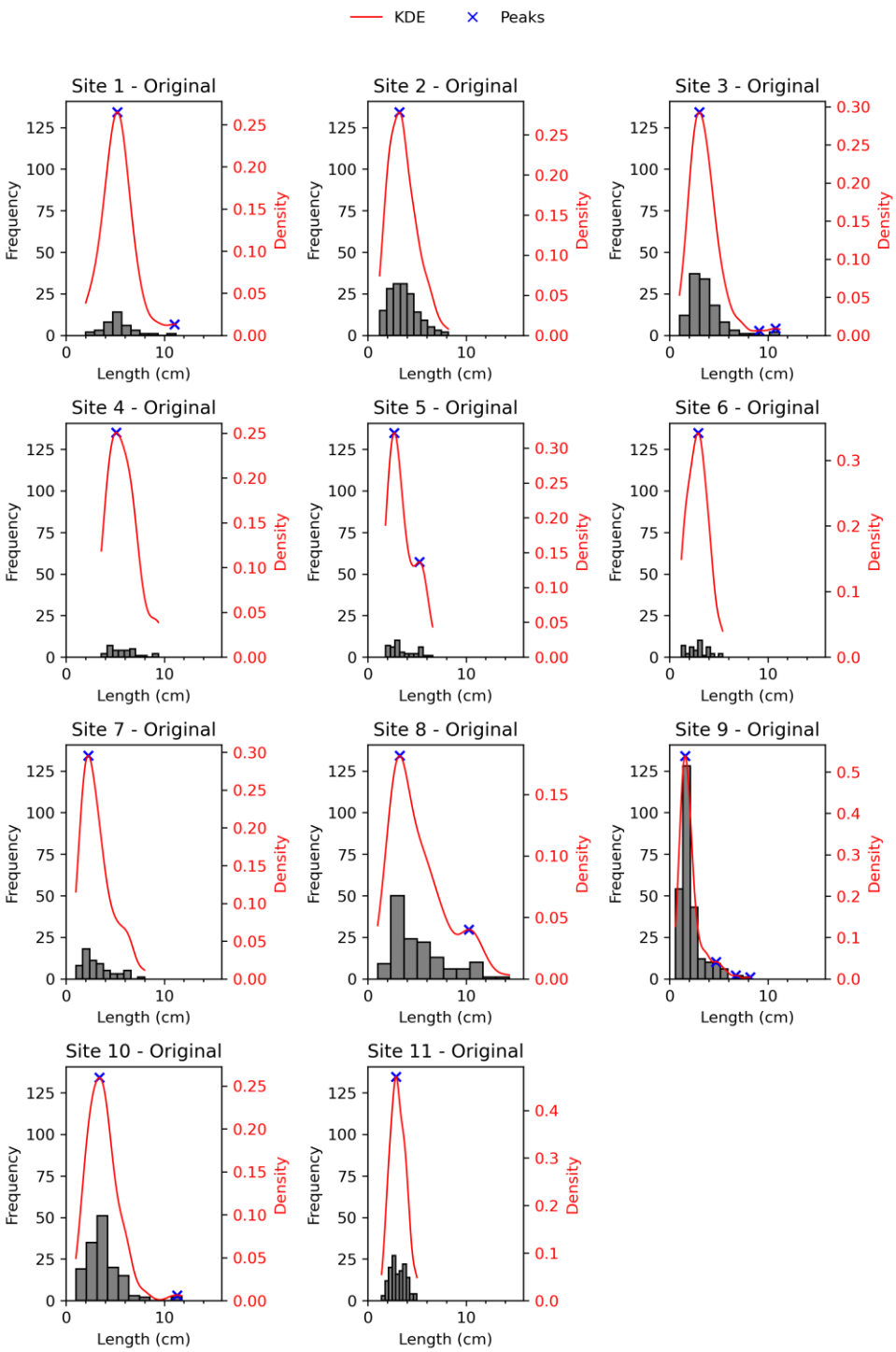
KDE
Peaks
Site 1 - Original
Site 2 - Original
Site 3 - Original
Site 4 - Original
Site 5 - Original
Site 6 - Original
Site 7 - Original
Site 8 - Original
Site 9 - Original
Site 10 - Original
Site 11 - Original
Frequency
Density
Length (cm)

(continued)

(B)

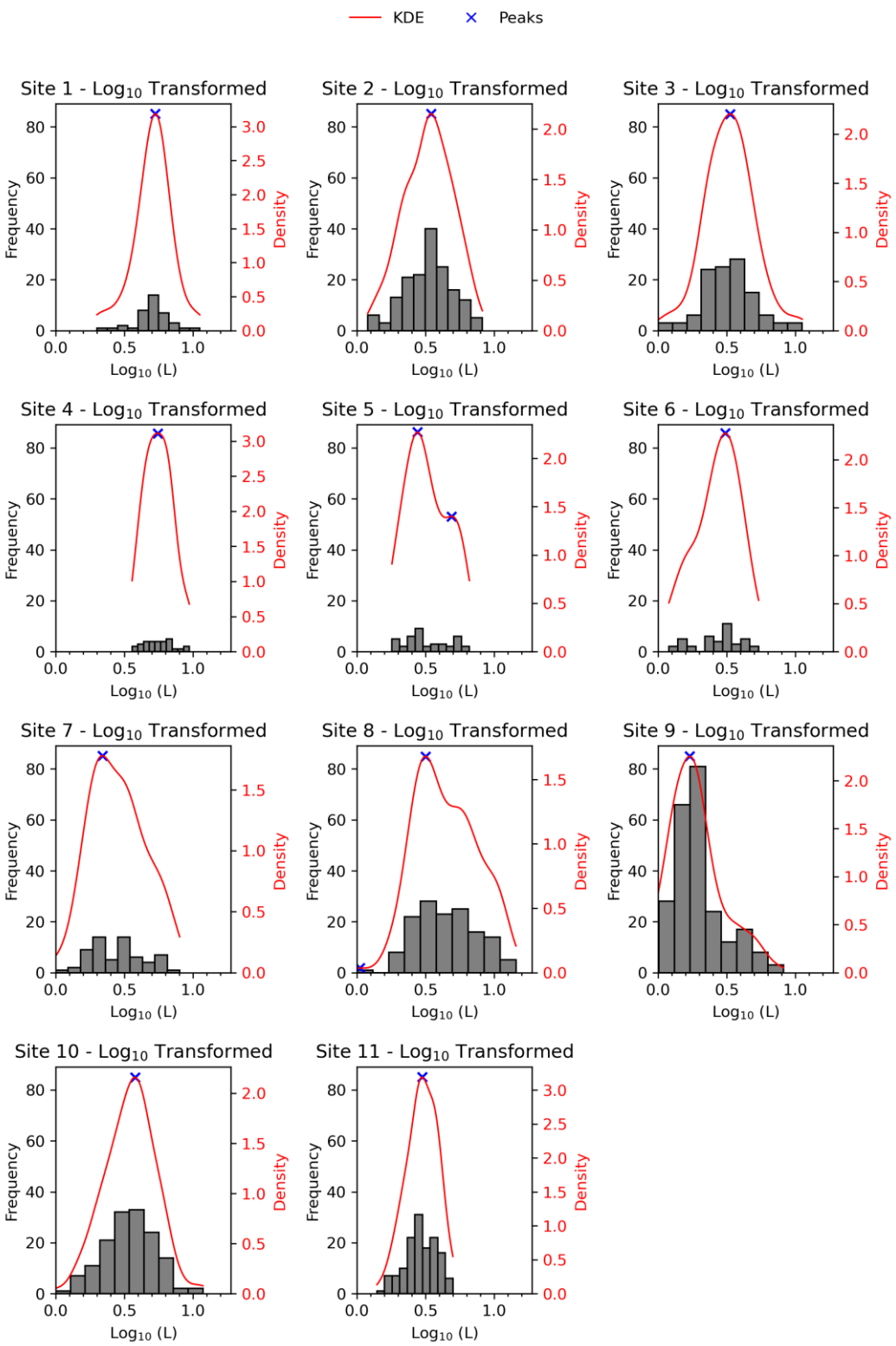

Figure B1: Histogram and Kernel Density Estimate of the (A) original and (B) Log_{10} transformed scallop length data from Trout Beck.

(A)

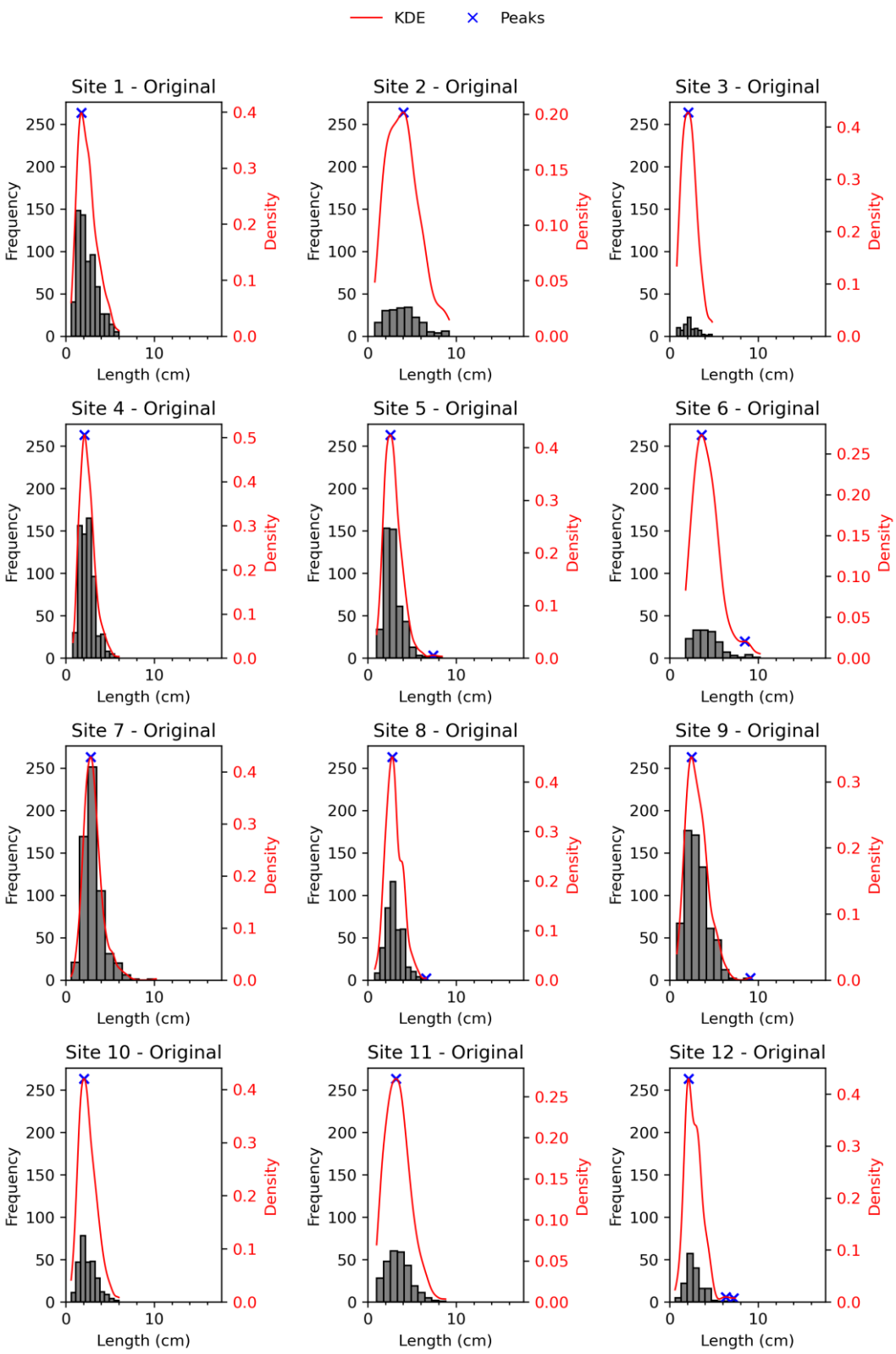
KDE
Peaks
Site 1 - Original
Site 2 - Original
Site 3 - Original
Site 4 - Original
Site 5 - Original
Site 6 - Original
Site 7 - Original
Site 8 - Original
Site 9 - Original
Site 10 - Original
Site 11 - Original
Site 12 - Original
Frequency
Density
Length (cm)

(continued)

(B)

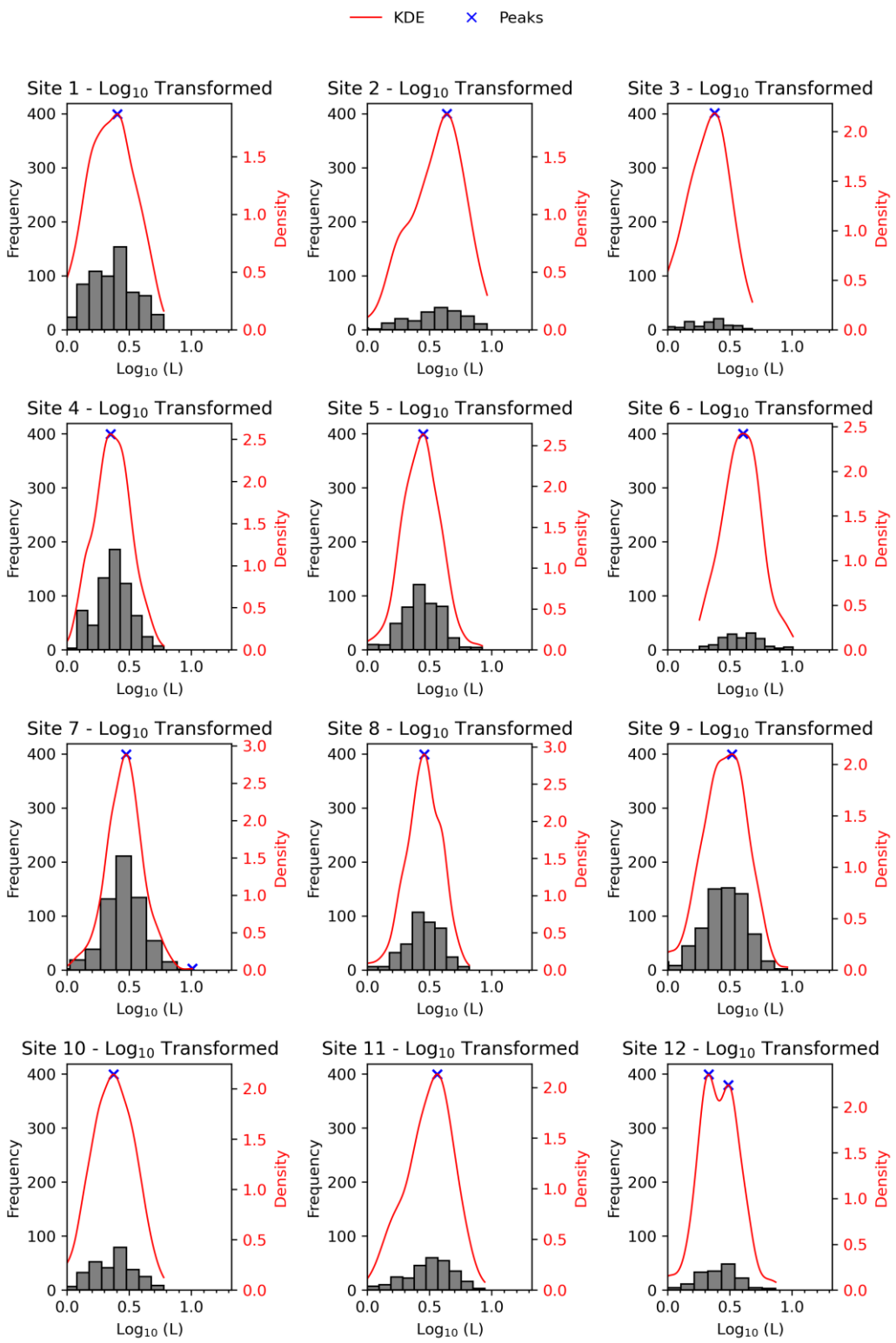
KDE
Peaks
Site 1 - Log10 Transformed
Site 2 - Log10 Transformed
Site 3 - Log10 Transformed
Site 4 - Log10 Transformed
Site 5 - Log10 Transformed
Site 6 - Log10 Transformed
Site 7 - Log10 Transformed
Site 8 - Log10 Transformed
Site 9 - Log10 Transformed
Site 10 - Log10 Transformed
Site 11 - Log10 Transformed
Site 12 - Log10 Transformed
Frequency
Density
Log10 (L)

(continued)

(C)

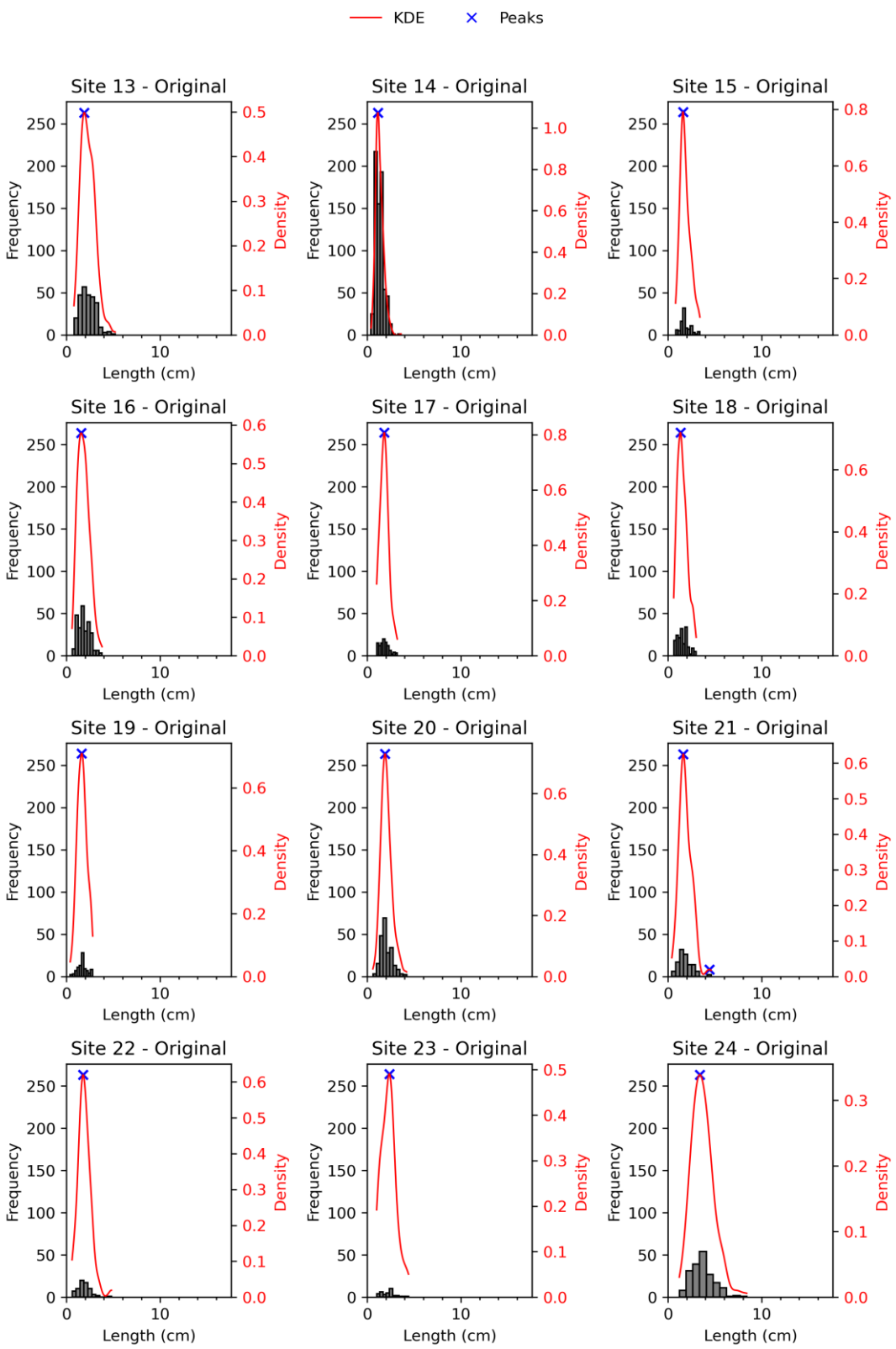
KDE
Peaks
Site 13 - Original
Site 14 - Original
Site 15 - Original
Site 16 - Original
Site 17 - Original
Site 18 - Original
Site 19 - Original
Site 20 - Original
Site 21 - Original
Site 22 - Original
Site 23 - Original
Site 24 - Original
Frequency
Density
Length (cm)

(continued)

(D)

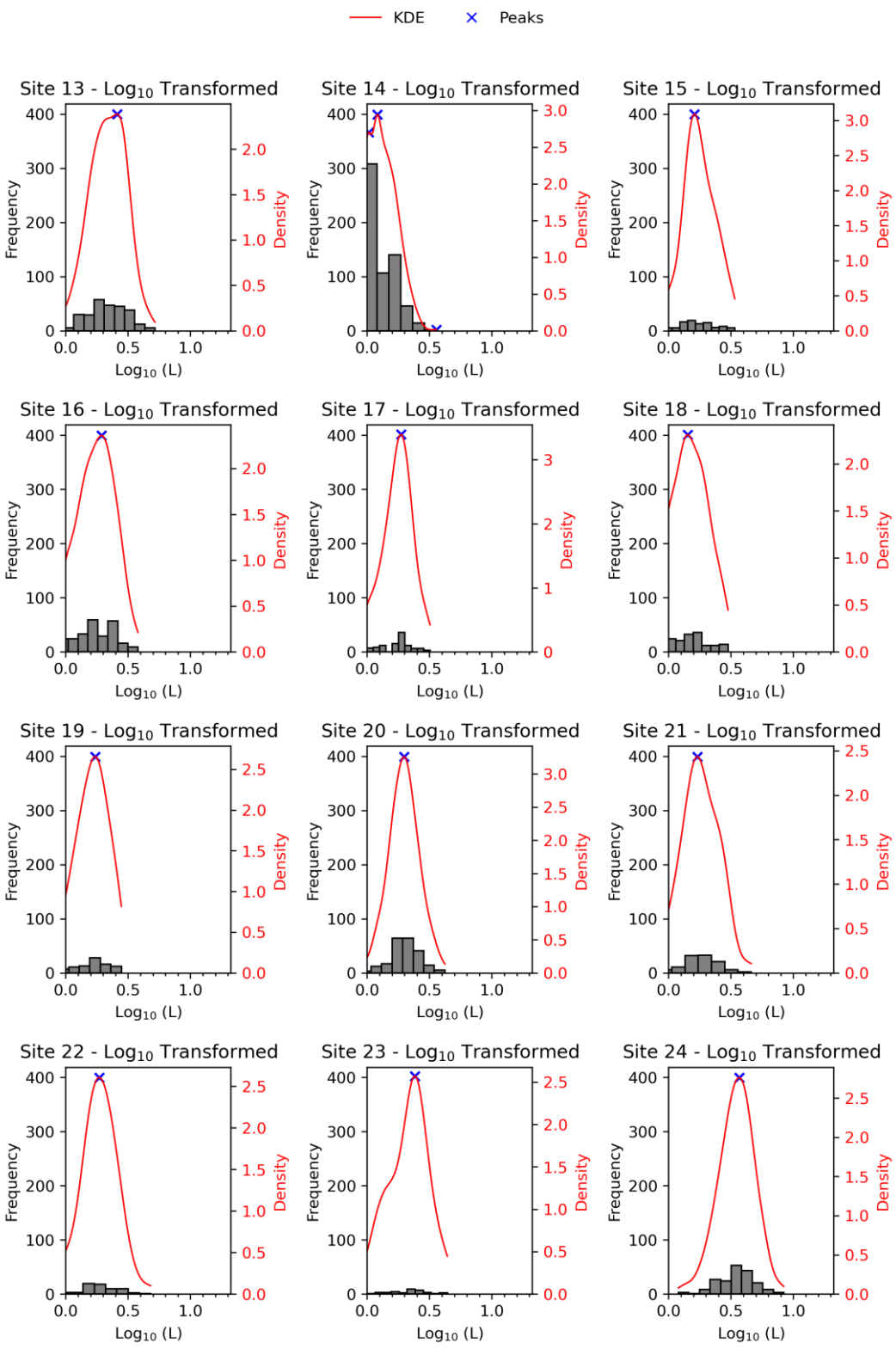
KDE
Peaks
Site 13 - Log10 Transformed
Site 14 - Log10 Transformed
Site 15 - Log10 Transformed
Site 16 - Log10 Transformed
Site 17 - Log10 Transformed
Site 18 - Log10 Transformed
Site 19 - Log10 Transformed
Site 20 - Log10 Transformed
Site 21 - Log10 Transformed
Site 22 - Log10 Transformed
Site 23 - Log10 Transformed
Site 24 - Log10 Transformed
Frequency
Density
Log10 (L)

(continued)

(E)

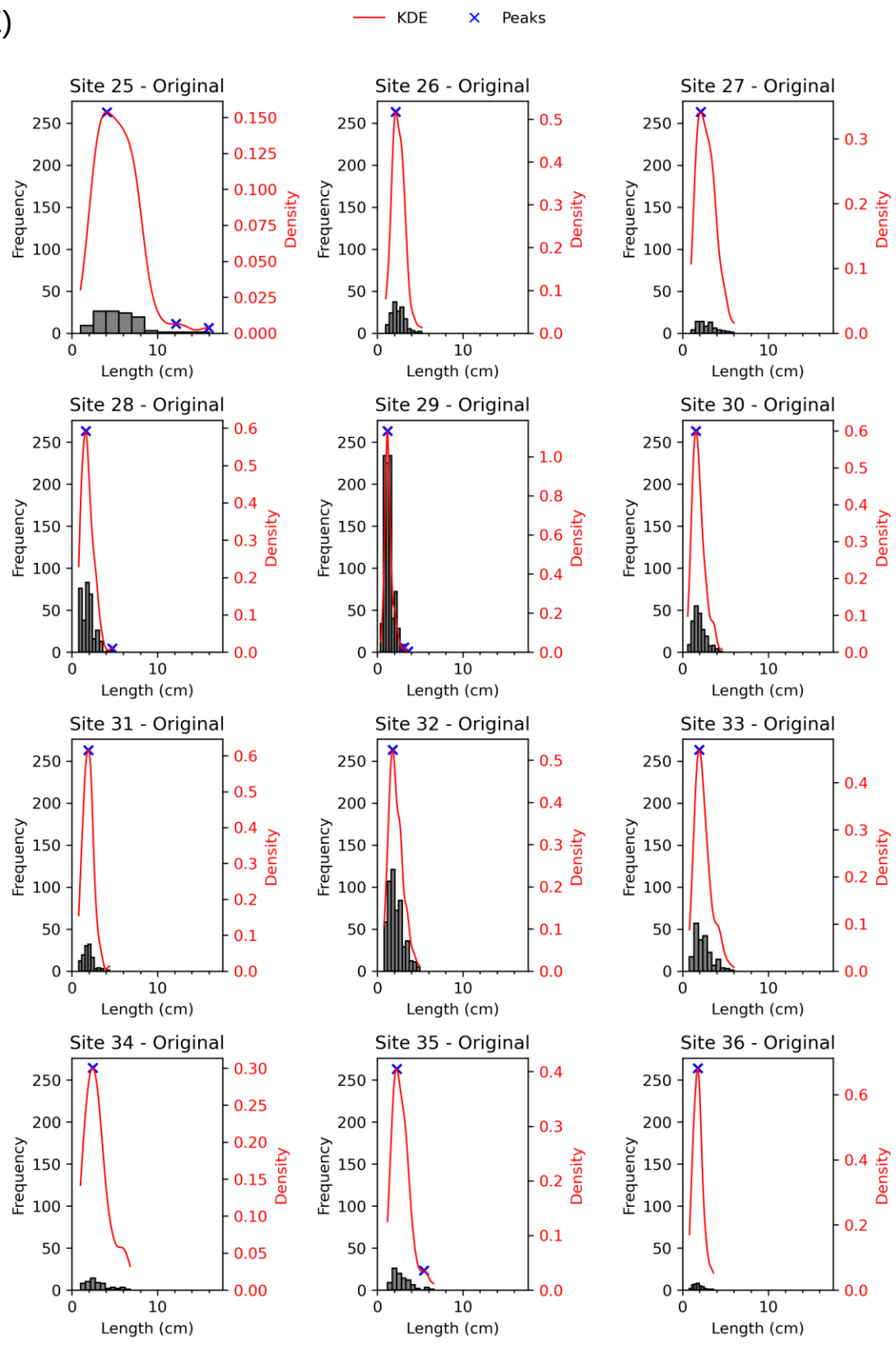
KDE
Peaks
Site 25 - Original
Site 26 - Original
Site 27 - Original
Site 28 - Original
Site 29 - Original
Site 30 - Original
Site 31 - Original
Site 32 - Original
Site 33 - Original
Site 34 - Original
Site 35 - Original
Site 36 - Original
Frequency
Density
Length (cm)

(continued)

(F)

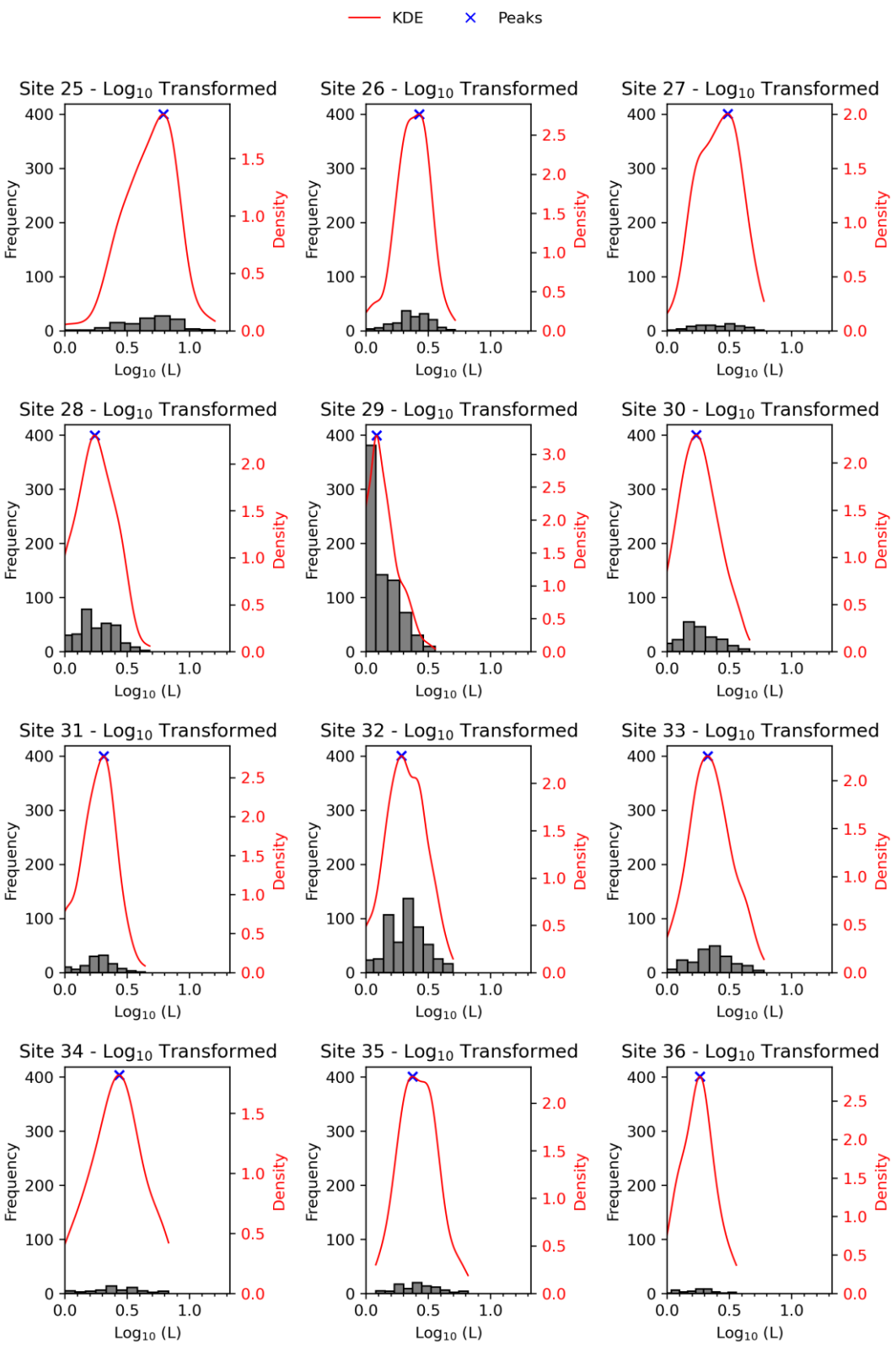
KDE
Peaks
Site 25 - Log10 Transformed
Site 26 - Log10 Transformed
Site 27 - Log10 Transformed
Site 28 - Log10 Transformed
Site 29 - Log10 Transformed
Site 30 - Log10 Transformed
Site 31 - Log10 Transformed
Site 32 - Log10 Transformed
Site 33 - Log10 Transformed
Site 34 - Log10 Transformed
Site 35 - Log10 Transformed
Site 36 - Log10 Transformed
Frequency
Density
Log10 (L)

(continued)

(G)

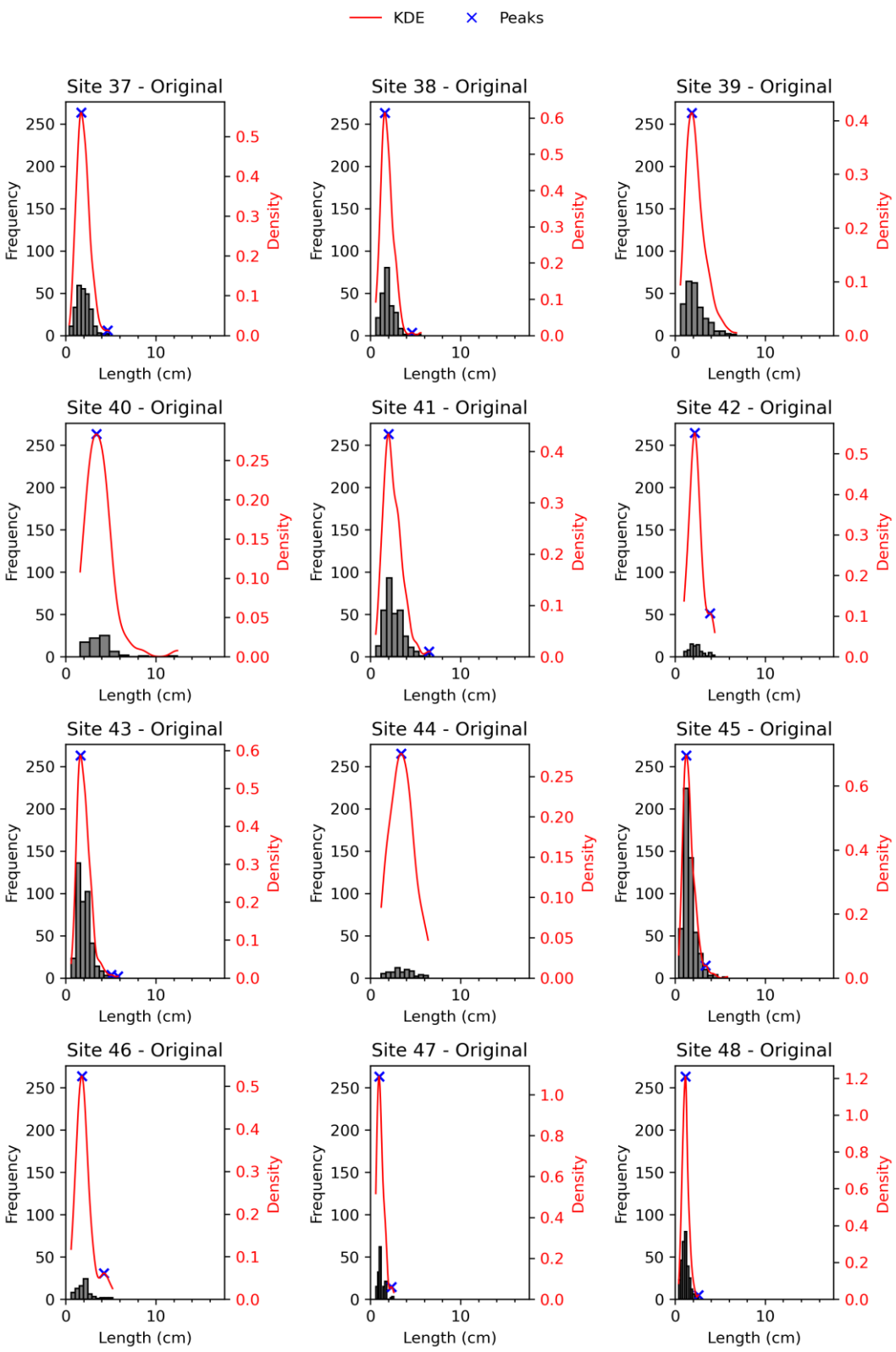
KDE
Peaks
Site 37 - Original
Site 38 - Original
Site 39 - Original
Site 40 - Original
Site 41 - Original
Site 42 - Original
Site 43 - Original
Site 44 - Original
Site 45 - Original
Site 46 - Original
Site 47 - Original
Site 48 - Original
Frequency
Density
Length (cm)

(continued)

(H)

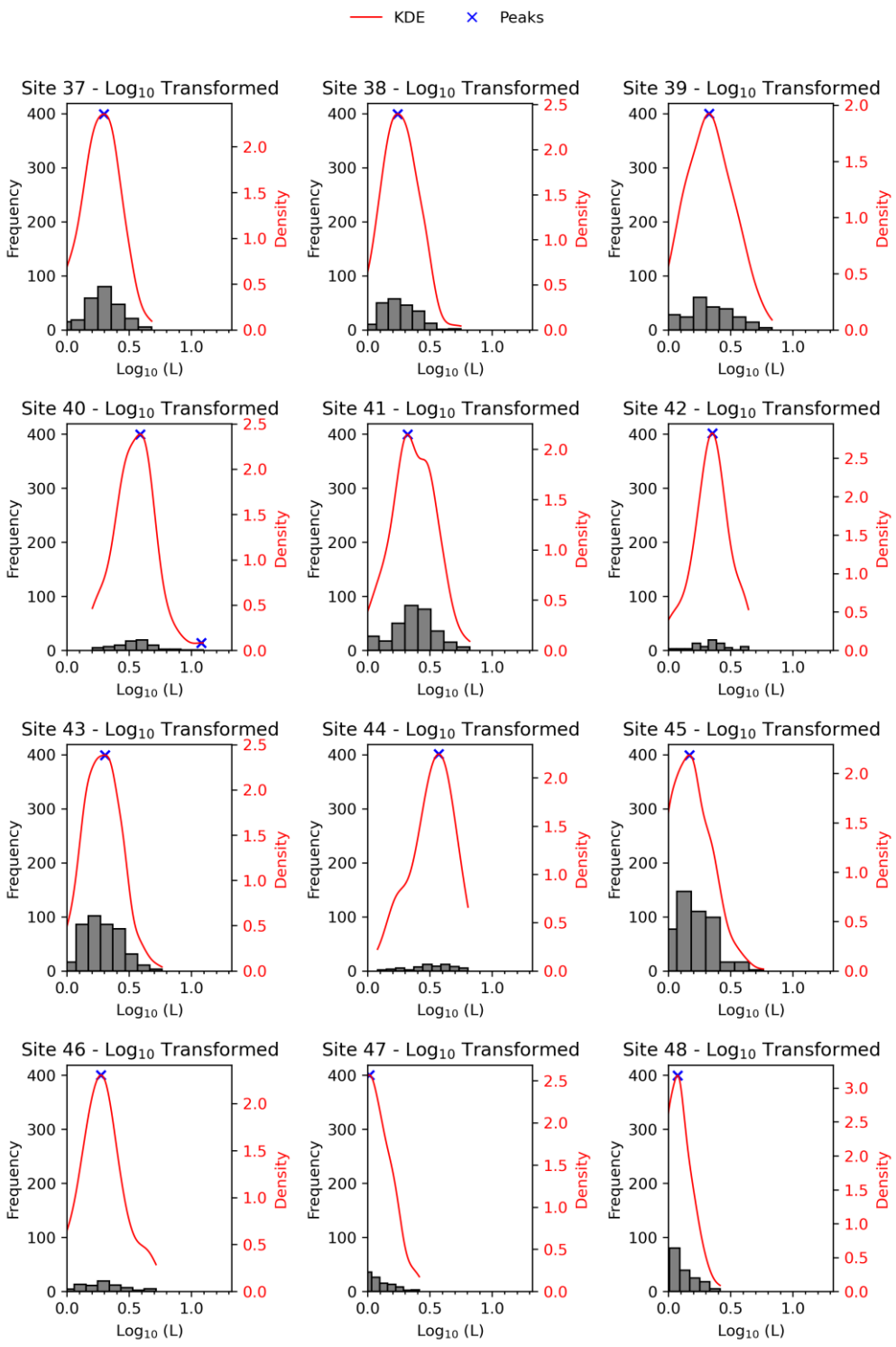

Figure B2: Histogram and Kernel Density Estimate for the scallop length data from Rough Sike. (A) Original - Sites 1 - 12, (B) Log_{10} - Sites 1 - 12, (C) Original - Sites 13 - 24, (D) Log_{10} - Sites 13 - 24, (E) Original - Sites 25 - 36, (F) Log_{10} - Sites 25 - 36, (G) Original – Sites 37 – 48, (H) Log_{10} – Sites 37 – 48.

7.3. Appendix C: Trout Beck and Rough Sike cross-section details

Table C1: Nearest cross-section sampled by Dingle et al. (in review) to each sample site at Trout Beck and Rough Sike.

Site number	Cross-section ID (Dingle et al., in review)
Rough Sike (RS)	
1	RS5
2	RS5
3	RS5
4	RS5
5	RS5
6	RS4
7	RS4
8	RS4
9	RS4
10	RS4
11	RS4
12	RS4
13	RS4
14	RS4
15	RS4
16	RS4
17	RS4
18	RS4
19	RS4
20	RS3
21	RS3
22	RS3
23	RS3
24	RS3
25	RS3
26	RS3
27	RS3

28	RS3
29	RS3
30	RS3
31	RS2
32	RS2
33	RS2
34	RS2
35	RS2
36	RS2
37	RS2
38	RS2
39	RS2
40	RS2
41	RS2
42	RS1
43	RS1
44	RS1
45	RS1
46	RS1
47	RS1
48	RS1
Trout Beck (TB)	
1	TB6
2	TB5
3	TB4
4	TB4
5	TB4
6	TB2
7	TB2
8	TB2
9	TB1
10	TB1
11	TB1

7.4. Appendix D: Scallop orientation

Table D1: Summary statistics of the scallop orientation distributions from sample sites at Trout Beck.

Site	Count	Circular Standard Deviation	Range	Skewness	Kurtosis	Modality
Site 1	39	14.7	50	-0.1	-1.1	Multimodal
Site 2	163	15.8	100	1.3	3.1	Unimodal
Site 3	116	12.0	62	0.2	-0.2	Unimodal
Site 4	30	8.5	46	-0.5	2.1	Unimodal
Site 5	40	13.4	63	0.6	0.5	Unimodal
Site 6	40	13.2	52	-0.2	-0.6	Multimodal
Site 7	63	9.0	51	1.0	2.1	Unimodal
Site 8	142	50.7	181	0.9	-0.7	Bimodal
Site 9	265	15.3	81	0.9	0.7	Unimodal
Site 10	147	9.9	59	0.2	0.3	Unimodal
Site 11	140	16.2	94	0.8	0.7	Unimodal

Table D2: Summary statistics of the scallop orientation distributions from sample sites at Rough Sike.

Site	Count	Circular Standard Deviation	Range	Skewness	Kurtosis	Modality
Site 1	644	16.9	121	0.1	0.6	Unimodal

Site	Count	Circular Standard Deviation	Range	Skewness	Kurtosis	Modality
Site 2	197	11.2	93	-0.4	2.7	Unimodal
Site 3	82	11.1	68	0.8	1.6	Unimodal
Site 4	662	21.9	130	-0.5	0.6	Unimodal
Site 5	465	16.8	137	0.9	2.6	Unimodal
Site 6	155	14.8	77	0.3	-0.1	Unimodal
Site 7	605	15.7	107	0.3	0.5	Bimodal
Site 8	396	14.5	123	-0.3	1.9	Unimodal
Site 9	671	19.4	148	-0.5	2.1	Unimodal
Site 10	286	31.0	198	0.1	0.4	Unimodal
Site 11	276	13.5	84	0.9	1.9	Unimodal
Site 12	161	20.6	103	-0.3	-0.3	Bimodal
Site 13	271	13.1	85	0.7	1.8	Unimodal
Site 14	705	17.1	149	0.5	1.8	Unimodal
Site 15	93	16.9	90	-0.4	0.4	Bimodal
Site 16	259	21.7	107	-0.1	-0.7	Bimodal
Site 17	105	19.5	102	0.1	-0.3	Multimodal
Site 18	169	15.7	83	0.3	-0.4	Bimodal
Site 19	92	16.2	85	-0.1	-0.1	Bimodal
Site 20	223	19.6	85	-0.1	-0.8	Bimodal
Site 21	117	20.9	125	-0.1	0.6	Unimodal
Site 22	70	22.0	81	0.0	-1.1	Bimodal

Site	Count	Circular Standard Deviation	Range	Skewness	Kurtosis	Modality
Site 23	35	15.6	61	0.2	-0.6	Bimodal
Site 24	191	13.7	69	0.3	-0.4	Unimodal
Site 25	111	12.5	61	0.5	-0.1	Unimodal
Site 26	156	24.0	131	0.5	-0.2	Unimodal
Site 27	69	33.1	130	-0.2	-0.8	Bimodal
Site 28	324	16.6	113	-0.3	0.8	Unimodal
Site 29	879	14.0	101	-0.1	0.4	Unimodal
Site 30	213	21.7	138	0.2	0.5	Unimodal
Site 31	120	17.5	72	1.0	0.1	Unimodal
Site 32	535	22.8	167	1.3	2.6	Unimodal
Site 33	204	18.1	95	-0.2	-0.2	Unimodal
Site 34	60	19.0	88	-0.1	-0.1	Bimodal
Site 35	93	16.5	112	-2.0	6.7	Unimodal
Site 36	37	29.5	127	0.2	-0.2	Unimodal
Site 37	256	23.9	126	0.0	-0.2	Bimodal
Site 38	224	31.2	163	0.6	-0.1	Bimodal
Site 39	244	21.8	166	-0.9	2.5	Unimodal
Site 40	74	26.0	128	0.0	0.0	Bimodal
Site 41	312	23.3	178	2.1	6.9	Unimodal
Site 42	74	23.1	107	0.8	0.3	Bimodal
Site 43	420	18.3	153	-0.6	3.7	Unimodal

Site	Count	Circular Standard Deviation	Range	Skewness	Kurtosis	Modality
Site 44	65	10.8	50	0.0	-0.3	Unimodal
Site 45	525	28.3	161	0.0	-0.2	Unimodal
Site 46	77	45.8	210	-1.4	1.2	Unimodal
Site 47	150	13.1	85	-0.5	1.3	Unimodal
Site 48	304	16.9	133	-1.0	3.1	Unimodal

8. References

BGS (2024) Alston Formation. The BGS Lexicon of Named Rock Units. British Geological Survey. Available from: https://webapps.bgs.ac.uk/lexicon/lexicon.cfm?pub=AG. Access date [25/07/2024].

Blumberg, P. N., and Curl, R. L. (1974) Experimental and theoretical studies of dissolution roughness. *Journal of Fluid Mechanics* 65(4): 735–751.

Bögli, A. (1980) A General View of Exokarst. In *Karst Hydrology and Physical Speleology* (1st ed.). Springer Berlin, Heidelberg.

Bortel, H. E. (2021) *Scallops Through Space and Time: A Study of Scallop Patterns and Consistency*. Ohio University.

Bretz, J. H. (1942) Vadose and Phreatic Features of Limestone Caverns. *The Journal of Geology* 50(6): 675–811.

Bushuk, M., Holland, D. M., Stanton, T. P., Stern, A., and Gray, C. (2019) Ice Scallops: A Laboratory Investigation of the Ice-Water Interface. *Journal of Fluid Mechanics* 873: 942–976.

Charlton, R. (2003) Towards defining a scallop dominant discharge for vadose conduits: some preliminary results. *Cave and Karst Science* 30: 3–7.

Charlton, R. (2009) *Chapter 7: Processes of erosion, transport and deposition*. In: Fundamentals of fluvial geomorphology. Routledge.

Checkley, D., and Faulkner, T. (2014) Scallop measurement in a 10m-high vadose canyon in pool sink, ease gill cave system, Yorkshire dales, UK and a hypothetical post-deglacial canyon entrenchment timescale. *Cave and Karst Science* 41: 76–83.

Claudin, P., Durán, O., Andreotti, B. (2017) Dissolution instability and roughening transition. *Journal of Fluid Mechanics*, vol. 832.

Cole, J. J., and Prairie, Y. T. (2014) Dissolved CO2 in Freshwater Systems☆. In *Reference Module in Earth Systems and Environmental Sciences*. Elsevier doi:10.1016/B978-0-12-409548-9.09399-4.

Coleman, J. C. (1945) An indicator of waterflow in caves. *Geological Magazine* 82(3): 138–139.

Cooper, M. (2018). Speleogenesis in Turbulent Flow. Graduate Theses and Dissertations. Retrieved from https://scholarworks.uark.edu/etd/2980.

Covington, M. D., Gulley, J. D., and Gabrovšek, F. (2015) Natural variations in calcite dissolution rates in streams: Controls, implications, and open questions. *Geophysical Research Letters* 42(8): 2836–2843.

Curl, R. L. (1966) Scallops and Flutes. Transactions of the Cave Research Group of Great Britain, Volume 7, Number 2, March 1966, pp 121-160.

Curl, R. L. (1974) Deducing Flow Velocity in Cave Conduits from Scallops. (36(2)): 1–5.

DEIMS-SDR (2023) Trout Beck - United Kingdom. R22. DEIMS.iD: https://deims.org/d767988a-34ab-4051-ac72-fe7204ffbe6f. Access date [23/08/2024].

Demir, T. (2000) *The influence of particle shape on bedload transport in coarse-bed river channels*, Doctoral thesis. Durham University.

Despain, J., Tobin, B., and Stock, G. (2016) Geomorphology and paleohydrology of Hurricane Crawl Cave, Sequoia National Park, California. *Journal of Cave and Karst Studies* 78(2): 72–84.

Dingle, E., Baynes, E., Hall, A., and Warburton, J. (in review) Erosion dynamics in carbonate bedrock channels inhibit weathering processes. *Earth Surface Processes and Landforms.*

Droin, A. (2021) *Delineation and morphometric analysis of micro-scale karstic forms (scallops) based on structure from motion digital elevation models*. University of Graz.

ECN (2024) Trout Beck. ECN site code: R22. Retrieved from https://ecn.ac.uk/sites/site/rivers/trout-beck#:~:text=Discharge%20is%20measured%20at%20an,fluctuations%20associated%20with%20the%20discharge. Access date [23/08/2024].

Evans, M. G., Burt, T. P., Holden, J., and Adamson, J. K. (1999) Runoff generation and water table fluctuations in blanket peat: evidence from UK data spanning the dry summer of 1995. *Journal of Hydrology* 221(3): 141–160.

Evans, C., Woodin, S., Lindsay, R. (2016) Atmospheric pollution. IUCN UK Committee Peatland Programme Briefing Note No. 13.

Farrant, A. R., and Smart, P. L. (2011) Role of sediment in speleogenesis; sedimentation and paragenesis. *Geomorphology* 134: 79–93.

Faulkner, T. (2013) Speleogenesis and scallop formation and demise under hydraulic control and other recharge regimes. *Cave and Karst Science* 40: 114–132.

Faulkner, T. (2022) The high-flow low-storage extreme in marble aquifers. [Published in the Proceedings of the 18th International Congress of Speleology, France, 2022, Vol 4, 129-132.].

Ford, D., and Williams, P. (2007) *Karst Hydrogeology and Geomorphology*. John Wiley & Sons.

Gale, S. J. (1984) The hydraulics of conduit flow in carbonate aquifers. *Journal of Hydrology* 70(1–4): 309–327.

Goodchild, M. F., and Ford, D. C. (1971) Analysis of Scallop Patterns by Simulation under Controlled Conditions. *The Journal of Geology* 79(1): 52–62.

Gradziński, M. (2002) Morphology of Czama Cave and its significance for the geomorphic evolution of the Kościeliska Valley (Western Tatra Mts.). 72: 255–262.

Hall, A. (2019) *Verification of and Expansion Upon the Use of Cave Scallops in Recreating Hydrogeologic Conditions in Karst Aquifers*. Ohio University.

Hammer, O., Lauritzen, S., and Jamtveit, B. (2011) Stability of Dissolution Flutes under Turbulent Flow. *Journal of cave and karst studies the National Speleological Society bulletin* 73.

Hancock, G., Anderson, R., and Whipple, K. (1998) Beyond Power: Bedrock River Incision Process and Form. *Washington DC American Geophysical Union Geophysical Monograph Series* : 35–60. doi:10.1029/GM107p0035.

Hurst, A. A., and Anderson, R. S. (2018) River channel lowering by upstream migration of bedrock steps. 2018: EP41B-2668. Presented at the AGU Fall Meeting Abstracts.

Johnson, C., Affolter, M., Inkenbrandt, P., and Mosher, C. (2017) 11.10: Karst. In *An Introduction to Geology*. Salt Lake Community College.

Kicińska, D., Hercman, H., and Najdek, K. (2017) Evolution of the Bystrej Valley caves (Tatra Mts, Poland) based on corrosive forms, clastic deposits and U-series speleothem dating. *Annales Societatis Geologorum Poloniae* 87: 101–119.

Lauritzen, S. (1989) *Scallop Dominant Discharge*. *Proceedings, 10 International Speleological Congress, Budapestth*.

Lauritzen, S. (1982) The paleocurrents and morphology of Pikhåggrottene, Svartisen, North Norway. *Norsk Geografisk Tidsskrift - Norwegian Journal of Geography* 36(4): 183–209.

Lundberg, J. (2019) Karren, cave. In *Encyclopedia of Caves*. Elsevier doi:10.1016/B978-0-12-814124-3.00070-4.

Lundberg, J., Carroll, W., Roberts, W., Mcfarlane, D., Buchroithner, M., and Rentergem, G. (2017) Analysis of scallops in Gomantong Caves, by GIS processing of 3D terrestrial laser scanner data. (Vol. 2). Presented at the Proceedings of the 17th International Congress of Speleology.

Maxson, J. H. (1940) Fluting and Faceting of Rock Fragments. *The Journal of Geology* 48(7): 717–751.

Murphy, P., and Moseley, M. (2012) Pre-mineralization vadose scallops associated with hematite at Hodbarrow, South Cumbria, UK. *Cave and Karst Science* 39: 115–118.

Palmer, A. (1991) Origin and morphology of limestone caves. GSA Bulletin 103(1): 1–21.

Richardson, K., and Carling, P. A. (2005) A typology of sculpted forms in open bedrock channels. In Richardson, K. and Carling, P. A. (Eds.), *A Typology of Sculpted Forms in Open Bedrock Channels* (Vol. 392). Geological Society of America.

Ristroph, L. (2018) Sculpting with flow. *Journal of Fluid Mechanics* 838: 1–4.

Ryb, U., Matmon, A., Erel, Y., Haviv, I., Katz, A., Starinsky, A., Angert, A., and Team, A. (2014) Controls on denudation rates in tectonically stable Mediterranean carbonate terrain. *Geological Society of America Bulletin* 126(3–4): 553–568.

Santanatoglia, G. (2023) *A fluid dynamics study using image processing of scallops on dissolving hard candy*, laurea. Politecnico di Torino.

Scikit Learn (2024) 2.8. Density Estimation. *Scikit-Learn*. Accessed: 7th August 2024 <https://scikit-learn/stable/modules/density.html. >.

Sharma, B. (2016) *Sediment Dynamics in a Bedrock Channel*. Durham University.

Simms, M. J., and Hunt, J. B. (2007) Flow capture and reversal in the Agen Allwedd Entrance Series, south Wales: evidence for glacial flooding and impoundment. *CAVE AND KARST SCIENCE* 34(2).

Skoglund, R., and Lauritzen, S. (2005) Maze caves in stripe karst: Examples from Nonshauggrotta, northern Norway.

Smith, H. M. (2004) *Significance of Bedrock Channel Morphology and Sediment Dynamics in a U.K. Upland River.*, Masters. Durham University.

Springer, G., and Hall, A. (2020) Uncertainties associated with the use of erosional cave scallop lengths to calculate stream discharges. *International Journal of Speleology* 49(1).

Springer, G., and Wohl, E. (2002) Empirical and Theoretical Investigations of Sculpted Forms in Buckeye Creek Cave, West Virginia. *Journal of Geology - J GEOL* 110: 469–481.

Tinkler, K., and Wohl, E. (1998) A Primer on Bedrock Channels. In *Rivers Over Rock: Fluvial Processes in Bedrock Channels*. American Geophysical Union (AGU) doi:10.1029/GM107p0001.

Turowski, J. M., Hovius, N., Meng-Long, H., Lague, D., and Men-Chiang, C. (2008) Distribution of erosion across bedrock channels. *Earth Surface Processes and Landforms* 33(3): 353–363.

Turowski, J. M., Hovius, N., Wilson, A., and Horng, M.-J. (2008) Hydraulic geometry, river sediment and the definition of bedrock channels. *Geomorphology* 99(1–4): 26–38.

Villien, B., Zheng, Y., and Lister, D. (2001) The scalloping phenomenon and its significance in flow-assisted corrosion. Presented at the Twenty Sixth Annual CNS-CNA Student Conference Toronto, Ontario, Canada.

Villien, B., Zheng, Y., and Lister, D. (2005) Surface Dissolution and the Development of Scallops. *Chemical Engineering Communications* 192(1): 125–136.

Whipple, K.X. (2004) Bedrock Rivers and the Geomorphology of Active Orogens. *Annual Review of Earth and Planetary Sciences* 32(1): 151–185.

Whipple, K.X, Hancock, G. S., and Anderson, R. S. (2000) River incision into bedrock: Mechanics and relative efficacy of plucking, abrasion and cavitation. *Geological Society of America Bulletin*.

Whipple, K.X., DiBiase, R. A., and Crosby, B. T. (2013) Bedrock Rivers. In *Treatise on Geomorphology*. Elsevier doi:10.1016/B978-0-12-374739-6.00254-2.

Wilson, A. (2009) *Fluvial bedrock abrasion by bedload: process and form*. University of Cambridge.

Woodward, E., and Sasowsky, I. D. (2009) A Spreadsheet Program (ScallopEx) to Calculate Paleovelocities From Cave Wall Scallops. *Acta Carsologica* 38(2–3).

Yang, T, and John, S. (1974) *Unit Stream Power for Sediment Transport in Natural Rivers*. Research Report. University of Illinois at Urbana-Champaign Water Resources Center.